METAL SALEN CATALYZED PRODUCTION OF POLYTRIMETHYLENE CARBONATE

A Dissertation

by

POULOMI GANGULY

Submitted to the Office of Graduate Studies
Texas A&M University
in partial fulfillment of the requirements for the degree of

DOCTOR OF PHILOSOPHY

May 2006

Major Subject: Chemistry

METAL SALEN CATALYZED PRODUCTION OF POLYTRIMETHYLENE CARBONATE

A Dissertation

by

POULOMI GANGULY

Submitted to the Office of Graduate Studies of
Texas A&M University
in partial fulfillment of the requirements for the degree of

DOCTOR OF PHILOSOPHY

Approved by:

Chair of Committee,	Donald J. Darensbourg
Committee Members,	Abraham Clearfield
	Francois P. Gabbaï
	Shankar P. Bhattacharyya
Head of Department,	Emile A. Schweikert

May 2006

Major Subject: Chemistry

ABSTRACT

Metal Salen Catalyzed Production of Polytrimethylene Carbonate.

(May 2006)

Poulomi Ganguly, B.S., St. Stephen's College; M.S., University of Delhi

Chair of Advisory Committee: Dr. Donald J. Darensbourg

Over the past decade the focus of our group has been production of polycarbonates through environmentally friendly routes. Continuing with this tradition, one such route is the ring opening polymerization of cyclic carbonates. The aliphatic polycarbonate derived from trimethylene carbonate, (TMC, 1, 3-dioxan-2-one), has been studied extensively for its potential use as a biodegradable polymer in biomedical and pharmaceutical systems. Its important applications include sutures, drug delivery systems and tissue engineering. To date, majority of the literature concerning catalysts for polymerization of TMC has been restricted to the use of simple Lewis acids with a marked absence of well defined and characterized catalysts. Metal salen complexes have been effective in the ring opening of cyclohexene oxide and the copolymerization of epoxide and carbon dioxide. The ability of this system as a catalyst for the polymerization of cyclic carbonates to polycarbonates is reported in this dissertation. The salen ligand is among the most versatile ligands in chemistry. Our attempts to optimize the catalytic activity by manipulating the salen structure and reaction

conditions are also discussed. Our initial efforts were concentrated in understanding the efficacy of Lewis acidic metal salen complexes (Al & Sn), as catalysts for this process. This was followed by the utilization of metal salen complexes of *biometals* as catalysts for the synthesis of these biodegradable polymers, as well as for the copolymerization of cyclic carbonates with cyclic esters. These copolymers are presently in great demand for their applications as sutures in the medical industry.

During the course of our investigations, a novel method of synthesizing poly-trimethylene carbonate, by the copolymerization of CO_2 and trimethylene oxide, has come to our attention. Surprisingly this reaction has received very little scientific exposure. We observed that metal salen derivatives, along with *n*-alkyl ammonium salts, were effective catalysts for the selective coupling of CO_2 and oxetane (trimethylene oxide) to provide the corresponding polycarbonate with only trace quantities of ether linkages. A section is also dedicated to our investigations in this area of research.

DEDICATION

This dissertation is dedicated to my parents (Bapia and Ma) for everything they have done for me. I am what I am today because of your love, support and encouragement. I know, Bapi, you would have been the happiest on the fulfillment of this dissertation. We will always miss you.

This is also dedicated to my sister, Paroma, for being the sunshine of our lives, and to my husband, Siddhartha, for always being there for me.

ACKNOWLEDGMENTS

I am extremely grateful to my advisor Dr. Donald J. Darensbourg, *Sir*, for being such a great advisor and giving me so many opportunities to learn not only in the lab but also outside it. I hope someday I can be not only a good chemist and a human being, but a great 'manager' like you. I am highly obliged to Dr. Clearfield and Dr. Gabbaï from the Department of Chemistry and Dr. Bhattacharyya (Electrical Engineering) for agreeing to serve on my committee. My heartfelt gratitude goes to Dr. Marcetta Y. Darensbourg for the kindness she showed me in the Fall of 2001, which I shall always remember.

My thanks and gratitude goes out to all the former members of the DJD group, not only for their mentoring but also for their advice and all their help. I would especially like to thank Dr. Damon R. Billodeaux for teaching me the ropes of crystallography. Current group members Eric Frantz, Jeremy Andreatta and Shawn Fitch are also to be thanked. Eric and Jeremy, I really appreciate your cheerful and enthusiastic disposition glimpses of which I got to witness during Open House and the TA skits.

I have been very fortunate to find some wonderful friends during these four years from each of whom I have learned so much. Wonsook, thanks for always being there for me, and if I already have not said it before, let me reaffirm, 'You are a Bond.' Shari, Hanan, Suparna, Ivy, Elky and Roxanne, your positive attitudes have taught me so much about life. I really value your friendship and will cherish it for the rest of my life.

Baba and Mamma, you are the best in-laws anyone could wish for. Everyone at Mamarbari, I don't have words to express my gratitude for all your love you showered over me over the years.

TABLE OF CONTENTS

CHAPTER Page

LIST OF TABLES

TABLE Page

LIST OF FIGURES

FIGURE Page

FIGURE Page

FIGURE Page

FIGURE Page

CHAPTER I

INTRODUCTION

For the past decade, the focus of the D.J. Darensbourg group has been enhancing the production of polycarbonates like polycyclohexylene carbonate and polypropylene carbonate through better catalyst design and environmentally friendly routes. Maintaining the tradition, for the first time, we center our attention to a completely different polycarbonate-Polytrimethylene Carbonate (PTMC).

This dissertation will investigate the two processes for making PTMC and our ability to increase their efficaciousness through better catalysts design - the more conventional route by the ring opening polymerization (ROP) of trimethylene carbonate and a novel one through the copolymerization of carbon dioxide and oxetane (Figure 1.1).

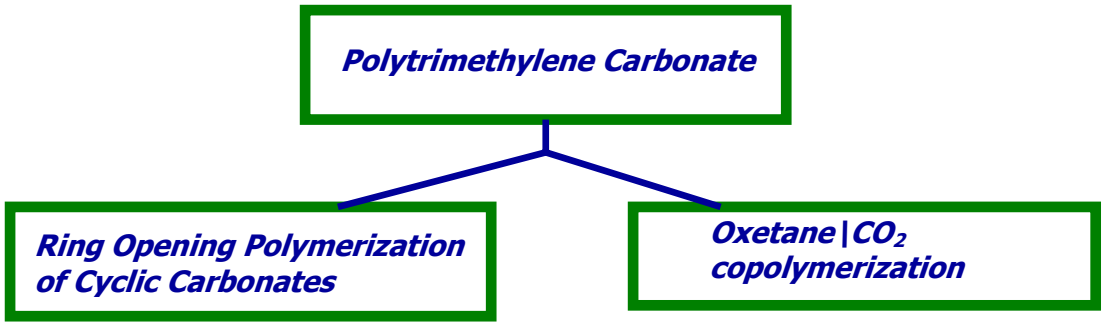

Figure 1.1: Routes for making polytrimethylene carbonate

This thesis follows the style of *Macromolecules*.

The industrial production of polycarbonates is accomplished by the interfacial polycondensation of phosgene and diols (Bisphenol A in case of General Electric's Lexan®). However phosgene is a highly toxic "nerve gas" and the reactions are carried out in a biphasic H_2O/CH_2Cl_2 solvent system (Figure 1.2).[1]

More recently another melt phase synthesis has been commercialized by GE, where Bisphenol A is reacted with diphenyl carbonate with phenol being the byproduct of the reaction.[2] Though a solvent free process, it requires a very high temperature of 300°C (in comparison to 40°C for interfacial polymerization) which results in an increase in the probability of side reactions along with the difficulty of removing the byproduct phenol completely from the system.

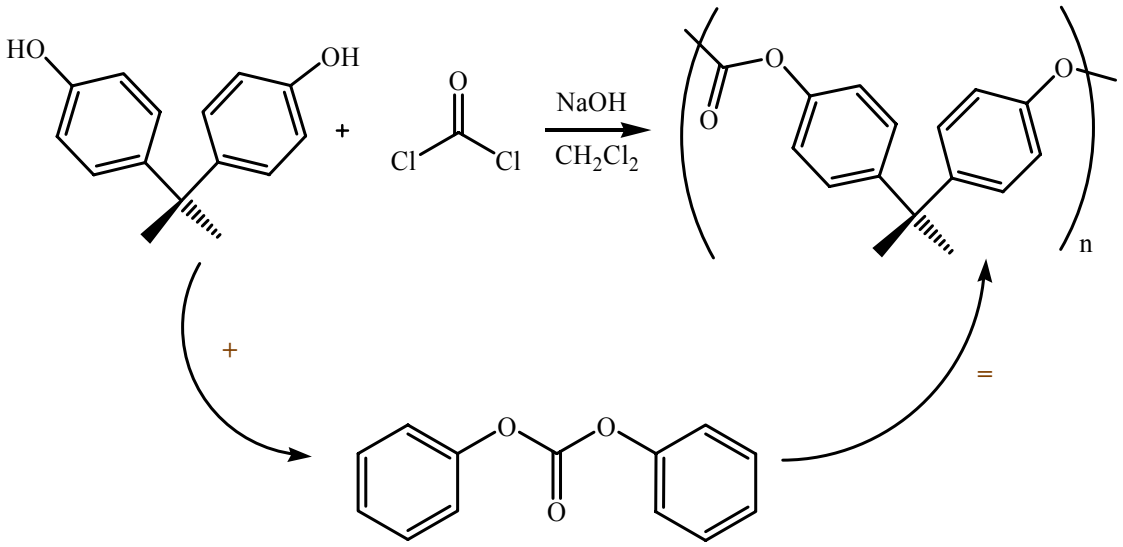

Figure 1.2: Industrial routes for synthesizing Bisphenol A polycarbonate

Hence there has always been an emphasis on the development of environmentally benign routes for making polycarbonates. The copolymerization of epoxide and CO_2 represents one such eco friendly way for making polycarbonates (Figure 1.3). For the last ten years the focus of our group has been designing efficient metal based catalysts for enhancing this process.

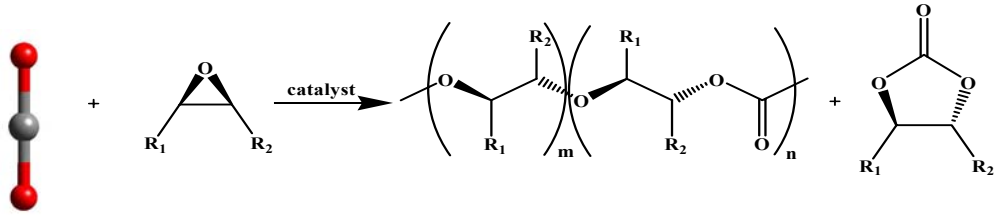

Figure 1.3: Copolymerization of epoxide and CO_2

The discovery of this process was made by Inoue, in 1969, who used a 1:1 mixture of diethyl zinc and water as catalyst.[3] However the high Lewis acidity of zinc resulted in consecutive ring opening of epoxide without CO_2 insertion. The first homogeneous catalyst for this process, developed by our group, was zinc based with bulk group in the 2,6 positions of the phenoxide ring.[4] The rate of the reaction was observed to be ten times faster than Inoue's catalyst. Over the years, most efficient catalysts designed by our group have been largely zinc based. Of late, the use of chromium salen catalysts in conjunction with a cocatalyst have surpassed all previous records of activities.[5] The rate of polymerization have increased exponentially along with > 99% CO_2 insertions and polydispersity indices ~ 1.0 (Figure 1.4).

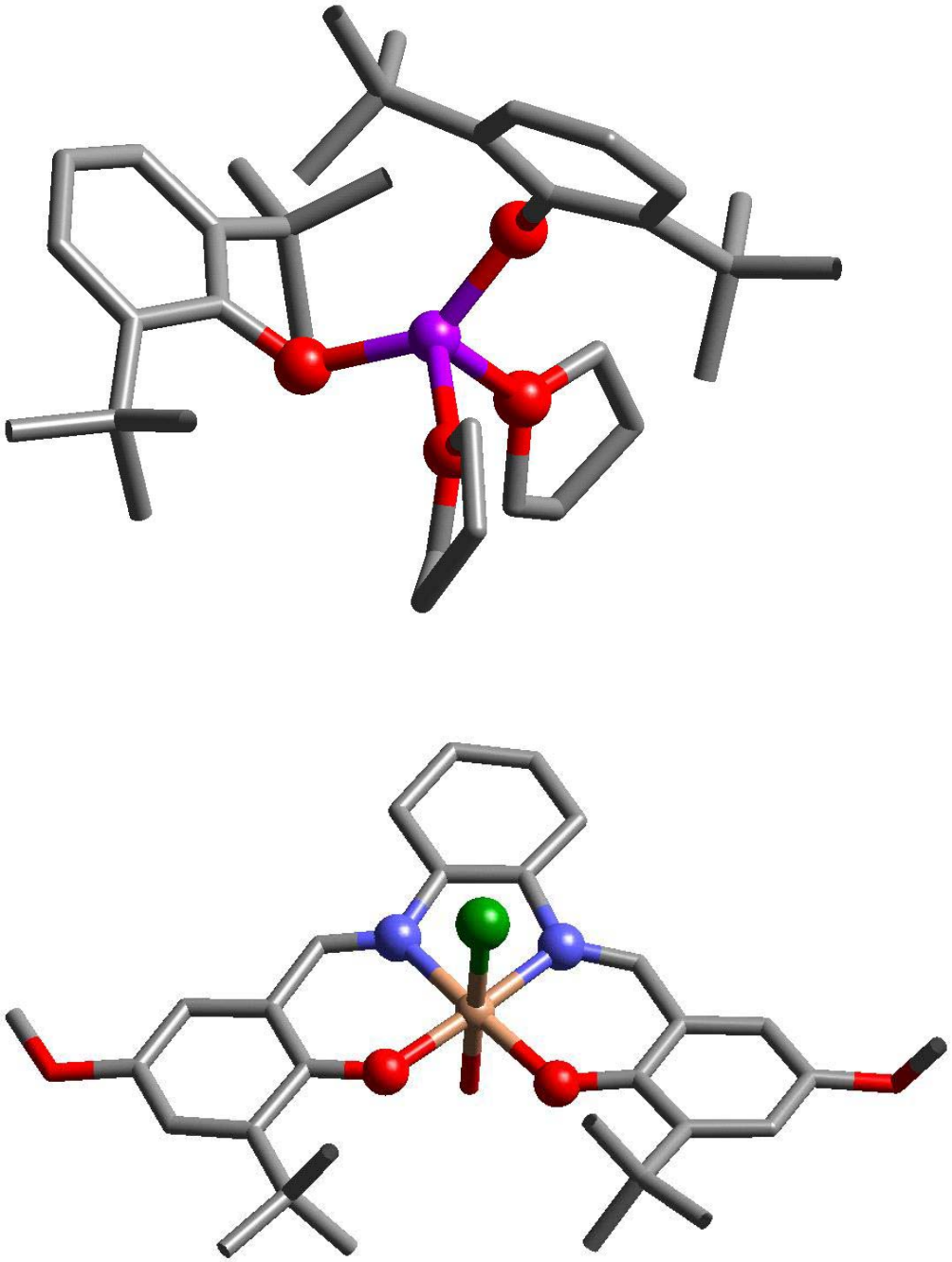

Figure 1.4: Efficient catalysts from the Darensbourg's group

Recently, we have decided to encompass an alternate environmentally friendly route of making polycarbonates into the realm of our research. Preparation of polycarbonates through the ring opening polymerization of cyclic carbonates is a very appealing process for obtaining high molecular weight polycarbonates. Though in the case of five membered cyclic carbonates, like propylene carbonate (Figure 1.5), polymerization is thermodynamically unfavorable, requiring high temperatures between 120°C-200°C and leading to a polymer with ether linkages due to the loss of CO_2.[6]

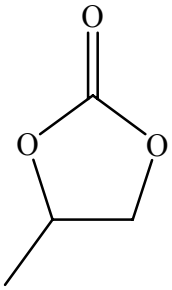

Figure 1.5:Skeletal representation of propylene carbonate

But, six or higher membered cyclic carbonates under certain conditions do give polymers free of any ether linkages at all even at moderate temperatures. A key focus of this dissertation will be the ring opening polymerization of one specific six membered cyclic carbonate-trimethylene carbonate (1,3–dioxan-2-one) (Figure 1.6).

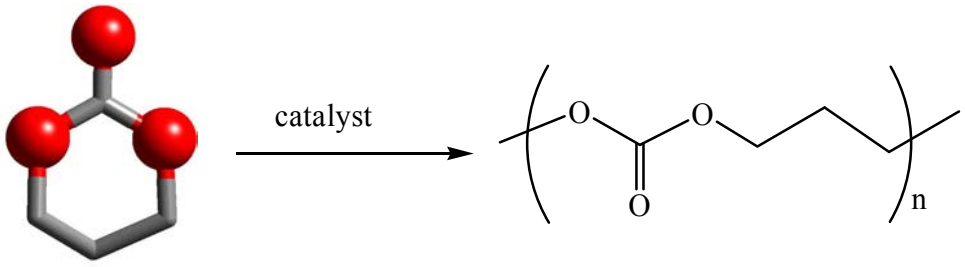

Figure 1.6 : Ring opening polymerization of trimethylene carbonate

Polytrimethylene Carbonate: Some Characteristic Properties

Polytrimethylene carbonate is an aliphatic polycarbonate. It falls in the useful class of biodegradable polymers and hence finds extensive applications in biomedical and pharmaceutical fields like sutures , drug delivery systems and tissue engineering.[7a,b] Infact out of the commercially available sutures, Maxon, (copolymer of glycolide and poly-TMC), introduced in 1985 and Caprosyn, (copolymer of lactide, ε-caprolactone, glycolide and poly-TMC), introduced in 2002 are very popular. Both these sutures are presently being produced by Syneture ™ a subsidiary of Tyco International. Other applications of PTMC include the preparation of scaffolds for the engineering of soft tissues such as heart muscle and the preparation of nerve conduits for guided nerve regeneration.[8]

Poly trimethylene carbonate is an amorphous polymer with a low glass transition temperature (T_g) of -14°C. High molecular weight PTMC shows good mechanical properties displaying high flexibility and tensile strength. When a sample of PTMC was implanted subcutaneously in rats, it showed a substantial weight loss during a six month period indicating enzymatic degradation.[9] One year after implantation the polymer had been completely resorbed and tissue at the site of implantation had completely regenerated.

Catalysts for the Ring Opening Polymerization of Trimethylene Carbonate

A summary of some of the widely used and active metal based catalysts will be presented in this section. Most of the activities have been expressed in percent yield of polymer . A small section has also been devoted to the use of enzymes as catalysts for this process. It is interesting to note, that catalyst development for the ring opening polymerization (ROP) of trimethylene carbonate is relatively recent area of research as compared to similar developments for lactides and lactones, even though the first polymer was obtained as early as the 1930s. Hence, few groups have dominated this area by their extensive research on a particular metal catalyst. Notable among them are the research groups of H.R. Kricheldorf (Germany), A. Albertsson (Sweden), Takeshi Endo (Japan), Richard Gross (USA) and Zhiquan Shen (China). For details regarding mechanistic research in this area the elegant review by G. Rokicki should be referred to.[10]

The first homopolymerization of TMC was conducted in the 1930s by Carothers and coworkers using potassium carbonate K_2CO_3 as the catalyst.[11a,b] However, the polymer obtained had a very low molecular weight of 4000kDa only. The interest in this project was rejuvenated by Kricheldorf and coworkers when he attempted to polymerize TMC with methyl triflate. However, he observed decarboxylation as a side reaction resulting in the formation of ether linkages.[12]

Following his work with methyl triflate, Kricheldorf and Schulz investigated boron halogenides. They found that boron halogenides may form crystalline complexes with TMC, but only complexes of BF_3 are active as initiators.[13] BF_3 initiated

polymerization gave high yields and molecular weights , but the resulting polymer contained ether linkages with the fraction of ether linkages increasing with temperature. This observation and the acceleration of polymerization in polar solvents suggested a cationic mechanism. A similar trend was also observed by Albertsson and Sjoling in their study of BF initiated polymerization of trimethylene carbonate.[14]

Sn Based Catalysts

Sn catalysts have been investigated extensively by Kricheldorf and coworkers over the past decade. Our aim out here is to give a general description of the variety of Sn based catalysts used by this pioneering group over the years.

The work on boron halogenides was followed by a similar study using tin tetrachlorides.[15] Unlike boron, $SnCl_4$, $SnBr_4$ and SnI_4 all afforded polyTMC with yields above 90%. In case of $SnCl_4$ and $SnBr_4$, decarboxylation was observed whereas SnI_4 gave a polymer free of all ether linkages along with higher molecular weights.

The next study was based on alkyltin chlorides. Numerous $BuSnCl_3$, Bu_2SnCl_2 and Bu_3SnCl initiated polymerization was conducted in bulk.[16] Yields above 90% were obtained with all three initiators, but reactivites decrease in the order $BuSnCl_3$ > Bu_2SnCl_2 > Bu_3SnCl. The order of reactivity also follows the acidic strength of these compounds. Kinetic studies in chloroform and nitobenzene suggest that Bu_3SnCl initiates a cationic mechanism but unlike $SnCl_4$ does not cause decarboxylation.

$SnOct_2$ (Sn(II) 2- ethylhexanoate) is the most widely used initiator in the technical production of polylactides and copolyesters of lactic acid. A high efficiency and approval by FDA are keys factors attributing to its popularity. Its catalytic efficacy

for the polymerization of trimethylene carbonate was investigated by Kricheldorf.[17] $SnOct_2$ initiated polymerizations of TMC were studied either in concentrated chlorobenzene at 80°C or in bulk at temperatures ≥ 120°C. Benzyl alcohol added as a coinitiator accelerated the polymerization process and allowed a control of the number average molecular weight via monomer/initiator ratio as is evident from Figure 1.7.

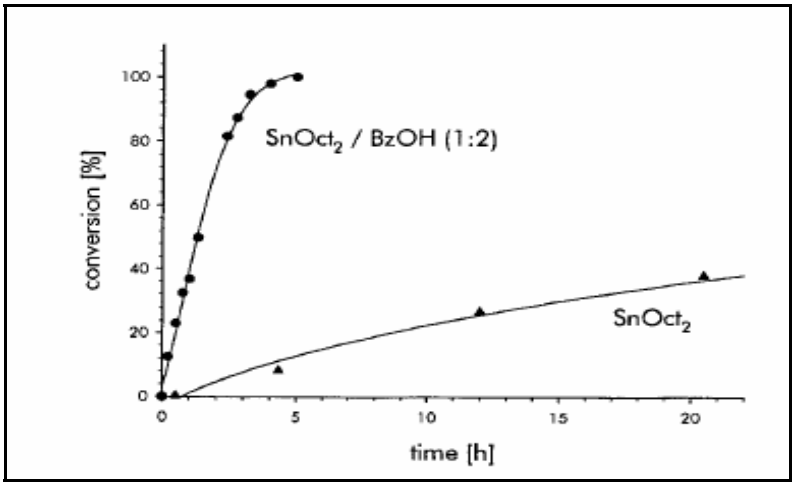

Figure 1.7: Time conversion curve of $SnOct_2$ initiated and Bzl-OH coinitiated polymerization of TMC

A similar study conducted with Bu_2SnOct_2 showed it to be a little less reactive than $SnOct_2$. [18] However, in this case the number average molecular weights did not parallel the monomer/initiator ratio indicating a complex polymerization mechanism.

An array of macrocyclic compounds of Sn have also been studied. They have all demonstrated high activities towards polymerization of trimethylene carbonate. Noteworthy are the use of 2,2-Dibutyl-2-stanna-1,3-dioxepane (DSDOP), Dibutyl Succinate and Dibutyl Adipate (Figure 1.8).[19,20] These macrocyclic tin based compounds are more reactive than their ethylhexanoate counterparts.

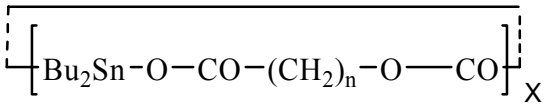

n= 2, X = 3, dibutyltin succinate

n= 4, X = 2, dibutyltin adipate

Figure 1.8: Generic structure of dibutyltin succinate and adipate

Rare Earth Complexes As Catalysts

The use of rare earth (III) metal halides as effective catalysts for polymerization of TMC was first investigated by Shen and coworkers.[21] The strong coordination of TMC on the rare earth ion induces the alkyl oxygen cleavage of TMC, indicating a cationic process. Polymerization is extremely fast and shows a complete absence of ether linkages.

The next catalyst of interest in this area were the lanthanide aryloxides, most commonly lanthanum tris(2,6-di-*tert* – butyl-4-methylphenolate) (Figure 1.9).[22] These lanthanum aryloxide compounds are extremely reactive towards the polymerization of TMC along with its other analog like DTC (2,2-dimethyltrimethylene carbonate). The polymerization is complete in 30 minutes at room temperature with a small amount of initiator ([monomer]:[initiator] = 1000). Shen has shown trimethylene carbonate to ring open via a route of acyl oxygen bond cleavage. Even in the case of DTC, a 97.9% yield was obtained in an hour maintaining the same M/I ratio at 15°C in toluene. The order of reactivity was found to be La > Nd > Dy ~ Y.[23]

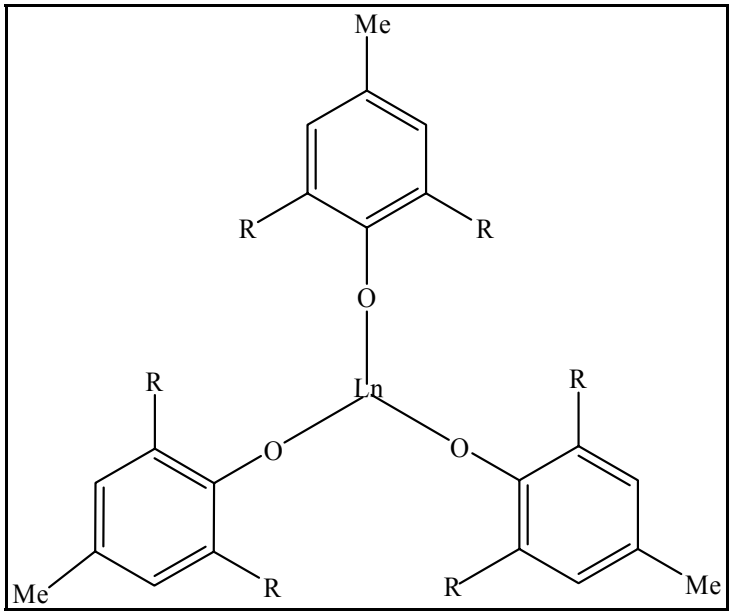

Figure 1.9:Generic diagram of $Ln(OAr)_3$

Among macrocyclic compounds, polymerization has been attempted with calix[8] arene –neodymium (Figure 1.10).[24] Under optimum conditions of M/I = 2000, 80°C and 16hrs polymer yield was 100%. A high dependence on the temperature was also found. The conversion and the molecular weight increases dramatically as temperature is increased from 50°C to 100°C. However, ether linkages were observed by ^{1}H NMR which indicate a cationic mechanism. In a more recent paper Shen and coworkers have compared the activities of *p-tert*-butyl calix [n] arene (n = 4, 6, 8) complexes of Nd, La, Y.[25]

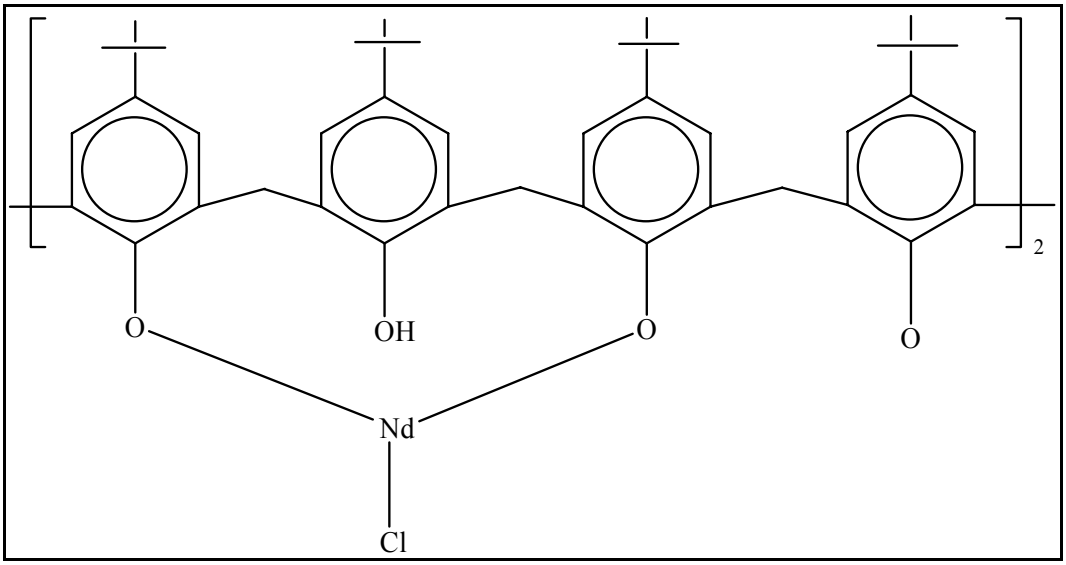

Figure 1.10: Shen's calix[8] arene-neodymium catalyst

Aggarwal and coworkers have reported the use of $LnCp_3$ complexes as well.[26] The order of activity was highly dependent on the size of the central metal atom Er ~ Gd > Sm> Pr > Ce. No decarboxylation was observed in the polymer chain. In a different publication the authors observed a system of SmI_2/Sm to be very active even at 70°C with a 80% yield of polymer after 15minutes only (M/I = 300).[27] Compounds like $Sm(C_5Me_5)_2(THF)_2$ and $SmMe(C_5Me_5)_2(THF)$ have been shown to be very active in homopolymerization of optically active *R*-1-Methyltrimethylene carbonate even at 0°C while lowering the temperature to -78°C resulted in no polymerization .[28]

Complexes of the type Ln-N instead of Ln-O or Ln-C were shown to be active by Zhou *et al.* by the study of a series of lanthanum gunidinate complexes $[RNC(NR'_2)NR]_3Ln$.[29] Both the substituents on the central metal atom as well the ligand shown an effect on the catalytic activity. The polymerization was found to be

first order in monomer concentration with the molecular weight of the polymer obtained increasing linearly with polymer yield. Mechanistic studies indicated a coordination insertion mechanism.

General Catalysts Used for the Polymerization of Trimethylene Carbonate

The polymerization of six membered cyclic carbonates like trimethylene carbonate (TMC) can be carried out by the use of both ionic and coordination initiators as well as enzymes. However polymers with high molecular weight, and therefore good mechanical properties , are obtained in the case of coordination polymerization. The idea of active initiators have undergone a change in the recent years from the typical tin based to more recently rare earth metals. However, there are still a few elements, which though active as initiators, deserve more extensive research and investigation. This section deals with some of those initiators both from the main group as well as transition metals.

Among the earliest papers on metal based initiators for polymerization of trimethylene carbonate are that of Albertsson and Sjoling.[14] A variety of initiators including $AlCl_3$, $Al(OiPr)_3$, $BF_3O(Et)_2$, $(Bu)_2SnO$, CH_3COOK and NaH were investigated for both melt and solution polymerization. They observed that the physical appearance of the polymer depended on the molecular weight. Low molecular polymers ($M_w < 6000$) were oily, viscous liquids containing mostly oligomers, whereas polymers with molecular weights between 6000 and 50,000 were soft and sticky. Materials with even higher molecular weights were more elastic and no longer sticky. All the Lewis acidic metals gave polymers with reasonably high molecular weights.

Hocker and coworkers have studied polymerization of DTC using porphyrin complex of aluminum (Figure 1.11).[30] It was shown that a halide (Cl) or alkyl (CH_3) attached to the aluminum were inactive for polymerization. Only alkoxy nucleophiles proved effective The reaction time was extremely slow at room temperature: after 100h only a 85% yield was obtained, though reaction time could be significantly reduced by increasing the temperature.

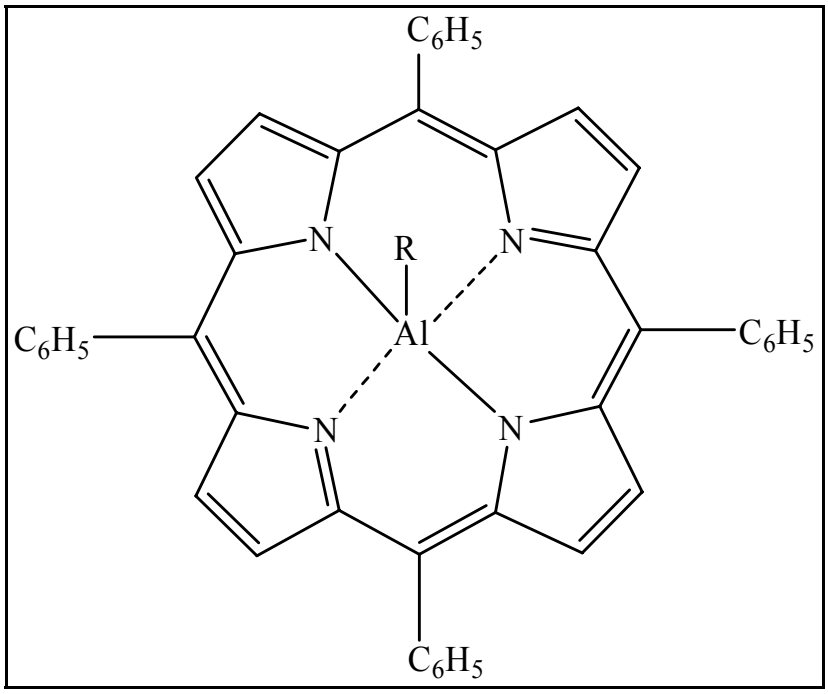

Figure 1.11: Generic structure of tetraphenyl porphyrin aluminum complex

Kricheldorf and coworkers reported the use of $TiCl_4$ for cationic polymerization of TMC.[31] Endo *et al*. have also observed the living polymerization of 1,3-dioxepan-2 one (7CC) with 2,2'-Methylenebis(6-*tert*-butyl-4methylphenolate) titanium dichloride as the catalyst (Figures 1.12 and 1.13). The molecular weight of the obtained polycarbonate could be controlled by changing the monomer:initiator ratio.[32] It is

appropriate to mention out here the use of another transition metal catalyst $Sc(OAr)_3$ by Shen and coworkers in their of copolymerization of TMC and ε-caprolactone.[33] They found that the rate of homopolymerization of TMC was comparable to that obtained in the case of organolanthanide compounds. Even at 0°C and M/I = 500 , the yield was as high as 69.9% in just 75 minutes in a solution of toluene.

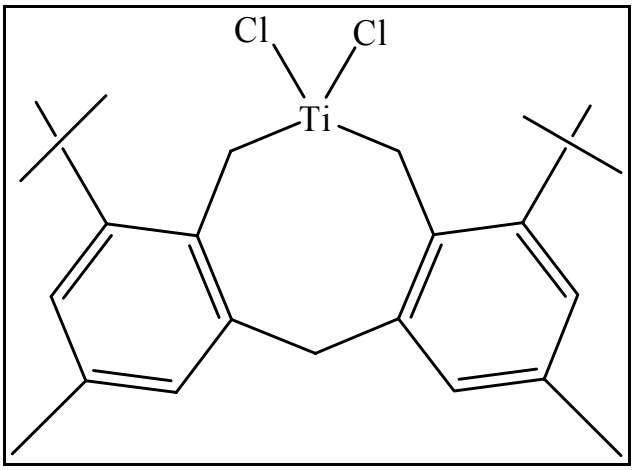

Figure 1.12: 2,2' methylenebis(6-tert-butyl-4-methylphenolate) titanium dichloride catalyst used by Endo

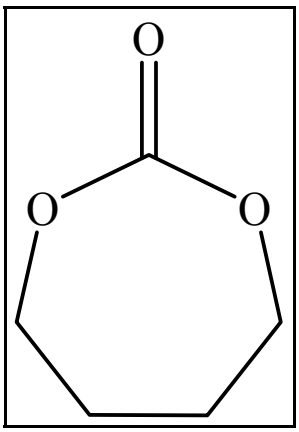

Figure 1.13: Generic strucure of 1,3-dioxepan-2-one (7CC)

The suitability of metal acetylacetonates as potential initiators have been tested by Dobryzynski *e. al.*[34] The attractiveness of acetylacetonates can be attributed to their ease of availability, relatively low price and easy storage. Low toxic metals like Zn (II), Fe (III) and Zr(IV) complexes were investigated. Though high conversions were obtained with all three complexes at 110°C, as shown in Figure 1.14 $Zn(acac)_2$ was the most effective catalyst as is evident from the graph which depicts the percent conversion of the monomer w.r.t each of the three catalysts as a function of time. .

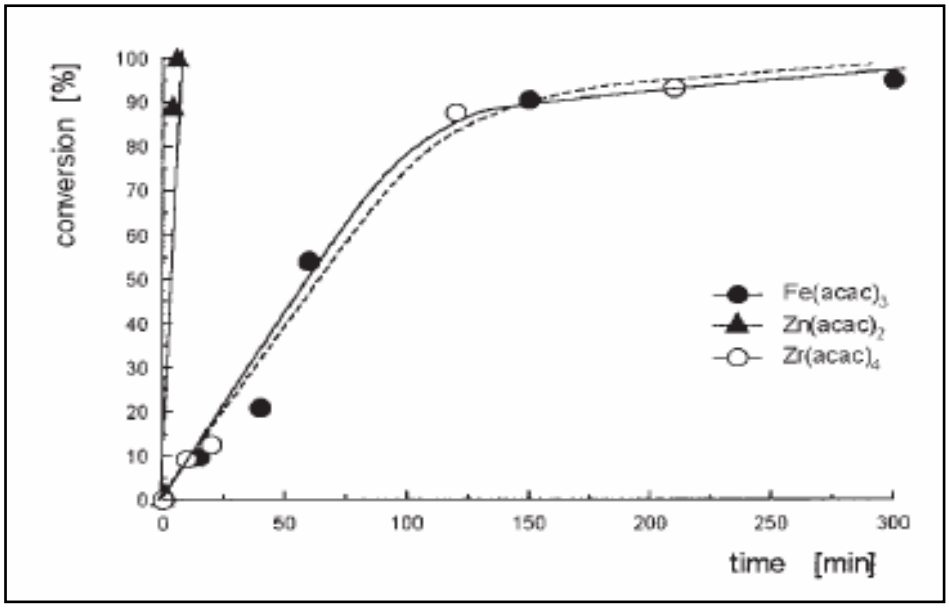

Figure 1.14: Comparison of the activities of the three catalysts as a function of % conversion and time

Enzyme Catalyzed Polymerization of Trimethylene Carbonate

A discussion on the available catalysts for the ring opening polymerization of trimethylene carbonate cannot be complete without a note on enzymatic polymerization. Polymerizations catalyzed by enzymes are fast emerging as a new synthetic method for polymer assembly. Enymatic polymerizations require relatively milder conditions than their chemical counterparts, besides enzyme catalysts are readily recyclable and biocompatible.

Matsumara *et al.* obtained high molecular weight poly trimethylene carbonate by using low quantities of porcine pancreatic lipase (PPL) as the catalyst at a reaction temperature between 60-100°C.[35] Gross and coworkers screened seven commercially available lipases for the bulk polymerization of TMC.[36] Novozyme-435 from *Candida Antarctica* was found to be the most active producing a polymer with no ether linkages due to decarboxylation. The highest molecular weight was obtained by conducting the reaction at 55°C. Interestingly, increasing the water content in these enzymes resulted and enhanced polymerization rates but decreased molecular weights. Bisht and coworkers have also shown the lipase Pseudomonas fluorescens to be active.[37]

Hence quite an extensive array of lipases have been screened for their catalytic efficiency for polymerization of trimethylene carbonate. Though enzymes do have a big advantage over their chemical counterparts due to their biocompatibility, activities obtained pale in front of commonly used chemical catalysts. Future efforts in this area is concentrated on designing new enzymes to optimize the yield of the polymer.

Conclusions

This section provides a summary of the most popular catalysts available today for the ring opening polymerization of trimethylene carbonate. Though the first homopolymerization of trimethylene carbonate was achieved in 1932, most of the research has been done in the past two and a half decades (Figure 1.15). Though the initial catalysts were simple initiators which underwent cationic initiation resulting in ether linkages in the polymer, presently emphasis is being laid on metal based initiators, where in most cases the ether linkages could be eliminated. Over this span of time, organolanthanide systems have overtaken tin based catalysts as being more active.

However, catalysts design and development for polymerization of trimethylene carbonate is still at a very nascent stage. Most of the catalysts utilized so far are simple commercially available Lewis acidic initiators. It is relevant to mention here, that for comparison we just need to look at the case of epoxide /CO_2 copolymerization reactions where turnover frequencies have skyrocketed from 1mol of epoxide consumed/mol catalyst-hr, (Inoue's catalyst 1969) to 760 mol of epoxide consumed /mol catalyst-hr (Cr-salen catalysts 2004), in a period of three and a half decades only. Hence, the future of catalysts design for polymerization of cyclic carbonate, should involve the use of structurally superior catalyst systems in an effort to enhance the reaction rates of polymerization - an issue we will to tackle in the pages of this dissertation.

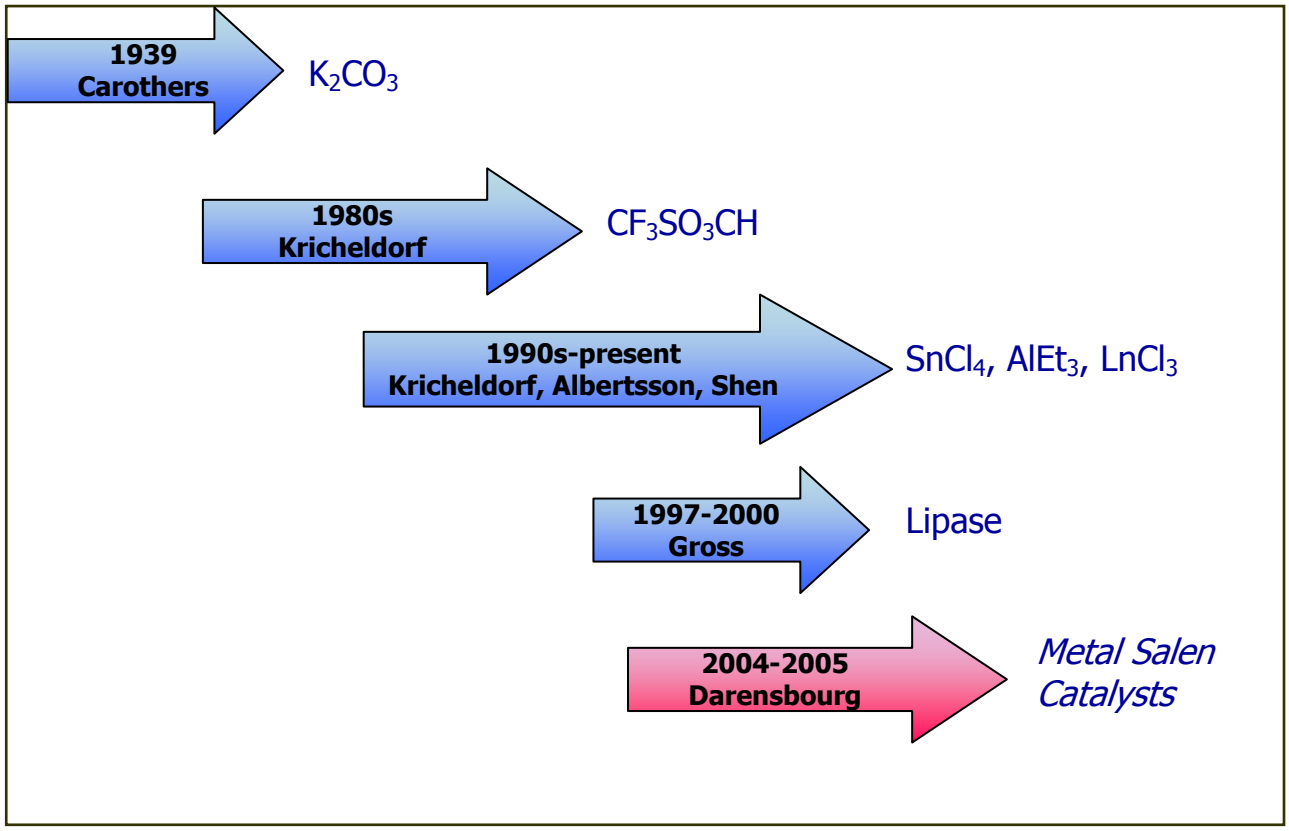

Figure 1.15: Timeline of catalyst development for the polymerization of trimethylene carbonate

CHAPTER II

RING OPENING POLYMERIZATION OF TRIMETHYLENE CARBONATE USING ALUMINUM (III) AND TIN (IV) SALEN CHLORIDE CATALYSTS*

Introduction

For several decades there has been much interest in the production of polycarbonates *via* the environmentally benign route of copolymerizing an epoxide and carbon dioxide. The intensity and success of efforts in this area have been greatly enhanced with the advent of effective homogeneous catalysts.[38] Unfortunately, the concomitant formation of the thermally stable five-membered ring cyclic carbonate from *aliphatic* epoxides and CO_2 has hindered the wide scale use of this approach.[5a] Although, there have been significant strides at developing better, more selective, catalysts for the coupling of propylene oxide and carbon dioxide to poly(propylenecarbonate), this still is a process which remains relatively underdeveloped.[39] An alternative pathway to aliphatic polycarbonates is the ring-opening polymerization (ROP) of six membered cyclic carbonates such as trimethylene carbonate. The analogous process involving five-membered cyclic carbonates affords polycarbonates with a significant quantity of ether linkages, e.g., the thermodynamically unfavored polymerization of propylene carbonate to poly(propylenecarbonate) is accompanied by a great deal of CO_2 loss.[40] However, it is possible under certain conditions to produce polycarbonates with no ether linkage, i.e., CO_2 loss, from six and higher membered cyclic carbonates (Figure 2.1).[13,15]

---

* Reprinted with permission from "Ring Opening Polymerization Of Trimethylene Carbonate Using Aluminum (III) And Tin (IV) Salen Chloride Complex" by D.J.Darensbourg, 2005. *Macromolecules,* 38, 5406-5410. © 2005 by American Chemical Society.

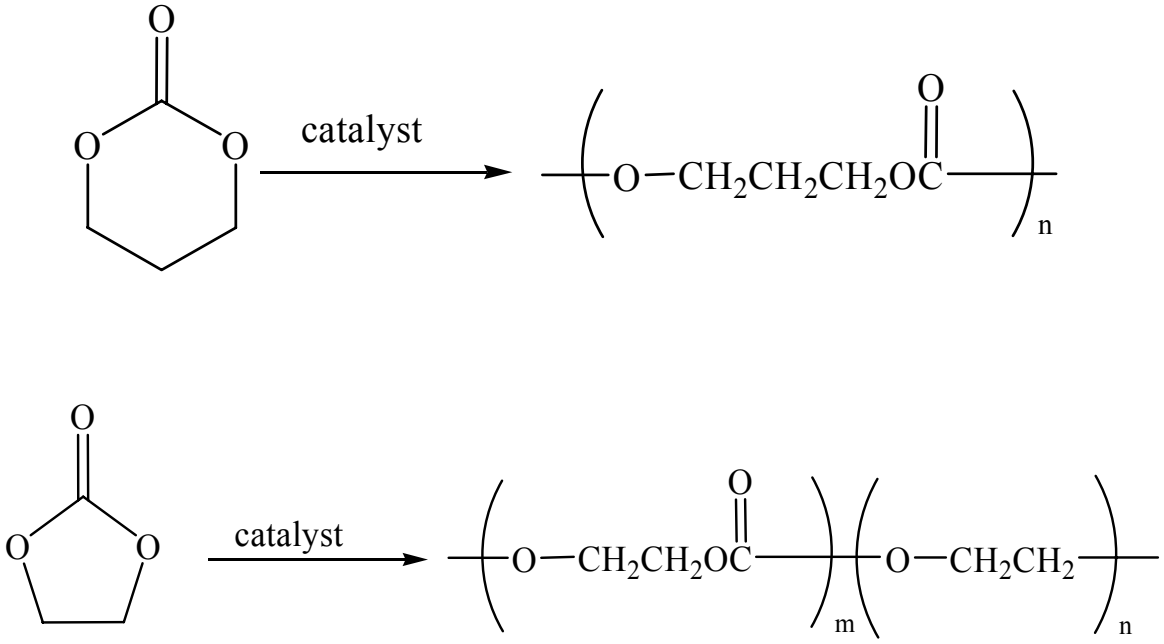

Figure 2.1: ROP of six and five membered cyclic carbonates

The polycarbonate derived from trimethylene carbonate (TMC or 1,3-dioxan-2-one) has been investigated quite extensively for its potential utilization as a biodegradable polymer in important biomedical and pharmaceutical applications, such as sutures, drug delivery systems, and tissue engineering.[7a,b] For the ROP of cyclic carbonates both cationic and anionic initiators have been shown to be effective.[13,41] Strong Lewis acids undergo cationic initiation to provide a polymer with ether linkages resulting from decarboxylation, where weaker Lewis acid initiate by an anionic mechanism providing polymer with 100% carbonate linkages.[42] Due to their Lewis acidic nature aluminum and tin salts have by far been the most popular catalysts for the ring-opening polymerization of trimethylene carbonate. However, thus far there has

been a marked absence of well-defined metal complexes employed as catalysts for this process.

Recently, our group has reported a variety of well-characterized metal catalysts systems for the copolymerization of cyclohexene oxide or propylene oxide and carbon dioxide. We have been able to optimize these reactions employing extremely robust metal salen complexes, with many of these systems affording copolymers with greater than 99% carbonate linkages and low polydispersity indices.[5b,43] This success has prompted us to examine the efficacy of such catalysts for the ring-opening polymerization of TMC.

Salen complexes are one of the most fundamental class of complexes in coordination chemistry today. The first salen complex was synthesized in 1933 by a condensation reaction of salicylaldehyde and ethylenediamine with various metal salts in a one-pot reaction.[44] Today more than 2,500 types of salen complexes have been synthesized and studied.[45] The key contributors to the popularity of the salen ligand is its ease of synthesis and the ability to modify and the sterics and the electronics of the ligand architecture by varying R_1,R_2 and R, to optimize a reaction (Figure 2.2).

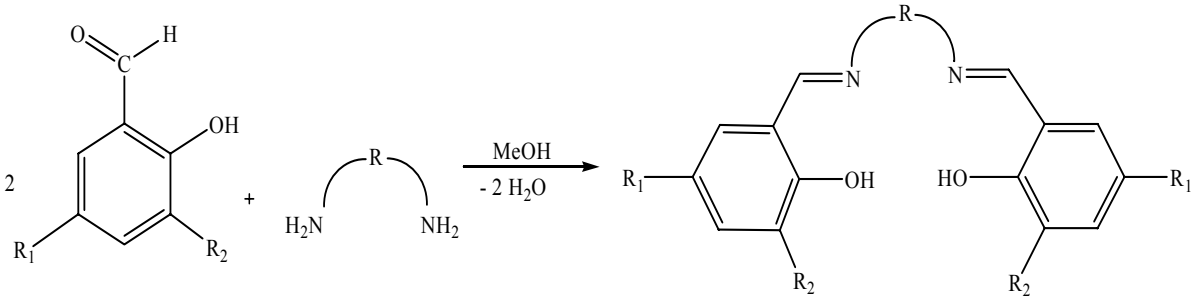

Figure 2.2: Skeletal representation of the sythesis of salen ligands

The discovery by Jacobsen and Katsuki of enentioselective epoxidation of unfunctionalized alkenes using chiral Mn(salen) complexes as catalysts intensified interest in these complexes as catalysts for prominent reactions.[46] Infact, today this reaction is used industrially for the production of the HIV protease inhibitor marketed by Merck. Today metal salen complexes are used extensively to catalyze a variety of reactions including asymmetric ring-opening of expoxides, epoxide\CO_2 copolymerization and cycloaddition of epoxide and CO_2 to synthesis of cyclic carbonates to name a few. Infact an elegant summary of these ligands and their various applications have been provided by Dr. Anssi Haikarainen in the dissertation titled ' Metal salen catalysts in the oxidation of lignin model compounds.'[47]

Relevant to our study, Cao and coworkers have recently reported the use of a novel salen aluminum alkoxide and its dimer to ring open trimethylene carbonate,[48a] and Chisholm has similarly demonstrated (salen)aluminum alkoxides to be effective catalysts for ROP of lactides.[48b] Herein, we have focused on Al(III) and Sn(IV) salen chloride compounds as catalysts for the ring opening polymerization of trimethylene carbonate. Efforts have been made to optimize the effectiveness of these catalysts by systematic variation of the electronics of the salen ligand. Figure 2.3 illustrates the generic structure of the Sn(IV) and Al(III) salen chloride complexes utilized in this study.

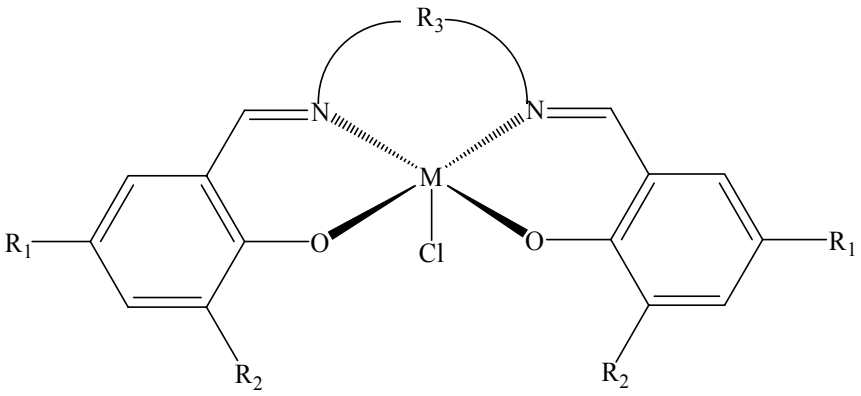

Figure 2.3: Generic diagram of a M salen chloride, where M=Al or SnY, R_2 and R_1 refers to the 3,5-positions of the phenolate rings respectively

Experimental Section

All syntheses were carried out under argon atmosphere using standard Schlenk and glovebox techniques. Acetonitrile was first dried by distillation into CaH_2 onto P_2O_5 followed by distillation onto CaH_2 and then freshly distilled from CaH_2 prior to use. Salicylaldehyde, ethylenediamine, and 1,2- phenylenediamine were purchased from Aldrich and used as received.

^1H NMR spectra were recorded on a 300 MHz Varian Unity Plus spectrometer. The spectra was calibrated using signals from the solvent and was reported downfield from $SiMe_4$

The methodology employed in the synthesis of the monomer is identical to that reported by Endo and coworkers using 1, 3 propanediol and ethylchloroformate.[49] The monomer was further purified by repeated crystallization in THF/diethylether.

All aluminum salen chloride catalysts were synthesized according to known literature procedures.[50-51]

General Synthesis of (salen)AlCl Complexes. A 50ml Schlenck flask was charged with 1.0 mmol of the H_2salen ligand and dissolved in 40ml of toluene. A 100ml Schlenk flask was charged with 1.0mmol of a 1.9M toulene solution of Et_2AlCl, and an additional 10ml of toluene was added. The ligand was cannulated into the flask containing the metal, and the mixture was stirred for 12h at room temperature. A yellow precipitate was observed. The reaction mixture was concentrated to ~10ml and approximately 30ml of hexanes was added to precipitate the product. The precipitate was collected by filtration and dried under vacuum.

Synthesis of {N,N-bis(3,5-di-chloro-salicylidene)-ethylene diimine} Sn(IV) Dichloride. $(Cl)_2salenH_2$ (0.406g, 1.0mmol) is dissolved with 20mL of THF in a 50mL Schlenk flask. The solution is transferred *via* cannula onto a 10mL THF suspension of KH (0.088g, 2.1mmol) in a separate 50mL Schlenk flask. Immediate evolution of H_2 gas is observed and the mixture is stirred 1h at room temperature to produce an orange solution of $K_2(Cl)_2$salen. A 50mL Schlenk flask fitted with a reflux condenser is charged with $SnCl_4$ (0.286g, 1.0mmol) and 10mL THF. The potassium salt solution is transferred *via* cannula onto the $SnCl_4$ mixture and refluxed overnight. The reaction mixture is cooled to room temperature, filtered, and the solvent removed *in vacuo*. The solid is washed with hexanes (2 x 20mL) to yield 0.275g of orange-yellow solid (46%). ^{1}H NMR (d_6-DMSO): δ = 4.18-4.29 (m, 4H, N-C*H*$_2$C*H*$_2$-N), 7.69(d, 2H, phenyl-*H*), 7.93(d, 2H, phenyl-*H*), 8.86(s, 2H, phenyl-C*H*=N).

Synthesis of {N,N-bis(3,5-di-chloro-salicylidene)-1,2-phenylene diimine} Sn(IV) Dichloride. (phen)$(Cl)_2$salenH_2 (0.300g, 0.66mmol) is dissolved with 20mL of THF in a 50mL Schlenk flask. The solution transferred *via* cannula onto a 10mL THF suspension of KH (0.053g, 1.32mmol) in a separate 50mL Schlenk flask. Immediate evolution of H_2 gas is observed and the formation of a deep red solution. The mixture is stirred 1h at room temperature and a red precipitate forms. The THF slurry transferred *via* cannula into a 50mL Schlenk flask fitted with a reflux condenser and charged with $SnCl_4$ (0.172g, 0.66mmol) in 10mL THF. The mixture is refluxed 3h to form a dark red-orange solution and a white precipitate. The reaction mixture is cooled to room temperature, filtered, and the solvent removed *in vacuo*. The solid is washed with hexanes (2 x 20mL) to yield 0.545g of orange solid (85%). X-ray quality crystals were grown by slow diffusion of pentane into a concentrated THF solution at -30°C over several days. ^{1}H NMR (d_6-DMSO): δ = 7.31-7.39(m, 2H, phenyl-*H*), 7.56-7.63 (m, 2H, N-phenyl-*H*), 7.92(d, 2H, N-phenyl-*H*), 8.21-8.24 (m, 2H, phenyl-*H*), 8.80 (s, 2H, phenyl-*H*), 9.57 (s, 2H, phenyl-C*H*=N).

Synthesis of {N,N-bis(salicylidene)-1,2-phenylene diimine} Sn(IV) (*n*-butyl)(chloride). (phen)salenH_2 (0.301g, 1.0mmol) is dissolved with 20mL of THF in a 50mL Schlenk flask. The solution transferred *via* cannula onto a 10mL THF suspension of KH (0.088g, 2.1mmol) in a separate 50mL Schlenk flask. Immediate evolution of H_2 gas is observed and the mixture is stirred 1h at room temperature to produce an orange solution of K_2(phen)salen. A 50mL Schlenk flask is charged with (Bu)$SnCl_3$ (0.283g, 1.0mmol) and 10mL THF. The potassium salt solution transferred *via* cannula onto the

(Bu)$SnCl_3$ and the mixture is stirred at room temperature overnight and the solvent removed *in vacuo*. The crude solid is extracted with CH_2Cl_2 (2 x 20mL). The filtrate is evaporated and the solid is washed with hexanes (2 x 20mL) to yield 0.460g of yellow-orange solid (87%). ^{1}H NMR: δ = 0.406 (t, 3H, CH_2-C*H*$_3$), 0.905-0.928 (m, 2H, CH_2-C*H*$_2$-CH_3), 1.21-1.23 (m, 2H, Sn-CH_2-C*H*$_2$ 1.37-1.38 (m, 2H, Sn-C*H*$_2$), 6.25-6.30 (m, 4H, phenyl-*H*), 6.56-6.59 (m, 4H, phenyl-*H*), 6.85-6.86 (m, 4H, N-phenyl-*H*), 7.47 (s, 2H, phenyl-C*H*=N). Elemental Analysis: Calculated for $C_{24}H_{23}N_2O_2SnCl \bullet CH_2Cl$ C: 49.18%, H: 4.13, N: 4.59; Found: C: 49.80%, H: 4.64%, N: 4.67%.

Kinetic Studies. TMC and the catalyst were weighed out in a schlenk flask in the desired monomer: initiator ratio followed by the addition of 10mL of dry solvent. The reaction vessel was placed into a preheated oil bath. The percent conversion of the monomer in time was calculated by manually sampling out a small aliquot of the solution, quenching it and analyzing by NMR.

Polymerization Runs. A typical melt polymerization run consisted of adding a 1g of the monomer to a previously flame dried schlenk flask. The monomer: initiator ratio was maintained at 350:1.The reaction was carried on at 95°C for 3h under argon atmosphere unless mentioned otherwise. The resulting polymer was purified by precipitation from dichloromethane, 5% HCl and methanol and then dried in vacuo. Turnover frequencies (mol of TMC consumed/mol of the catalyst-hr) were calculated by actually weighing the vacuum dried polymer.

Results and Discussion

We have examined several aluminum and tin(salen) chloride derivatives for the ring-opening polymerization of trimethylene carbonate, where the substituents in the 3,5-positions of the phenolate moieties were systematically varied. A typical melt polymerization run consisted of adding a 1.0 g of TMC to a previously flame dried Schlenk flask. The monomer: initiator ratio was maintained at 350:1, and the reaction was carried on at 95ºC for 3 h under an argon atmosphere, unless mentioned otherwise. The resulting polymer was purified by precipitation from dichloromethane, 5% HCl, and methanol and then dried *in vacuo*. Turnover frequencies (mol of TMC consumed/mol of the catalyst-hr) were calculated by actually weighing the vacuum dried polymer. All polymer runs show the complete absence of ether linkages even at high temperatures of 140°C.

However, monitoring the reaction posed a challenge. Our group has been using ASI ReactIR1000™ to monitor the epoxide/CO_2 copolymerization reactions by *in situ* infrared spectrometry (Figure 2.4a). However in our, the carbonyl stretch of both the monomer and the polymer occur at the position of 1750cm^{-1}. Hence we have had to depend on ^{1}HNMR solely for our studies which shows an upfield shift as the monomer converts to the polymer (Figure 2.4b).

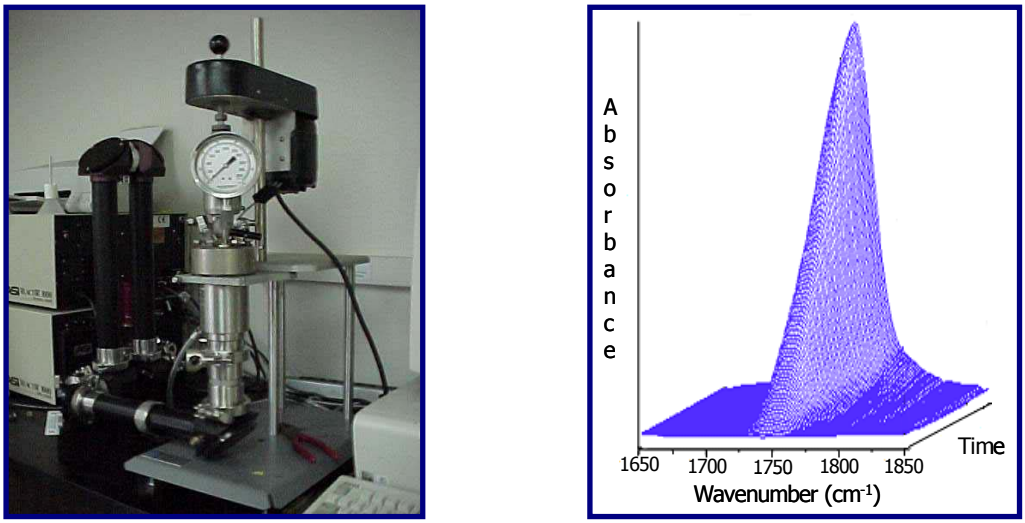

(a)

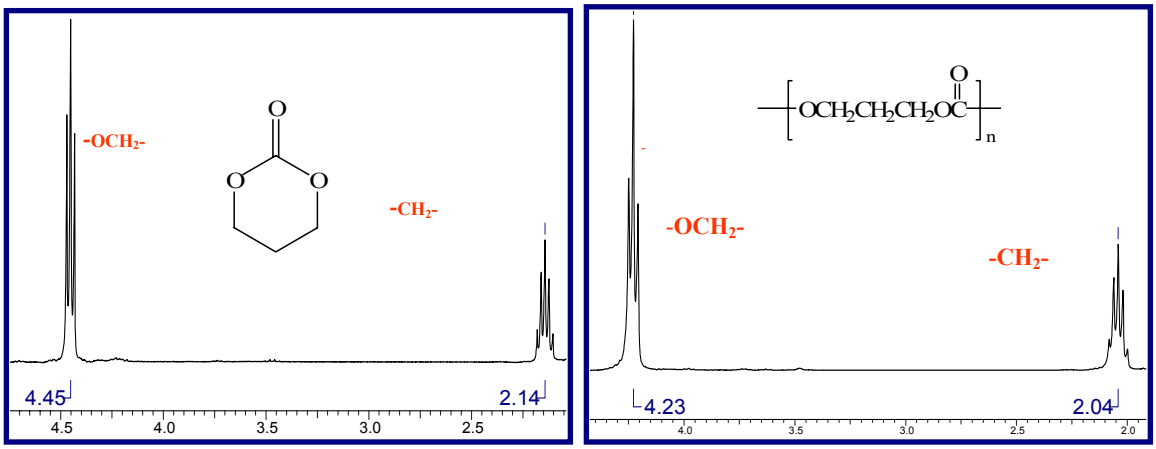

^{1}H NMR of TMC in $CDCl_3$ **^{1}H NMR of Poly-TMC in $CDCl_3$**

(b)

Figure 2.4: **(a)**: Monitoring the reaction by ASI ReactIR™ 1000. **(b)**. Monitoring the reaction by ^{1}HNMR

All (salen)AlCl derivatives examined successfully initiated the ring-opening polymerization of trimethylene carbonate, as shown in Table 2.1, though to varying extents. The most active catalyst was N,N'*bis*(3,5-dichlorosalicylidene) phenylenediimine aluminum(III) chloride. A steady increase in the monomer conversion was observed on substituting the 3 and 5 positions in the phenolate ring with a bulkier group such as *t*-butyl or chloro. A substantial increase, around 80%, in the catalytic activity is observed between entry 1 and 6 as depicted in Figure 2.5. Besides, these bulky substituents serve to enhance the solubility of the salen complexes. We have also attempted to optimize the catalytic activity of these derivatives by manipulating the salen backbone. An electron withdrawing backbone results in an increase in the activity as shown in Table 2.2. Although as is evident from the trend in Table 2.3, changes in backbone (21% increase from cyclohexylene to phenylene backbone).do not have as pronounced an effect on the performance of the catalyst as that of the substituents on the phenolate ring (80%) (Figure 2.6). Studies by Gibson and coworkers have indicated that increasing the electrophilicity of the metal center by adding electron withdrawing groups to the phenolate rings of the salen ligands increases the complexes ability to catalyze the ring-opening polymerization of (D,L)- and (L)-lactide at ambient temperature.[51] Our results are in coherence with those of Gibson's for lactide polymerization.

Table 2.1. Polymerization results on varying the substituents in the 3,5-positions of the phenolate rings for (salen)Al(III)Cl complexes containing a phenylene backbone.[a]

Entry	R_1	R_2	TOF[b]
1	H	H	45.5
2	H	Phenyl	46.6
3	H	*t*-butyl	49.6
4[c]	*t*-butyl l	*t*-butyl	72.3.
5	Cl	Cl	81.3

[a] Each reaction was performed in melt maintaining a monomer: initiator ratio (M/I) as 350:1at 95°C for 3h. [b] The TOF was determined by weighing the polymer after precipitating in 5% HCl and MeOH, and drying in a vacuum oven and is reported as mol of TMC / mol Al-h. [c] M_w = 26248 with a PDI of 1.66

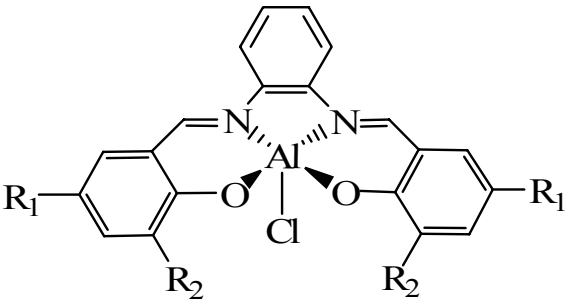

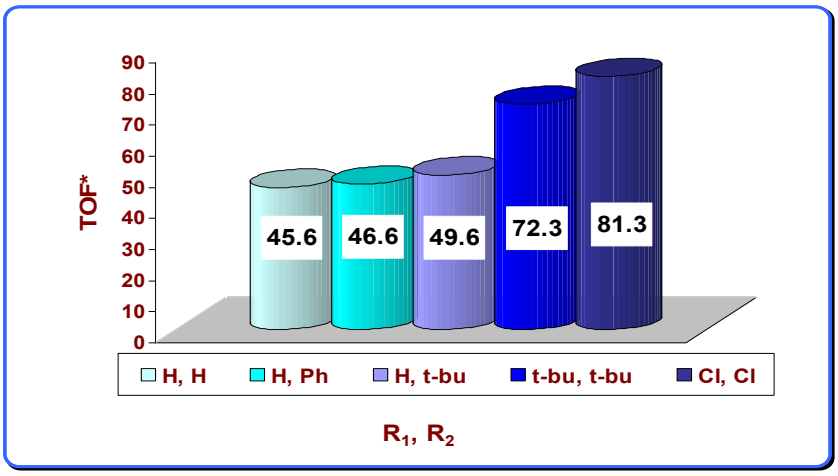

Figure 2.5: Effect of changing the ligands at the 3,5position of the phenolate ring

Table 2.2. Polymerization results for varying the backbone for (salen)Al(III)Cl complexes where the substituents in the 3,5-positions of the phenolate ring are *t*-butyl groups.[a]

Entry	R_3	TOF[b]
1	Cyclohexylene	59.5
2	Ethylene	62.6
3	Naphthalene	69.7
4	Phenylene	72.3.

[a] Each reaction was performed in melt maintaining a monomer: initiator ratio (M/I) as 350:1at 95°C for 3h. [b] The TOF was determined by weighing the polymer after precipitating in 5% HCl and MeOH, and drying in a vacuum oven and is reported as mol of TMC / mol Al-h.

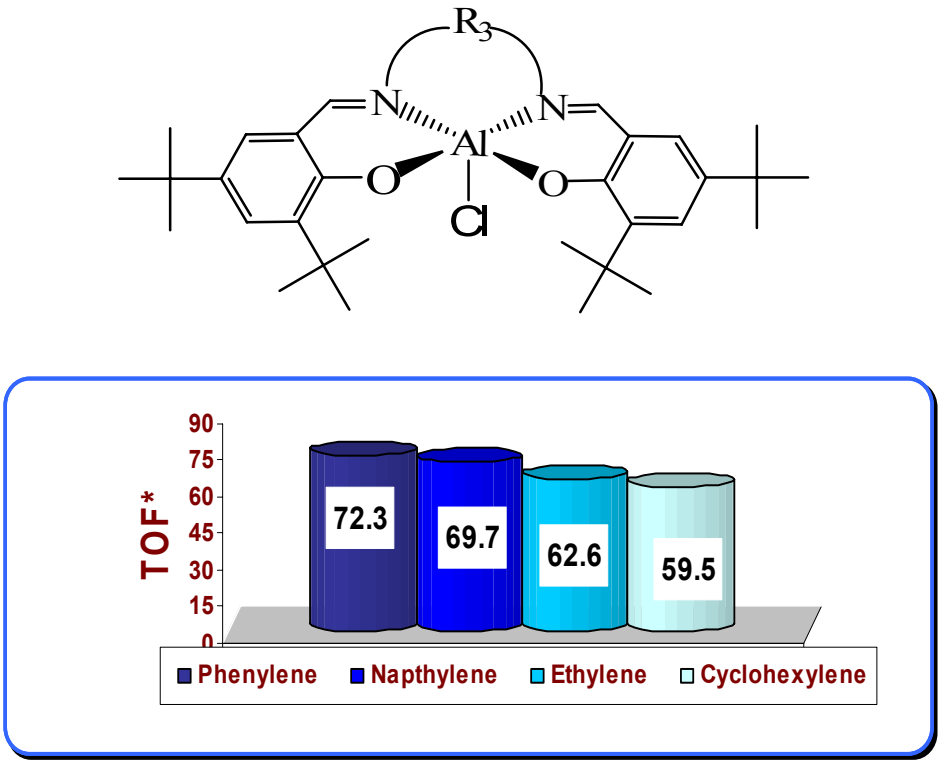

Figure 2.6: Effect of changing the backbone of the salen ligand

We also tried to extend our study to the change of the initiator. An aluminum salen like entry 4 (Table 2.3 and Figure 2.7) was synthesized with the ethoxide group (OEt) as the initiator. Melt polymerization was carried out for 2h at 90°C. A comparison of the TOF values indicated that, ethoxide is a better initiator than the chloride.

Table 2.3. Polymerization results for varying the initiator X for (salen)Al(III)X complexes containing a ethylene backbone where the substituents in the 3,5-positions of the phenolate ring are *t*-butyl groups.[a]

Entry	X	TOF[b]
1[c]	OEt	104.8
2	Cl	78.7

[a] Each reaction was performed in melt maintaining a monomer: initiator ratio (M/I) as 350:1at 90°C for 2h. [b] The TOF was determined by weighing the polymer after precipitating in 5% HCl and MeOH, and drying in a vacuum oven and is reported as mol of TMC / mol Al-h. [c] M_w = 23986 with a PDI of 1.61

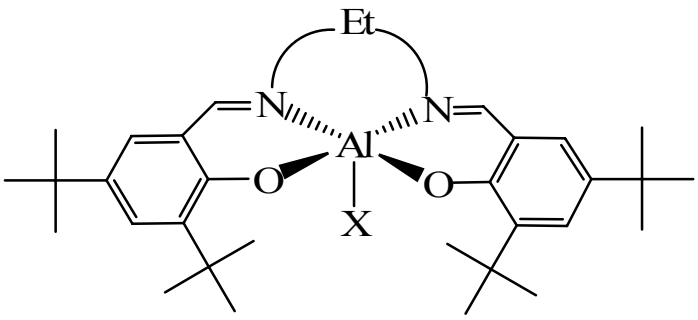

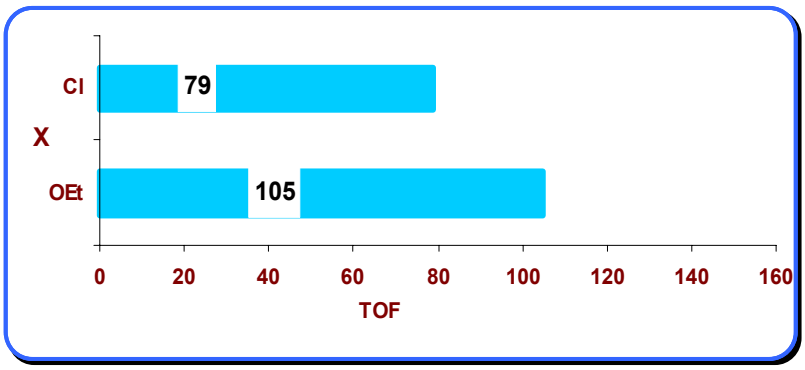

Figure 2.7: Effect of changing the initiator (salen)Al(III)X complexes

Cyclic carbonates like TMC have traditionally been polymerized using a variety of tin-based initiators like tin(IV) tetrahalides and tin(II) octanoate. The polymerization runs, employing tin(IV) salen derivatives were carried out under the same conditions as their aluminum counterparts. Though the tin compounds do ring open trimethylene carbonate, as is evident from Table 2.4 and Figure 2.8, the activity is much reduced. {N,N'-*bis*(3,5-dichloro-salicylidene)-1,2-phenylene diimine} Sn(IV) dichloride, (entry 3, Table 2.4) our most active tin salen shows a turnover frequency of 22, a reduction in activity by one-fourth in comparison to the corresponding aluminum catalyst (entry 6, Table 2.1). It should be noted that the dependence of activity on the electronics of the salen structure follows the same trend seen for aluminum. Hence, an increase in the Lewis acidity of the metal center corresponds to an increase in the rate of polymerization.

Table 2.4. Polymerization results for (salen)Sn(X)Y complexes.[a]

Entry	R_1	R_2	backbone	Y	X	TOF[b]
1	H	H	phenylene	*n*-Butyl	Cl	13
2	Cl	Cl	ethylene	Cl	Cl	17
3	Cl	Cl	phenylene	Cl	Cl	22

Each reaction was performed in melt maintaining a monomer: initiator ratio (M/I) as 350:1at 95°C for 3h.
[b] The TOF was determined by weighing the polymer after precipitating in 5% HCl and MeOH, and drying in a vacuum oven and is reported as mol of TMC / mol Snl-h..

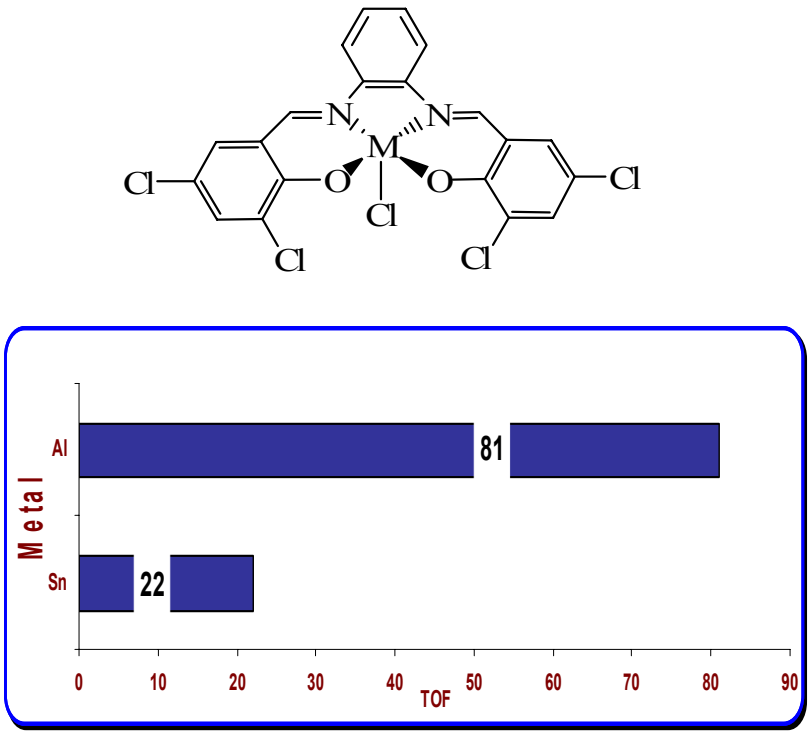

Figure 2.8: Comparison of turnover frequencies of Al(III) and Sn(IV) salen

Though detailed mechanistic study was not an aim of our investigation, our preliminary results indicate a "coordination–insertion" mechanism, which proceed by the coordination of the monomer to the active metal species followed by its insertion into the metal-nucleophile bond. All kinetic studies have been conducted using {N,N-bis(salicylidene)-1,2-phenylene diimine} Al(III)(chloride) . The rate of polymerization in a weakly polar solvent like toluene (dielectric constant 2.4) was found to be 4.1 times faster than 1,1,2,2,tetrachloroethane (TCE) (dielectric constant 10.8) indicating a coordination mechanism (Figure 2.9). The linear time dependence of the semi-logarithmic plot of $\ln(A-A_0)/(A-A_t)$ also demonstrates that the polymerization is first order in monomer under the conditions used in this study.

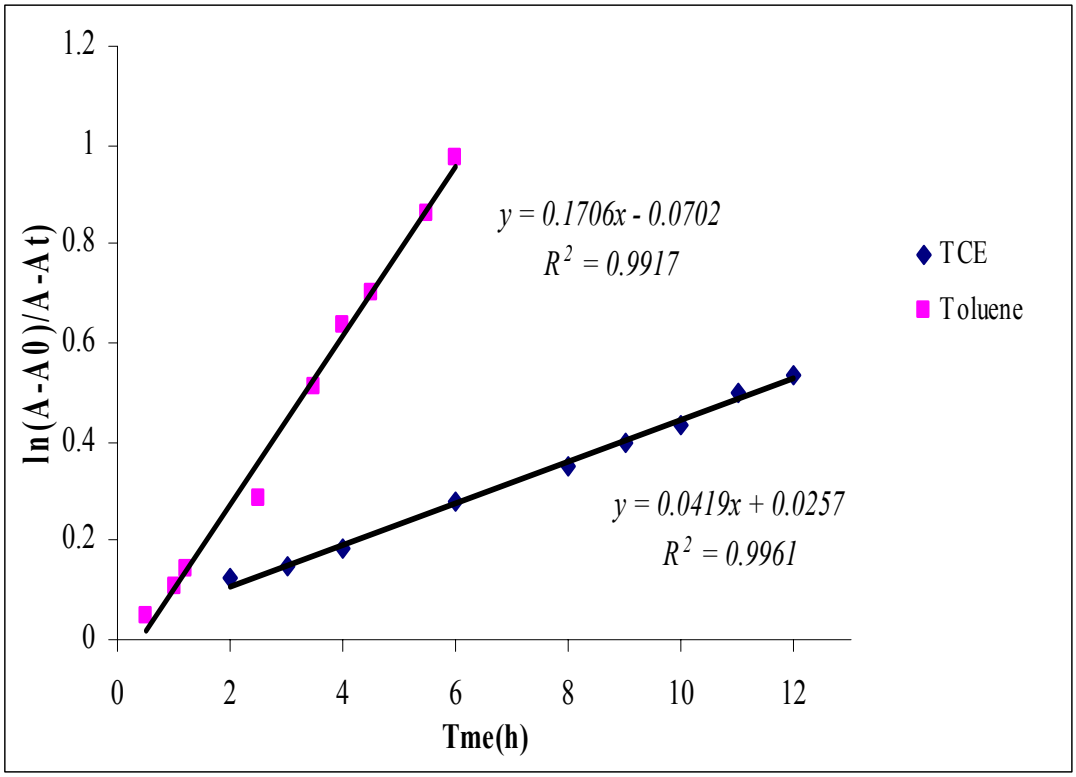

Figure 2.9: Rate of polymerization in Toluene vs. 1,1,2,2,-Tetrachloroethane (TCE) as monitored by NMR while maintaining the monomer: catalyst as 15:1 at 80°C.

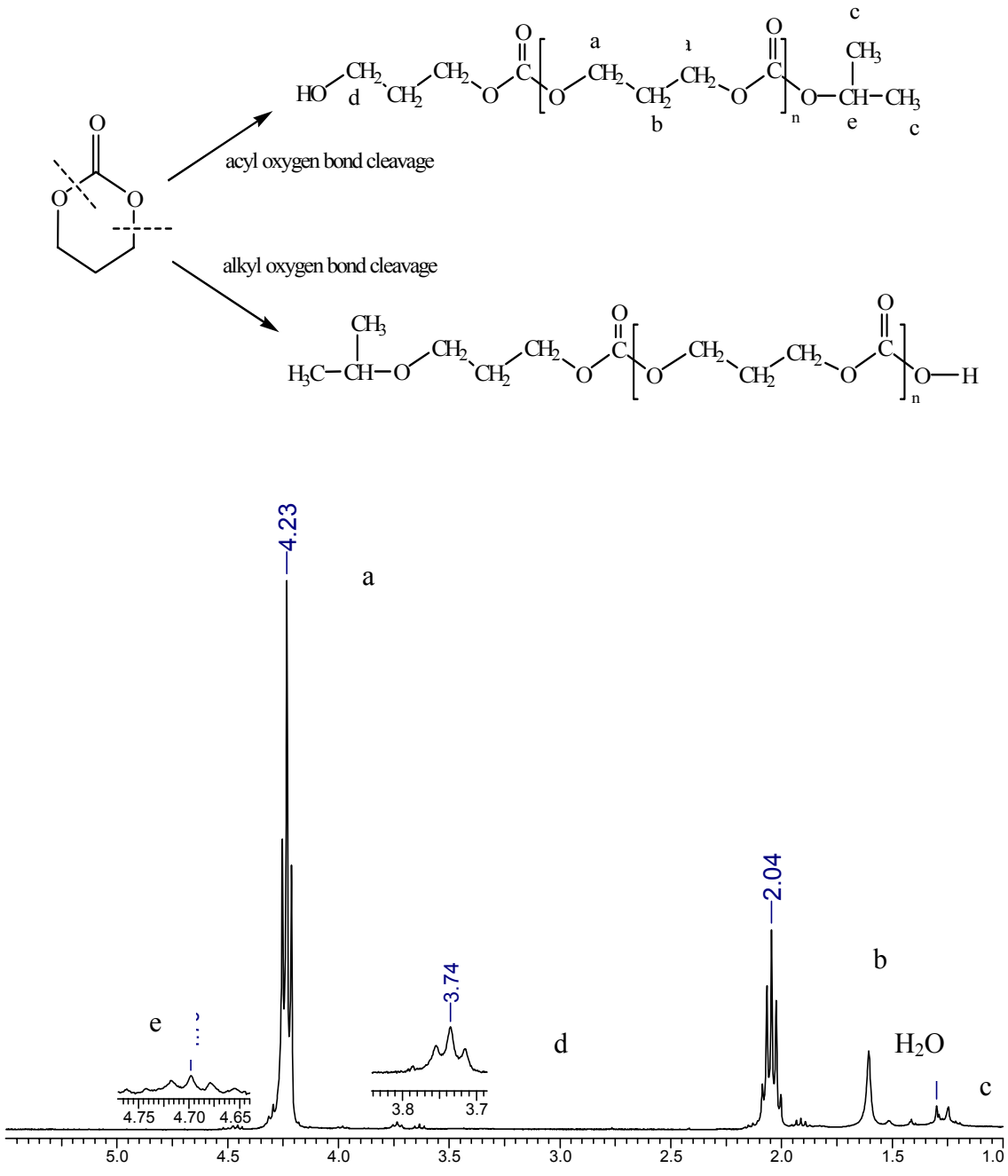

Figure 2.10: Sample of poly (trimethylene carbonate) terminated by isopropanol in $CDCl_3$

A sample of low-molecular weight polyTMC terminated by 2-propanol exhibited peaks in the ^{1}H NMR spectra consistent with this mechanism as predicted by Shen and coworkers, that is, the monomer inserts into the growing polymer chain *via* acyl-oxygen bond cleavage (Figure 2.10).[23]

To get a better insight into the TMC polymerization by these metal salen complexes , the kinetics was studied in TCE by NMR. Table 2.5 summarizes the rate constants at various concentrations of the catalysts and temperatures. All runs in Table 2.5 have been conducted by dissolving the catalyst in 10mL of 1,1,2,2-tetrachloroethane (TCE). TCE is a chlorinated solvent with a high boiling point of 147°C. Both the monomer and the polymer are soluble in TCE even at high conversions (unlike toluene) thus enhancing the ease of monitoring. The rate of polymerization was found to be first order in both monomer and catalyst concentration (Figure 2.11). Activation parameters $\Delta H^{\neq}$= 51 KJ/mol and $\Delta S^{\neq}$= -141J/mol were calculated from the Eyring plot of ln(k/T) vs. (1/T) (Figure 2.12).

Table 2.5. Polymerization rate constants using {N,N-bis(salicylidene)-1,2-phenylene diimine} Al(III)(chloride) as the catalyst.

Entry[a]	[Al](mol\l)	Temperature (°C)	k(mol\lsec)
1	0.0047	95	0.0057
2	0.0064	95	0.0070
3	0.0082	95	0.0093
4	0.0119	95	0.0126
5	0.0135	95	0.0149
6	0.0135	80	0.0085
7	0.0135	110	0.0369
8	0.0135	125	0.0771
9	0.0135	140	0.1087

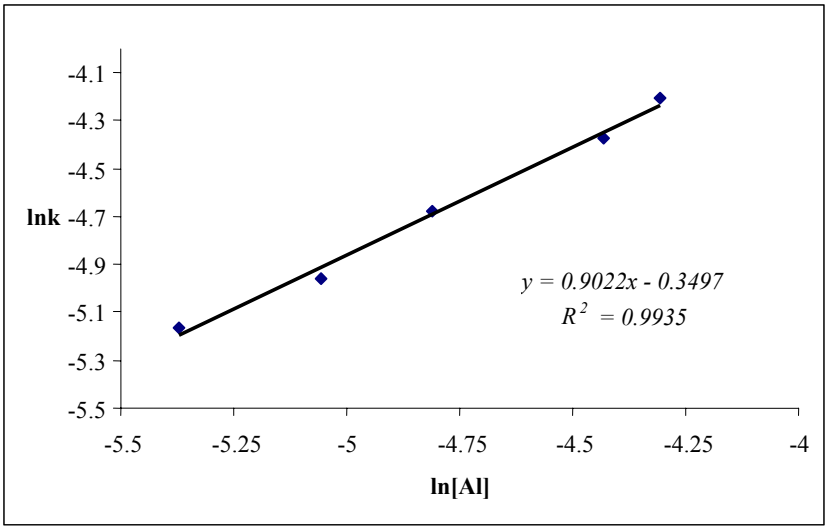

Figure 2.11. Plot of ln k vs. ln[Al]

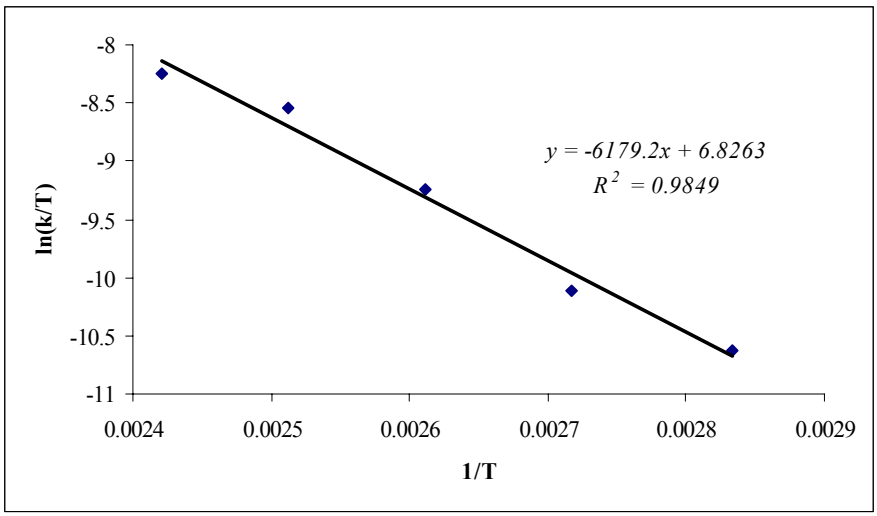

Figure 2.12: Eyring plot

Conclusions

In this chapter we have demonstrated that salen derivatives of Al(III) and Sn(IV) are effective catalysts for the ring-opening polymerization of trimethylene carbonate to afford polycarbonates with *no* ether linkages. We have been able to optimize the catalytic activity of these metal complexes by manipulating the salen structure. Our results indicate that an electron withdrawing, sterically unencumbering salen backbone enhances the activity of both aluminum and tin salen derivatives. A significant decrease is observed in the performance of Sn(IV) compounds in comparison to the Al(III) complexes which can be attributed to the reduction in Lewis acidity of the metal center, even though $SnCl_2$ and $Sn(Oct)_2$ are the commonly utilized catalysts commercially.

No ether linkages were observed in the polymer samples even at high temperatures of 140°C. The ether linkages usually appear as a triplet at 3.43ppm on the

^{1}HNMR spectra. A polymer of M_w of 27,000 and PDI of 1.63 was obtained from the most active aluminum salen catalyst.

CHAPTER III

THE USE OF Ca(II) SALEN COMPLEXES FOR THE RING OPENING POLYMERIZATION OF TRIMETHYLENE CARBONATE

Introduction

Continuing the discussion from the previous two chapters, we have seen that **a**liphatic polycarbonates, obtained from polymerization of cyclic carbonates, and their copolymers are slowly gaining popularity in a number of biomedical and pharmaceutical applications due to their biodegradable nature. These cyclic carbonates have also been recognized as 'a novel class of monomers' showing expansion in volume on polymerization.[52] The polymerization of trimethylene carbonate (TMC or 1,3-dioxan-2-one) can be carried out with the use of both ionic and coordinated initiators as well as enzymes. Our recent success with the use of well defined and characterized trivalent aluminum salen complexes as catalysts for the ring opening polymerization of TMC, generated interest in the utility of biometals as catalysts for this process.[53] Due to the difficulty in removing trace amounts of catalyst residues from the polymer, organometallic complexes based on non toxic biometals would be an ideal option.

For the purpose of our investigation we have chosen salen complexes of zinc, magnesium and calcium. These three elements are among the thirty-five key minerals present in the human body. While both calcium and magnesium are macrominerals with 1200mg and 35mg being present in human body in a 70kg human, zinc is micromineral with approximately 2g being present in the body.

Organozinc, calcium and magnesium compounds have also proved to be active catalysts for polylactide production. The β-diiminate zinc complexes developed by Coates have shown rapid living polymerization of *rac*-LA at room temperature [54] More recently Chisholm and coworkers have compared a series of monomeric amide and aryloxide tris-pyrazolyl borate complexes of calcium, magnesium and zinc to investigate their efficacy for polymerization of lactides.[55] Feijan and coworkers have investigated the of calcium alkoxides generated *in situ* for similar kind of polymerization.[56] Bu_2Mg have been used as a catalyst for ring opening polymerization of DMC (2,2-Dimethyltrimethylene carbonate) by Keul *et al*.[57] In a recently published article Dobrzynski and coworkers have used acetylacetonate complexes of zinc, iron and zirconium to investigate polymerization of both TMC and DMC.[34]

A coinitiator is essential for M^{2+} salen systems since they do not have a nucleophile attached unlike the M^{3+} systems. Usually diols and alcohols have been used for such kind of chemistry. Our group has achieved excellent results with the use of anionic cocatalysts in the case of epoxide / CO_2 copolymerization.[58] Hence, we decided to investigate the use of such catalysts with our M^{2+} salen catalyst systems, which will be presented in this chapter.

Experimental

Unless otherwise specified, all manipulations were performed using a double manifold Schlenk vacuum line under an atmosphere of argon or an argon filled glovebox. Toluene and tetrahydrofuran were freshly distilled from sodium/benzophenone. Acetonitrile was first dried by distillation from CaH_2 onto P_2O_5

followed by distillation onto CaH_2 prior to use. Both CH_2Cl_2 and 1,1,2,2-tetrachloroethane (TCE) were freshly distilled from P_2O_5. Trimethylene Carbonate was purchased from Boehringer Ingelheim. It was recrystallized from tetrahydrofuran and diethyl ether, dried under vacuum and stored in the glovebox. Potassium hydride was purchased from Aldrich as a mineral oil emulsion, washed with hexanes (3 x 30mL), and dried under vacuum prior to use. Salicylaldehyde, ethylene diamine, 1,2-phenylenediamine and 1,2-napthylene diamine were purchased from Aldrich and used as received. The corresponding salen ligands were synthesized according to literature procedure.[59] The synthesis of magnesium and zinc salens have been previously described in literature.[60a,b] PPN^+Cl^- (bis(triphenylphosphoranylidene)ammonium chloride) were purchased from Aldrich and recrystallized dichloromethane/ether before use, and $PPN^+N_3^-$ was synthesized according to published procedure.[61] Tetra-*n*-butylammonium halides (Aldrich) were recrystallized from acetone/ether twice before use. Tetra-*n*-butylammonium azide (TCI) was stored in the freezer of the glovebox immediately upon arrival. ^1H NMR spectra were recorded on Unity+ 300MHz and VXR 300MHz superconducting NMR spectrometers. Infrared spectra were recorded on a Mattson 6021 FT-IR spectrometer with DTGS and MCT detectors. Analytical elemental analysis was provided by Canadian Mircoanalytical Services Ltd. Molecular weight determinations (M_w and M_n) were carried out at the New Jersey Center for Biomaterials, Rutgers University.

General Synthesis of Ca(II) (salen) Complexes. H_2Salen (1.0 eq.) and NaH (5 eq.) were dissolved in THF. After stirring at room temperature overnight, extra NaH was

filtered and sodium salt was transferred *via* cannula through a medium porosity frit packed with Celite to a schlenk flask containing CaI_2(1.1 eq.). The reaction mixture became clear and stirred at room temperature overnight. THF was removed under low pressure and dichloromethane was added to the reaction mixture followed by filtration to remove NaI. The desired complex after removing dichloromethane was dried in *vacuo*.

Synthesis of {N,N-bis(3,5-di-*tert*-butyl-salicylidene)-ethylene diimine} Ca (II). Using the general method, 0.492 g of N,N'-*bis*(3,5-di-*tert*-butylsalicylidene)-1,2-ethylenediimine (1.0 mmol) and 0.322 g of CaI_2 (1.1 mol) were dissolved in 30 ml of THF. The final product was a pale yellow solid (0.522 g, 98 % yield). Elemental analysis calculated (%) for $C_{32}H_{46}N_2O_2Ca$: C, 72.41; H, 8.74; N, 5.28; found: C, 66.79; H, 8.65; N, 4.97. ^{1}H NMR ($CDCl_3$, 300 MHz); δ 8.20(s, CH=N, 2H), 7.26(d, 2H), 6.94(d, 2H), 3.81(s, NH_2, 4H), 1.56(s, 18H), 1.35(s, 18H).

Synthesis of {N,N-bis(3,5-di-*tert*-butyl-salicylidene)-1,2-phenylene diimine} Ca(II). Using the general method, 0.275 g of N,N'-*bis*(3,5-di-*tert*-butylsalicylidene)-1,2-phenylenediimine (0.50 mmol) and 0.162 g of CaI_2 (0.55 mol) were dissolved in 20 ml of THF. The final product was a yellow solid (0.272 g, 94 % yield). Elemental analysis calculated (%) for $C_{36}H_{46}N_2O_2Ca$: C, 76.39; H, 7.69; N, 4.45; found: C, 66.77; H, 7.58; N, 4.26. ^{1}H NMR ($CDCl_3$, 300 MHz); δ 8.64(s, CH=N, 2H), 6.94-7.27(m, 8H), 1.43(s, 18H), 1.25(s, 18H).

Synthesis of {N,N-bis(3,5-di-*tert*-butyl-salicylidene)-1,2-napthylene diimine} Ca(II). Using the general method, 0.304 g of N,N'-*bis*(3,5-di-*tert*-butylsalicylidene)-1,2-naphthylenediimine (0.50 mmol) and 0.162 g of CaI_2 (0.55 mol) were dissolved in

20 ml of THF. The final product was a brown solid (0.292 g, 93 % yield). Elemental analysis calculated (%) for $C_{40}H_{48}N_2O_2Ca$: C, 74.70; H, 8.01; N, 4.84; found: C, 65.29; H, 7.89; N, 4.40. ^{1}H NMR ($CDCl_3$, 300 MHz); δ 8.73(s, CH=N, 2H), 7.08-7.92(m, 10H), 1.45(s, 18H), 1.35(s, 18H).

Synthesis of {N,N-bis(3,5-di-*tert*-butyl-salicylidene)-ethylene diimine} Al(III) Et. This is an adaptation of a procedure described in literature by Dzugen and Goedken. A 50ml Schlenk flask was charged with salenH_2 in 30ml of CH_3CN. A second 50ml Schlenk flask was charged with 1.0 equiv. of a 1.9M toluene solution $AlEt_3$. A 10ml volume of CH_3CN was added, and the solution was cannulated onto the ligand mixture. The mixture was stirred at room temperature for 2h and the solvent removed under reduced pressure.

Polymerization Runs. A typical melt polymerization run consisted of adding a 1g of the monomer to a previously flame dried schlenk flask. The monomer: initiator: coinitiator ratio was maintained at 350:1:1.The reaction was carried on at 86°C for only 15 minutes under argon atmosphere. The resulting polymer was purified by precipitation from dichloromethane, 5% HCl and methanol and then dried in vacuo. Turnover frequencies (mol of TMC consumed/mol of the catalyst-hr) were calculated by actually weighing the vacuum dried polymer.

Kinetic Studies. TMC, catalyst and the cocatalyst were weighed out in a schlenk flask in the desired monomer:initiator: coinitiator ratio followed by the addition of 10mL of dry 1,1,2,2-tetrachloroethane (TCE) . The reaction vessel was placed into a preheated oil bath. The percent conversion of the monomer in time was calculated by

manually sampling out a small aliquot of the solution, quenching it and analyzing by ^{1}HNMR.

Results and Discussion

Melt Polymerization Results. We have examined several (salen) derivatives of calcium and compared them to magnesium, zinc and aluminum salens for the ring-opening polymerization of trimethylene carbonate. A typical melt polymerization run consisted of adding a 1.0 g of TMC to a previously flame dried Schlenk flask. The monomer:initiator:coinitiator ratio was maintained at 350:1:1, and the reaction were carried on at 86ºC for only 15 minutes under an argon atmosphere, with tetra *n*-butyl ammonium chloride as the coinitiator unless mentioned otherwise. The resulting polymer was purified by precipitation from dichloromethane, 5% HCl, and methanol and then dried *in vacuo*. Turnover frequencies (mol of TMC consumed/mol of the catalyst-hr) were calculated by actually weighing the vacuum dried polymer. All polymer runs show the complete absence of ether linkages even at high temperatures of 140°C which appear as a triplet at 3.4-3.5 ppm on ^{1}HNMR spectra (Figure 3.1). Studies conducted, focused on varying the central metal atom, sterics and electronics of the ligand architecture and the cocatalyst used.

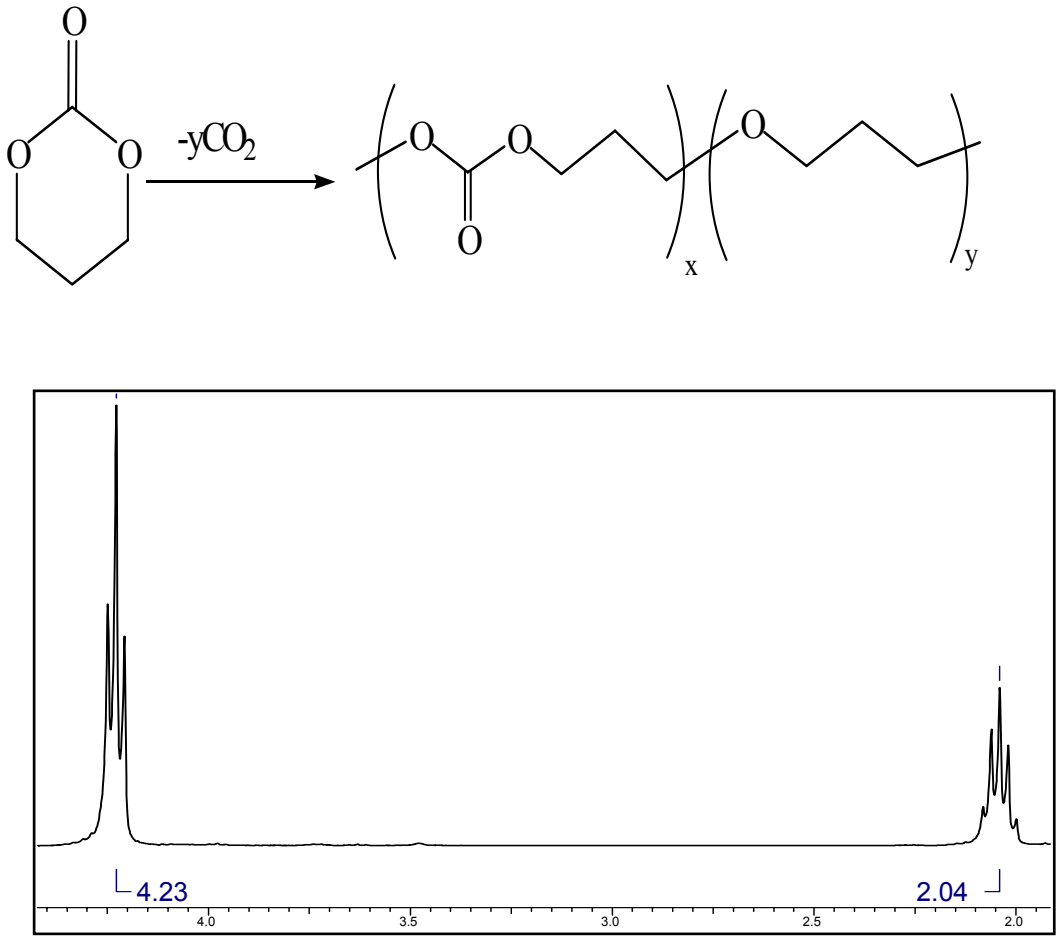

Figure 3.1: ^{1}HNMR of polyTMC in $CDCl_3$ with ether linkages absent

The purpose of our first study was to investigate biometals as catalysts for ring opening polymerization of trimethylene carbonate. Biometals are ideal catalysts for these systems due to their application as biodegradable polymers as has been discussed in the introduction. The Ca, Zn and Mg in the salen systems are present in their +2 oxidation state and a coinitiator was needed for polymerization. Hence to compare it with our existing most efficient Al(III) salen nucleophile catalysts we needed an Al(III)

salen compound in which the axial nucleophile would be uninvolved in the polymerization process, thus justifying the need for an external initiator. Damon Billodeaux of our group has shown that in the case of (salen)Al(III)(ethyl) complexes the axial alkyl group does not participate in the polymerization process, making it an ideal candidate for comparision.[50b]

Table 3.1 and Figure 3.2 summarize our results on the change in catalytic activity by changing the metal center. Ca is by far the most active metal, displaying an increase in activity which is 107% faster than magnesium salen complex and 131% faster than the aluminum catalyst. One reason for this could be the larger size of Ca in comparison to both Mg and Al. Besides both the Ca and Mg are harder ions whereas Zn is much softer. The difference in the activity between Ca and Zn is 349%.

Table 3.1. Polymerization results on varying the central metal atom (salen)M complexes containing an ethylene backbone and tetra-*n*-butyl groups in the 3,5 –positions of the phenolate ring.[a]

Entry	M	TOF[b]
1	Zn	250
2	Al	485
3	Mg	541
4	Ca	1123

[a] Each reaction was performed in melt maintaining a monomer:initiator: [*n*-$Bu_4N]^+Cl^-$ratio as 350:1:1 at 86°C for 15 mins. [b] The TOF was determined by weighing the polymer after precipitating in 5% HCl and MeOH, and drying in a vacuum oven and is reported as mol of TMC / mol M-h.

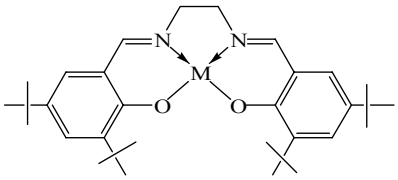

M= Ca^{2+},Mg^{2+},Zn^{2+}

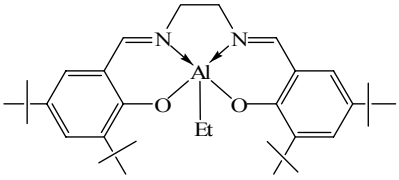

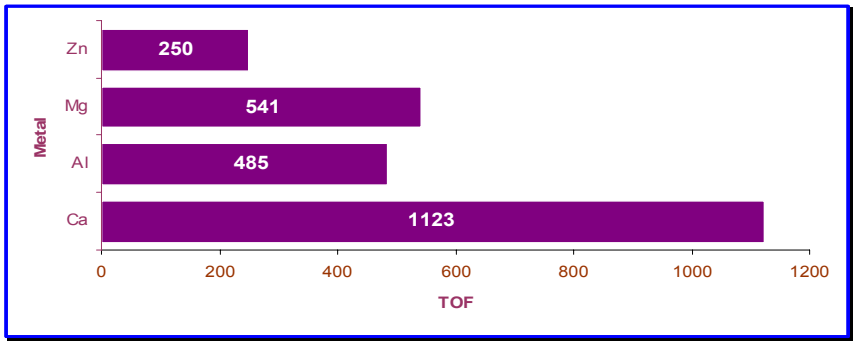

Figure 3.2: Effect of changing the metal center

We have conducted an exhaustive study on the effects of changing the ligand architecture on catalytic activity for the ring opening polymerization of the trimethylene carbonate using aluminum salen catalysts. Hence, the purpose of this study here was just to confirm if the trends were similar or different in the case of Ca(II) salens than the previous case. All (salen)Ca derivatives examined, successfully initiated the ring-opening polymerization of trimethylene carbonate, as shown in Table 3.2, though to varying extents (Figure 3.3). The most active catalyst was N,N'*bis*(3,5-di-*tert*-butylsalicylidene)napthylenediimine Ca(II). The monomer conversion increased by 2.7 times as the 3 and 5 positions in the phenolate ring were substituted with a bulkier group *t*-butyl group as is evident from Entry 1 and 2 of Table 3.3. This is consistent with our results obtained from aluminum salen catalysts which showed a similar increase in the catalytic activity on varying the 3,5 position of the phenolate ring. Besides, the bulky *t*-butyl substituents serve to enhance the solubility of the salen complexes. We have also attempted to optimize the catalytic activity of these derivatives by manipulating the salen backbone. An electron withdrawing, rigid and planar backbone results in an increase in the activity (Figure 3.4). Although as is evident from the trend in Table 3.3, changes in backbone do not have as pronounced an effect on the performance of the catalyst as that of the substituents on the phenolate ring. There is a change in catalytic activity of only 8% between the ethylene backbone and the most active napthylene backbone, a trend consistent with that seen for aluminum salen catalysts in the previous chapter.

Table 3.2. Polymerization results on varying the substituents in the 3,5-positions of the phenolate rings for (salen)Ca(II) complexes containing a phenylene backbone.[a]

Entry	R_1	R_2	TOF[b]
1	H	H	416
2	*t*-butyl	*t*-butyl	1175

[a] Each reaction was performed in melt maintaining a monomer:initiator:*n*-$[Bu_4N]^+Cl^-$ ratio as 350:1:1 at 86°C for 15 minutes. [b] The TOF was determined by weighing the polymer after precipitating in 5% HCl and MeOH, and drying in a vacuum oven and is reported as mol of TMC / mol Ca-h.

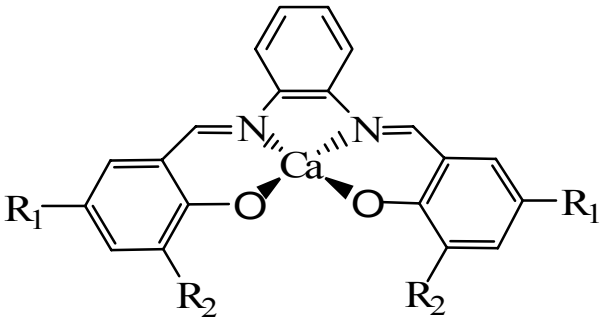

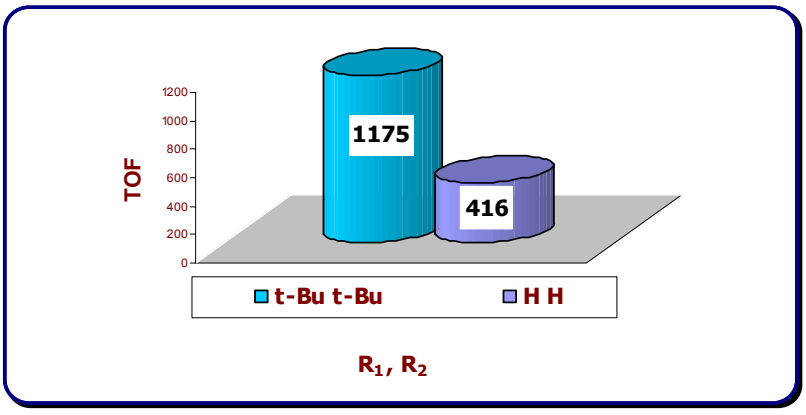

Figure 3.3: Effect of changing the ligands on the 3,5 -phenolate moiety

Table 3.3. Polymerization results for varying the backbone for (salen)Ca(II) complexes where the substituents in the 3,5-positions of the phenolate ring are *t*-butyl groups.[a]

Entry	R_3	TOF[b]
2	Ethylene	1123
3	Phenylene	1175
4	Naphthylene	1270

[a] Each reaction was performed in melt maintaining a monomer:initiator: *n*-$[Bu_4N]^+Cl^-$ ratio as 350:1:1at 86°C for 15 minutes. [b] The TOF was determined by weighing the polymer after precipitating in 5% HCl and MeOH, and drying in a vacuum oven and is reported as mol of TMC / mol Ca-h.

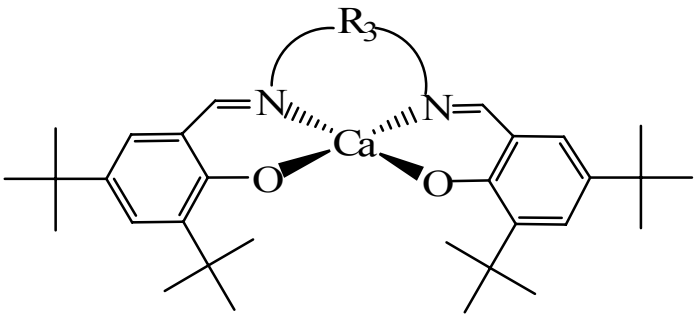

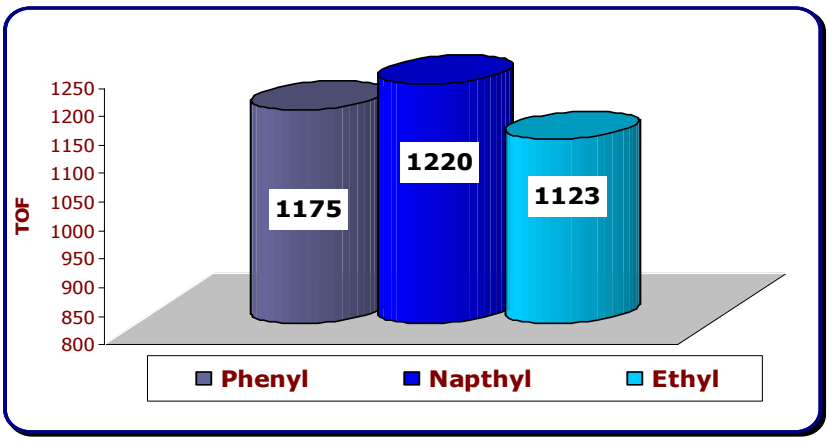

Figure 3.4: Effect of changing the backbone of the (salen)Ca(II) complex

The fourth study conducted with regards to melt polymerization was varying the coinitiator used. A literature survey suggested that for our systems of cylic carbonates alcohols and diols have always been used. However, our group has seen remarkable results with the use of ionic cocatalysts in the case epoxide\CO_2 coploymerization.[4] Two varieties of ionic salt cocatalysts were used PPN^+X^- (*bis* (triphenylphosphorylidine)ammonium) or $Bu_4N^+X^-$ (*n*-butyl ammonium).

Due to the non-interacting nature of the cation, PPN salts are very popular today. However, they are rather expensive and insoluble in the commonly available organic solvents. Hence an alternate option was Bu_4N^+ salts. These salts have the benefit over their PPN^+analogs of being relatively inexpensive and readily soluble in organic solvents. In this study we have not only investigated the effect of variation of the cation PPN/Bu_4N^+ but also the anion X= Cl^-, N_3^- and Br^-. Table 3.4 and Figure 3.5 summarizes our results. Turnover frequencies were slightly better in the case of the PPN salts, which could be attributed to the interacting nature of the Bu_4N^+cation. Catalytic activity follows the trend of N_3^-> Cl^-> Br^-which can logically be attributed to the initiator strength.

Table 3.4. Polymerization results on varying the cocatalyst in Ca(II)(salen) complexes containing an ethylene backbone and tert-butyl groups in the 3,5 –positions of the phenolate ring.[a]

Entry	Cocatalyst	TOF[b]
1	$Bu_4N^+Br^-$	766
2	$Bu_4N^+Cl^-$	1123
3	$Bu_4N^+N_3^-$	1183
4	PPN^+Cl^-	1221
5	$PPN^+N_3^-$	1286

[a] Each reaction was performed in melt maintaining a monomer:initiator: coinitiator ratio as 350:1:1 at 86°C for 15 mins. [b] The TOF was determined by weighing the polymer after precipitating in 5% HCl and MeOH, and drying in a vacuum oven and is reported as mol of TMC / mol Ca-h.

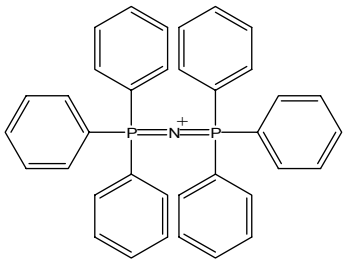

PPN

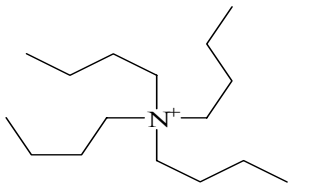

Tetra-*n*-butylammonium

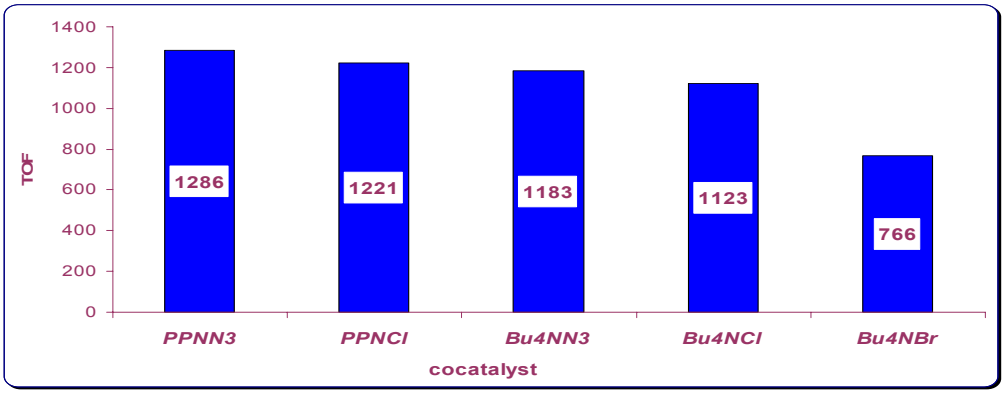

Figure 3.5: Effect of varying the cocatalyst

Due to initiator strength of these anionic catalysts by themselves we also conducted a control reaction where 1eq of PPNCl by itself was added to 1g of TMC maintaining the monomer:initiator ratio as 350:1. The reaction was conducted at an elevated temperature of 97°C instead of our usual temperature of 86°C for an hour. It was seen that the though PPNCl by itself did polymerize TMC, the polymer had a small amount of ether linkages, which appeared as a triplet at 3.4 ppm on the ^{1}HNMR spectra. TOF was a diminished 345. Hence, it confirmed our doubts that both the catalyst and cocatalyst was essential to obtain the high reactivities that have been displayed by these Ca catalyst \ anionic cocatalyst systems.

While determining the molecular weights of our polymer samples, it was observed that that the number-average molecular weight linearly increased with the ([M]/[I]). In addition the molecular weights determined by GPC were very close to the theoretical molecular weights (M_{nth} = [M]/[I].MW_{TMC} Conversion%.) as shown in Table 3.5. This indicated almost all the catalyst participated in the ring opening , the molecular weights of the polymers can be predicted by the molar ratio of the monomer to initiator and the monomer conversion. These observations showed that the reaction conformed to the pseudoliving mechanism and the controlled nature of polymerization (Figure 3.6). PTMC samples obtained at various M/I ratios also show the same narrow molecular weight distribution.

Table 3.5. The dependence of molecular weights of PTMC on M/I ratios. [a]

Entry	M/I	Mn x 10^{-4}		PDI
		GPC	Theor.	
1	275	3.0	2.8	1.76
2	350	3.7	3.4	1.76
3	500	5.6	5.0	1.61
4[b]	700	6.3	6.7	1.48

a Reactions conducted at 88°C for 30 minutes using {N,N-bis(3,5-di-*tert*-butyl- salicylidene)-phenylene diimine}Ca (II) as catalyst and 1eq of $PPNN_3$ as cocatalyst.b. Entry 4 run time 45 minutes.

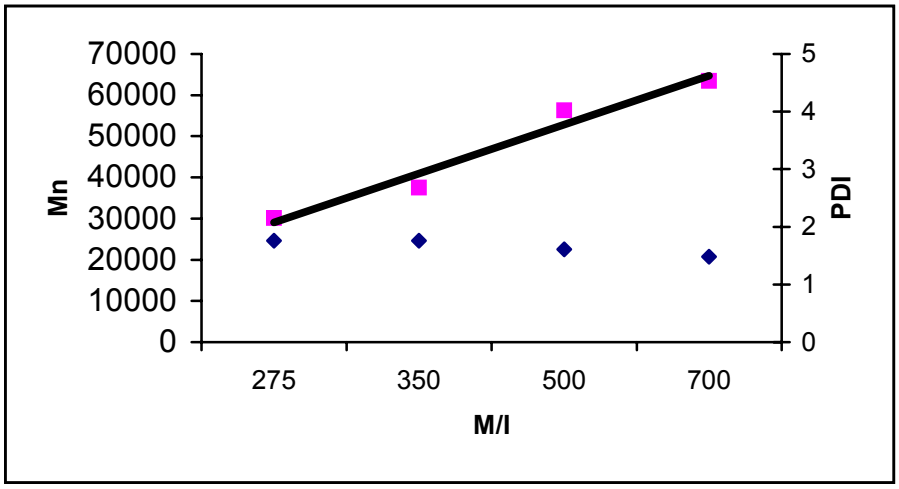

Figure 3.6: Plot of the dependence of molecular weight of PTMC on M/I ratios

Kinetic Studies

We have also conducted preliminary kinetic measurements. All kinetic studies have been conducted using {3,5-di-*tert*-butyl-(salicylidene)-1,2-ethylene diimine}Ca(II). with 1eq of *n*-$[Bu_4N]^+Cl^-$ at 110°C unless mentioned otherwise. As was seen in our previous study with aluminum(III)salens, the rate of polymerization in a weakly polar solvent like toluene (dielectric constant 2.4) was found to be faster than 1,1,2,2,tetrachloroethane (TCE) (dielectric constant 10.8) indicating a coordination mechanism. Although the reaction is slower in TCE, high boiling chlorinated solvents are usually used for such kinetic studies due to high solubility of both the monomer and polymer, thus facilitating the ease of sampling. The reaction was monitored by taking out a small aliquot of the reaction mixture after regular intervals of time and monitoring by ^{1}HNMR.

Figure 3.7a is a typical monomer consumption time dependence plot. The linear time dependence of the semi-logarithmic plot in Figure 3.7b , $\ln(A-A_0)/(A-A_t)$ vs. time demonstrates that the polymerization is first order in monomer . Table 3.6 summarizes the rate constants at various concentrations of the catalyst, cocatalyst and temperatures.

Table 3.6. Rate constants at varying the concentrations of the catalyst and cocatalyst and temperature

Entry	[Ca](mol\l)	Eq. of *n*-$[Bu_4N]^+Cl^-$	Temperature (°C)	k(mol\l sec)
1	0.0028	1.0	110	0.0426
2	0.00356	1.0	110	0.0666
3	0.0049	1.0	110	0.0749
4	0.0056	1.0	110	0.0889
5	0.0049	1.0	102	0.0625
6	0.0049	1.0	125	0.0995
7	0.0049	1.0	135	0.1141
8	0.0049	0.7	110	0.0572
9	0.0049	0.5	110	0.0439
10	0.0049	0.28	110	0.0247

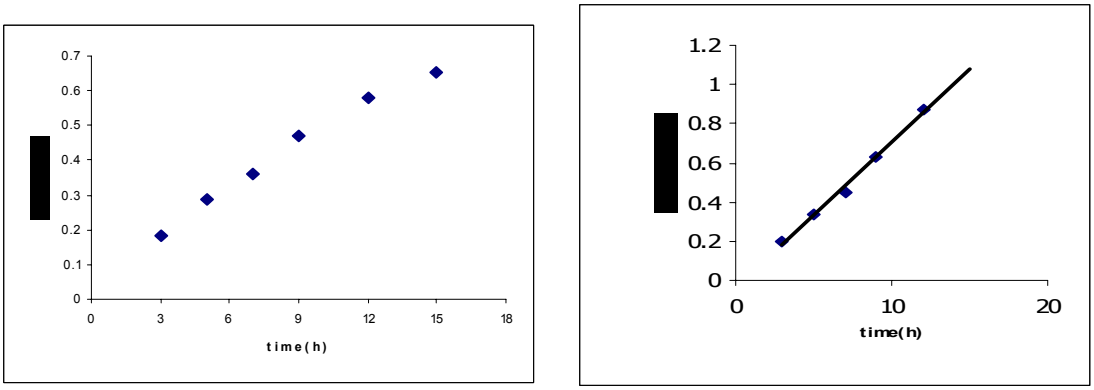

(a) **(b)**

Figure 3.7: (a): Plot of monomer conversion vs. time dependence. **(b)**: Semilogarithmic plot depicting order with respect to monomer concentration

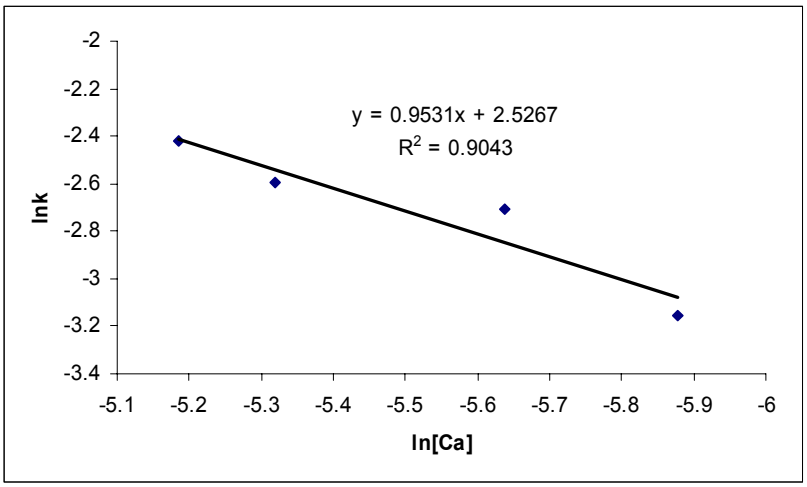

Figure 3.8: Plot of ln k vs. ln[Ca] to determine the order with respect to [catalyst]

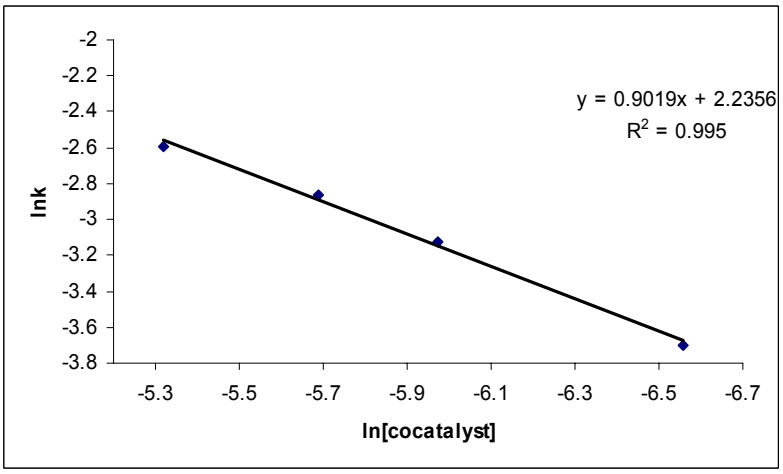

Figure 3.9: Plot of ln k vs. ln[cocatalyst] to determine the order with respect to cocatalyst concentration

Figure 3.8 and Figure 3.9 illustrate the correlation of polymerization rate versus the concentration of the Ca catalyst. These data disclose that the polymerization is first order w.r.t catalyst concentration. A first order dependence was also observed w.r.t to cocatalyst concentration as seen in Figure 3.9**.** Activation parameters $\Delta H^{\neq}$= 20.12 ±

1.040 KJ/mol and $\Delta S^{\neq}$= -216.11 ± 2.665 J/mol were calculated from the Eyring plot of ln(k/T) vs. (1/T) (Figure 3.10).

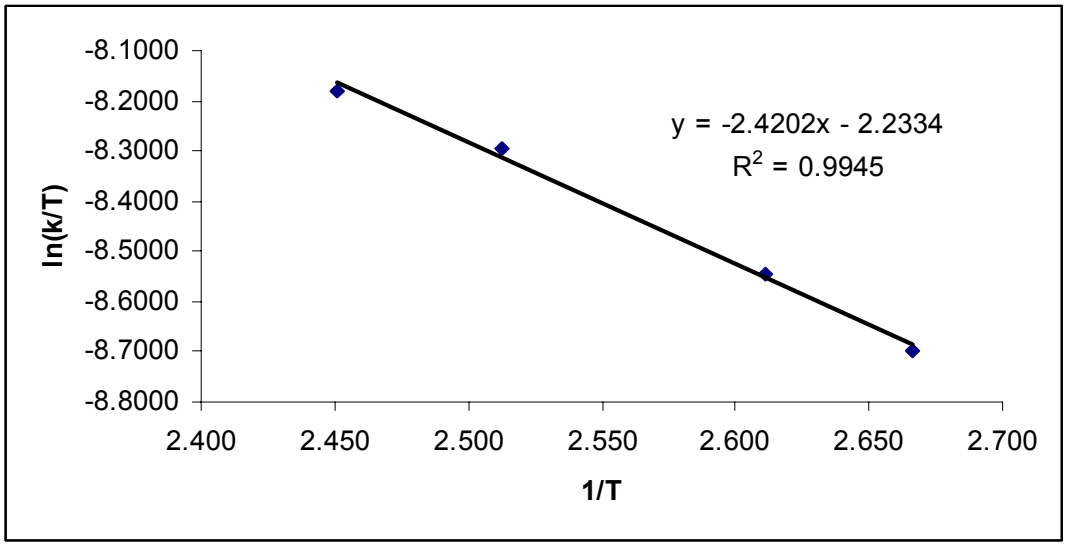

Figure 3.10: Eyring plot to calculate the activation parameters

We have tried to get an insight into the ring opening mechanism by both NMR, as well as infra red spectroscopy. The ^{1}HNMR spectra we obtained by terminating a low-molecular weight sample of the polymer with 2-propanol was similar as the one obtained in our previous study with Al salen catalysts which gives an indicating of monomer insertion into the growing polymer chain by breaking the acyl oxygen bon instead of the alkyl oxygen bond (Figure 3.11). This method of detecting the mode of insertion has been used by Shen and coworkers numerous times.[23]

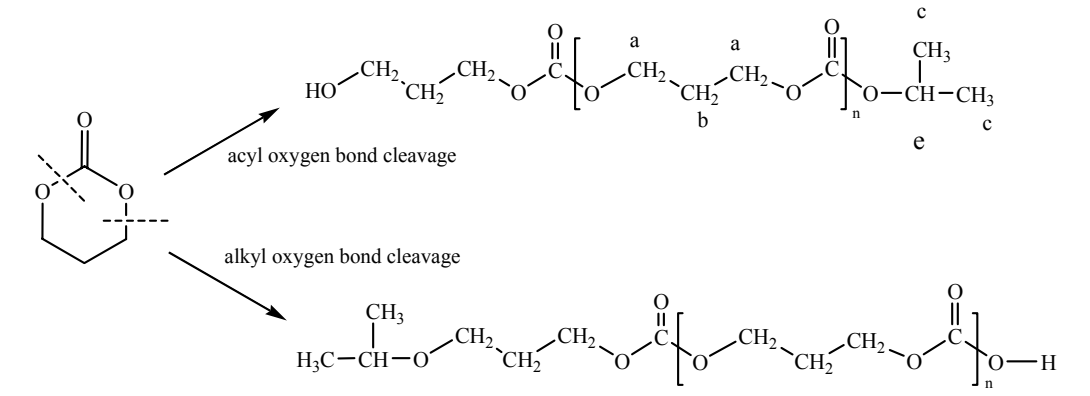

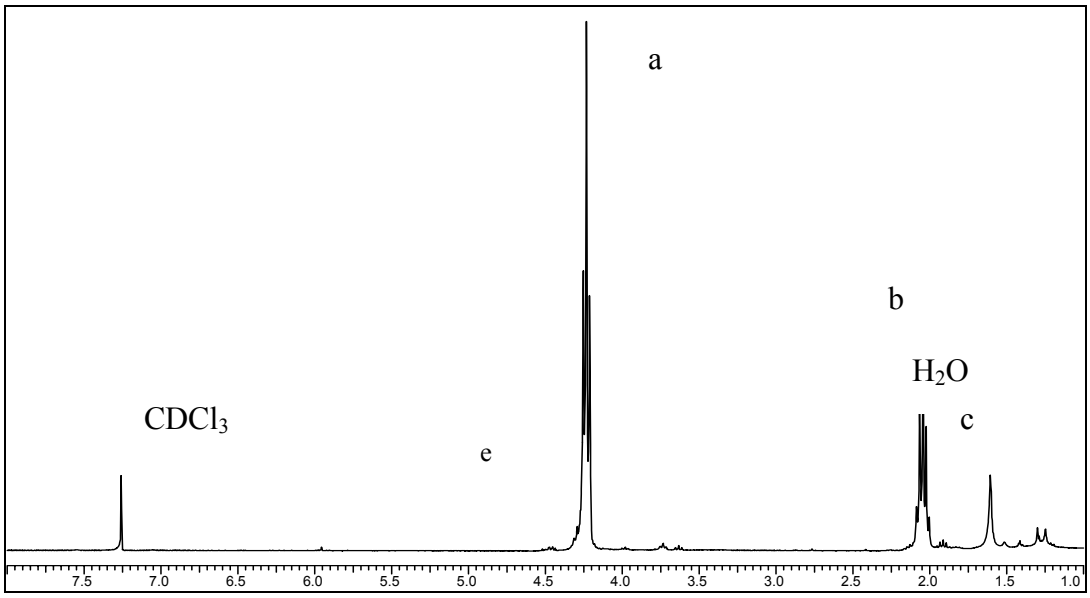

Figure 3.11: ^{1}HNMR of poly (trimethylene carbonate) terminated by 2-propyl alcohol in $CDCl_3$

The azide stretch is a very important spectroscopic probe in vibrational spectroscopy. A low molecular weight sample of polyTMC from a reaction catalyzed by {3,5-di-*tert*-butyl-(salicylidene)-1,2-ethylene diimine}Ca(II) and 1eq.$[Bu_4N]^{+}N_3$, showed an azide stretch at 2102 cm^{-1} representative of an organic azide as shown in Figure 3.12. Figure 3.13 shows the plausible initiation step with N_3^- as the initiator.

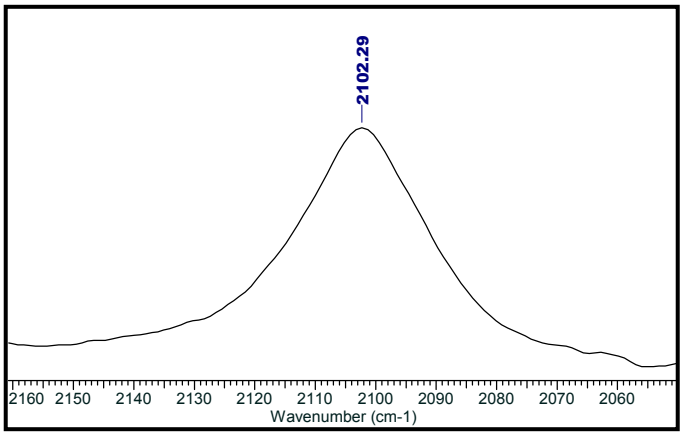

Figure 3.12: Infrared stretch of azide end group in polymer

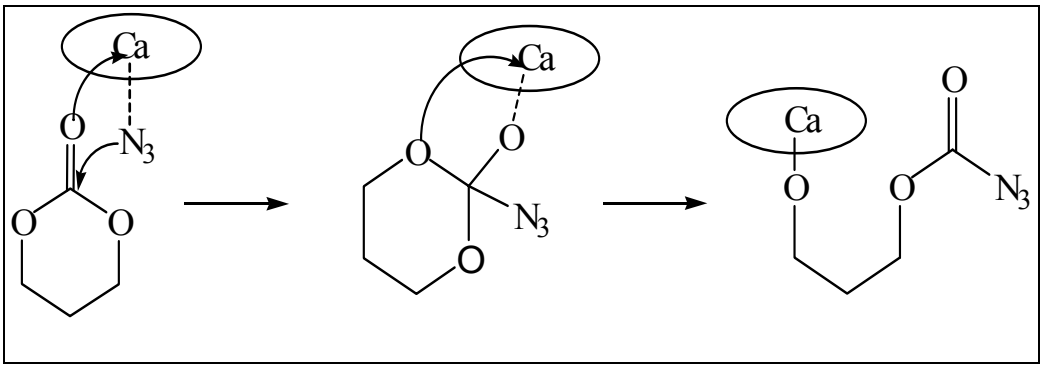

Figure 3.13: Plausible initiation of ring opening polymerization of TMC

Conclusions

The ring opening polymerization of trimethylene carbonate using Ca (II), Mg(II) and Zn(II) salen catalysts have been reported here. This is our third study in the series of main group metal salen complexes after Al(III) and Sn(IV) complexes. Unlike the previous two metal systems which already had an initiator bound to the metal, we have had to use an external initiator like PPN^+X^- or $[Bu_4N]^+X^-$ in this case.

With the Ca(II) catalysts we have obtained very high reactivities compared to both our aluminum(III) and tin(IV) catalysts (Figure 3.14). Besides, the added advantage of Calcium being a biometal is definitely a bonus. Though salen complexes of other biometals like Zn and Mg were also investigated, their efficiencies faded in the light of the high turnover frequencies obtained for Ca(II) systems. The activities have also been enhanced by electronically or sterically modifying the salen architecture. We have also conducted preliminary kinetic and mechanistic studies. The extremely mild conditions for the reaction (15minutes at 86°C, 1eq of cocatalyst) should also be remembered. Our initial kinetic studies indicate first order dependence w.r.t monomer, catalyst and cocatalyst. There is evidence of a coordination insertion mechanism where the end group of the polymer has been confirmed both by infra red spectroscopy. Another significant increase is the molecular weight of the polymer. Keeping all conditions the same, the molecular weight increases 2.2 times in the Ca salen.

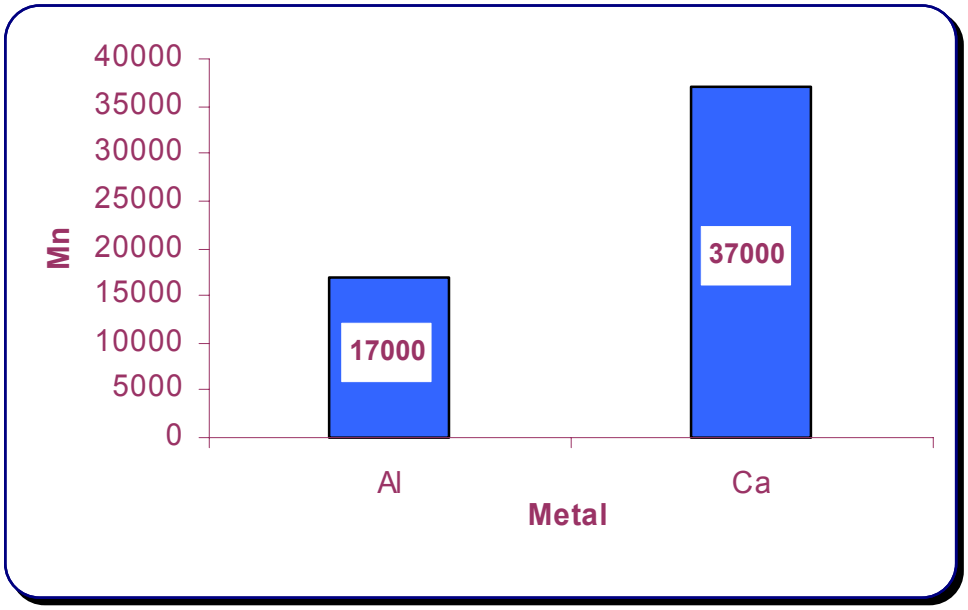

Figure 3.14: Comparison of M_n of the polymer obtained from Al(III) and Ca(II) catalysts

As has been discussed in Chapter I, rare earth initiators have shown very good activities for these cyclic monomer systems. However, while making a choice of catalyst for commercial use, the cost and long term toxicity should be taken into consideration. Metals like Ca definitely come out as a winner in both these aspects. The activities can be further enhanced as has been witnessed in both Chapters II and III with a very good ligand system like the salen , just by modifying the environment around the metal.

Future efforts in this area will concentrate on the copolymerization of TMC with cyclic esters having complementary properties. The thermal and mechanical properties of these copolymers can be designed according the composition of each monomer using these very effective metal salen catalysts.

CHAPTER IV

COPOLYMERIZATION OF ε-CAPROLACTONE AND TRIMETHYLENE CARBONATE USING Ca(II) SALEN COMPLEXES

Introduction

The properties of polymers can be modified either by physical blending or by chemical copolymerization. Copolymerization is an effective method for the synthesis of tailor made polymers. Both thermal and mechanical properties of the copolymer are highly dependent on the composition of the monomers. Relevant to this, copolymers of aliphatic polycarbonates are of great interest for their use in bioresorbable suture filament, artificial skin, prostheses, bone fixation plates, ligature clamps and galenic formulations.[62]

Poly(ε-caprolactone) (PCL) is a very attractive polymer with biocompatibility, non-toxicity and permeability. However, besides being brittle, the hydrophobicity and rather high crystallinity of PCL, decreases its compatibility with soft tissues and lower its biodegradability, which is usually disadvantageous for medical applications.[63] Poly (trimethylene carbonate) (PTMC), an amorphous aliphatic polycarbonate, displays high elasticity at room temperature but degrades slowly in aqueous solution.[64] Due to the carbonate linkage being more hydrophobic than the ester, a copolymer between the above mentioned monomers is expected to be more stable to *in vitro* hydrolysis and hence have a longer shell life than polyesters. However, because the hydrolysis is faster *in vivo* the copolymer can be used as a bioabsorbable material.[41]

Copolymers are classified on the basis of arrangement of the two monomers in the polymer chain (Figure 4.1).[65] Random copolymers contain repeating units arranged in a purely random fashion i.e. the probability of finding a given monomeric unit at any given site in the chain is independent of the nature of neighboring units at that position. Random copolymers are represented as poly (A-ran-B),

On the other hand block copolymers contain blocks of monomers of the same type, a block being defined as a portion of the polymer molecule in which the monomeric units have at least one constitutional or configurational feature absent from the adjacent portions. Block copolymers are named as poly A-block-polyB.

A graft copolymer contains a main chain of polymer consisting of one type of monomer, with branches made of a second type of monomer. It is named as poly A-graft-poly B where A is the monomer of the main chain (always named first) and B is the monomer of the side chain.

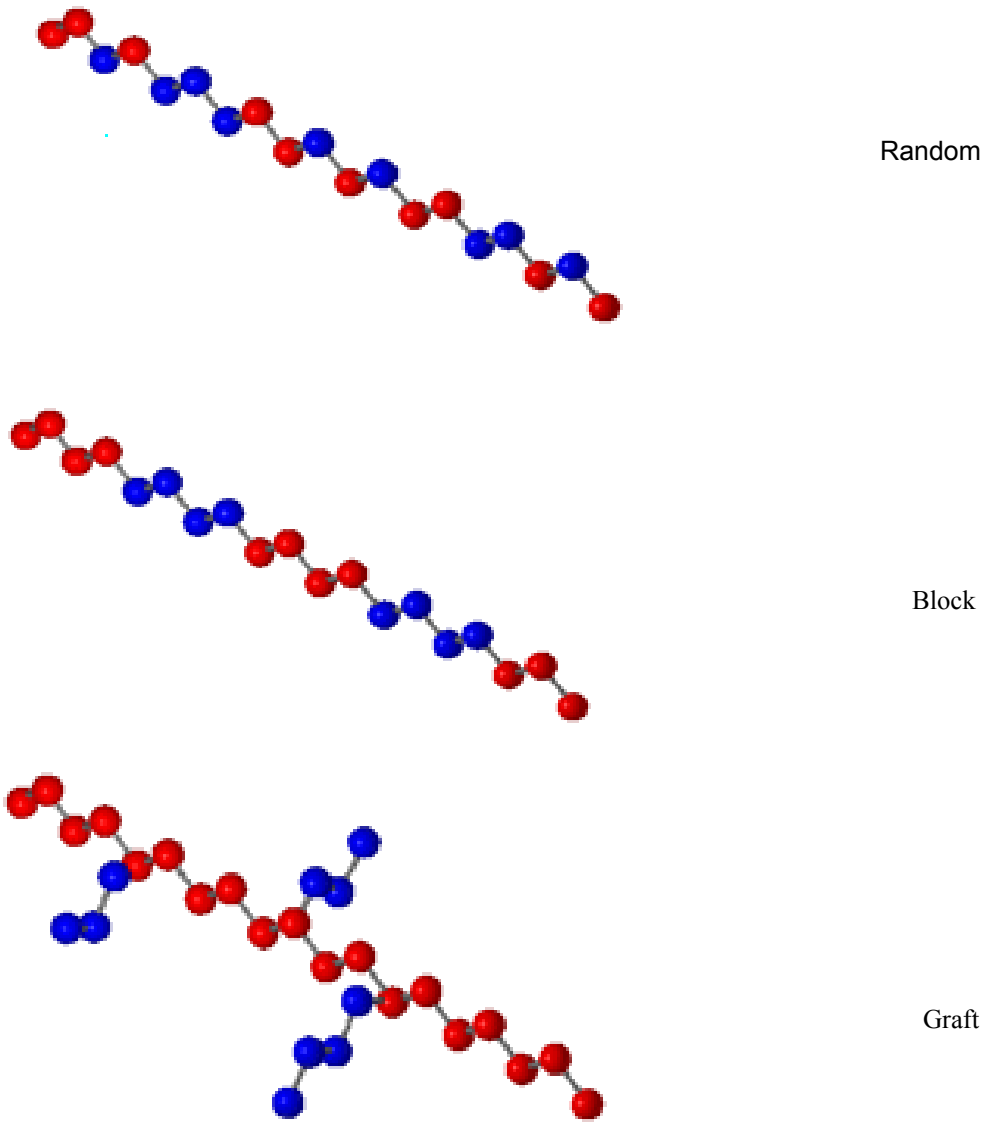

Figure 4.1: Strucure of copolymers

Both random and block copolymerization of trimethylene carbonate and ε-caprolactone have been effectively carried out using tin-octanoate,[66] aluminum isopropoxide,[67] rare-earth metal chlorides and alkoxides.[68] Rare earth metal alkoxides have by far been the most active catalyst for these copolymerization reactions. Lipases have been used as catalysts in the copolymerization of ω-pentadecalactone and TMC by Gross and coworkers.[62] The recent elegant works of Shen and coworkers using a scandium catalyst have been referred to throughout this study.[33]

Our success with the use of Calcium salen anionic cocatalyst system in the homopolymerization of TMC, as discussed in the previous chapter, prompted us to investigate the efficacy of these catalysts in the copolymerization of TMC / ε-caprolactone both for random and block polymerization. Its advantages as a non-toxic catalyst system has been exploited by a number of groups in the polymerization of lactides.

In this chapter, I shall discuss our preliminary results with the synthesis of poly(ε-caprolactone-co-trimethylene carbonate) using Ca (II) salen catalysts.

Experimental

CL (Aldrich) was dried and distilled over CaH_2 before use. TMC (Boehringer Ingelheim) was recrystallized from THF\diethyl ether and stored in the glovebox under argon. All manipulations were conducted under inert atmosphere using Schlenk techniques. All other solvents used were freshly distilled from their required reagents before use.

The synthesis of the Ca and Al salen catalysts have been discussed in detail in the previous two chapters. All Bis(triphenylphosphoranylidene)ammonium salts were recrystallized from dichloromethane/ether before use. Tetra-*n*-butylammonium halides were recrystallized twice from acetone/ether. All catalysts and cocatalysts were stored in the glovebox. ^{1}H NMR spectra were recorded on Unity+ 300MHz and VXR 300MHz superconducting NMR spectrometers.

Polymerization. The molar ratio of the monomers were maintained at 1:1 unless mentioned otherwise. The monomer: initiator ratio (M/I where $M=M_{TMC} + M_{CL}$) was kept at 700:1. The catalyst used was {N,N-bis(3,5-di-*tert*-butyl- salicylidene)-ethylene diimine}Ca (II) unless mentioned otherwise.

For *random copolymerization* both the monomers were added simultaneously along with the catalyst and the cocatalyst. The reaction was allowed to go on at 86°C for 2 hrs. Solution studies were conducted to understand the rate of the copolymerization reaction with respect to each monomer. A 1:1 ratio of the two monomers were added to a Schlenk flask along with the catalyst {N,N-bis(3,5-di-*tert*-butyl- salicylidene)-ethylene diimine}Ca (II), 1eq of [Bu4N]Cl and 10ml of TCE (1,1,2,2,-tetrachloroethane). . The monomer: initiator ratio was maintained at 700:1 and the temperature at 110°C. The reaction rate was monitored by taking out an aliquot after regular intervals of time and sampling it by ^{1}HNMR.

For *block copolymerizations*, two techniques were used which can be referred back to two different research groups. According to the technique used by Feijan and coworkers, in a Schlenk flask to a prepolymerized sample of TMC, the required amount

of CL was added along with the catalyst.[69] Polymerization was terminated after desired time followed by precipitation from acidified methanol.

The second technique followed was the more conventional approach used by Shen and coworkers.[68] 1g of TMC was polymerized with the required amount of catalyst maintaining the M:I ratio of 350:1. After an hour an equal equivalent of caprolactone was added to the same Schlenk flask and the reaction allowed to continue for a desired time.

The percent conversion of monomers were calculated with ^{1}HNMR. The resulting polymer was dissolved in dichlomethane and precipitated out of acidified methanol (5% HCl), washed several times in methanol, filtered and dried under *vacuo*. Turnover frequencies (mol of monomer consumed/ mol of catalyst-hr) were calculated from the conversions obtained by NMR.

Results and Discussion

Both simultaneous and sequential copolymerization of trimethylene carbonate and ε-caprolactone were attempted. Anionic cocatalysts like bis(triphenylphosphoranylidene)ammonium (PPN^+X^-) salts and *n*-butylammonium salts $(Bu_4N)^+X^-$ were used as cocatalysts.

Homopolymerization of trimethylene carbonate with Ca salen catalysts have already been discussed in the previous chapter. Catalyst {N,N-bis(3,5-di-*tert*-butyl-salicylidene)-ethylene diimine}Ca (II) showed an 80% conversion to polyTMC in just 15 minutes at 86°C (TOF = 1123). On the contrary, the same catalysts showed a conversion of only 20% in the case of poly CL even after 2 days under the same temperature as above (TOF = 5.8). Hence we had a catalyst system which was extremely good for one of our monomers (TMC) while being equally poor for our second monomer system (ε-CL) – a situation which for which we could find no precedence in the available literature..

Simultaneous Copolymerization of Trimethylene Carbonate and ε-Caprolactone

Random or simultaneous copolymerization was conducted at 86°C for 2hrs. The monomer: initiator ratio was maintained as 700:1 with a $monomer_1$:$monomer_2$ ratio of 1:1 unless mentioned otherwise. All polymerization reactions were conducted under melt condition with {N,N-bis(3,5-di-*tert*-butyl- salicylidene)-ethylene diimine}Ca (II) as the catalyst unless mentioned otherwise. The nature of the cocatalyst as well as the ratio were varied, the effect of which is discussed in Table 4.1 and Figure 4.2.

Table 4.1. Random copolymerization of CL with TMC using {N,N-bis(3,5-di-*tert*-butyl-salicylidene)-ethylene diimine}Ca (II) as the catalyst and different coinitiators.

Entry	Cocatalyst	Eq. of cocatalyst	TOF[b]	Content of diad (%)[c]		
				TMC-TMC	CL-CL	TMC-CL,CL-TMC
1	$Bu_4N^+Cl^-$	1.0	221.3	70.94	4.87	24.19
2	$Bu_4N^+Cl^-$	2.0	235.5	62.54	6.13	31.33
3	$Bu_4N^+N_3^-$	2.0	295.1	42.20	8.44	49.04
4	PPN^+Cl^-	1.0	253.7	54.88	8.13	36.99
5	$PPN^+N_3^-$	1.0	289.4	48.83	9.81	41.36
6	PPN^+OAc^-	1.0	189.7	93.65	1.79	4.56
7[d]	$Bu_4N^+Cl^-$	2.0	334.1	49.25	8.59	42.16
8[e]	PPNCl	1.0	204.5	94.34	7.31	13.53

[a] Each reaction was performed in melt maintaining a $monomer_1$:$monomer_2$ ratio of 1:1 at 86°C for 2h. [b] TOF was calculated as (mole of monomers consumed/ mole of catalyst-hr). [c]The content of the diad was determined by NMR.[d] Reaction conducted at 110°C.[e] {N,N-bis(3,5-di-*tert*-butyl- salicylidene)-ethylene diimine}Al (III) used as catalyst

As is evident from the first six entries of the above table of results both the chloride and azide nucleophiles are effective for copolymerization of TMC with CL with N_3^- being more effective than Cl^- (14.2%).. It is surprising to note that PPNOAc, which is an effective co initiator for polymerization of TMC with the same catalyst system shows a diminished activity for the copolymerization reaction. As has been observed before due to the non-interacting nature of the counter ion , the PPN salts are better initiators than their *n*-butylammonium counterpart.

Entry 7 of Table 4.1 shows the temperature dependence of the copolymerization reaction when the reaction has been conducted at an elevated temperature of 110°C. As would be expected the TOF increases by 42% from entry 2 on increasing the temperature by about 24°C. Entry 8 uses {N,N-bis(3,5-di-*tert*-butyl- salicylidene)-

ethylene diimine}Al (III) instead of the Ca(II) analog. This study was conducted since it has been shown in literature that CL can be polymerized more effectively by aluminum catalysts. However, the activity diminishes by around 24% in comparison to Entry 4 which is similar to the trend observed in the homopolymerization of TMC in the previous chapter. This result again indicates that the rapid polymerization of TMC by the Ca/Al catalysts enhances the simultaneous polymerization of CL.

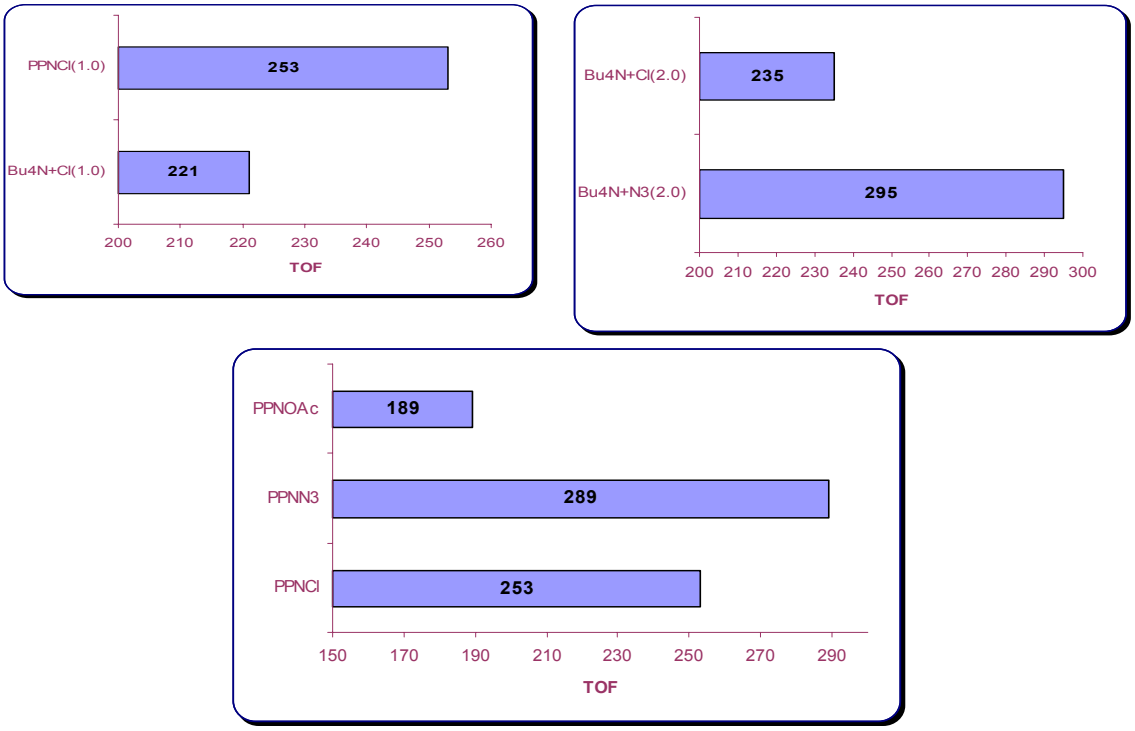

Figure 4.2: Effect of change of coinitiator on the turnover frequencies of TMC-CL random copolymerization

^{1}HNMR was used extensively to monitor the percent conversions. The average composition of each polymer was calculated by integrating the area of the signals of [CH_2O] group of ε-CL unit at 2.3ppm and the signal [$CH_2CH_2CH_2$] group of TMC at 2.1ppm as shown in Figure 4.3.. The region between 4.0 - 4.3ppm show four groups of peaks indicating four kinds of diads. These peaks indicate a direct bonding of the CL and TMC units

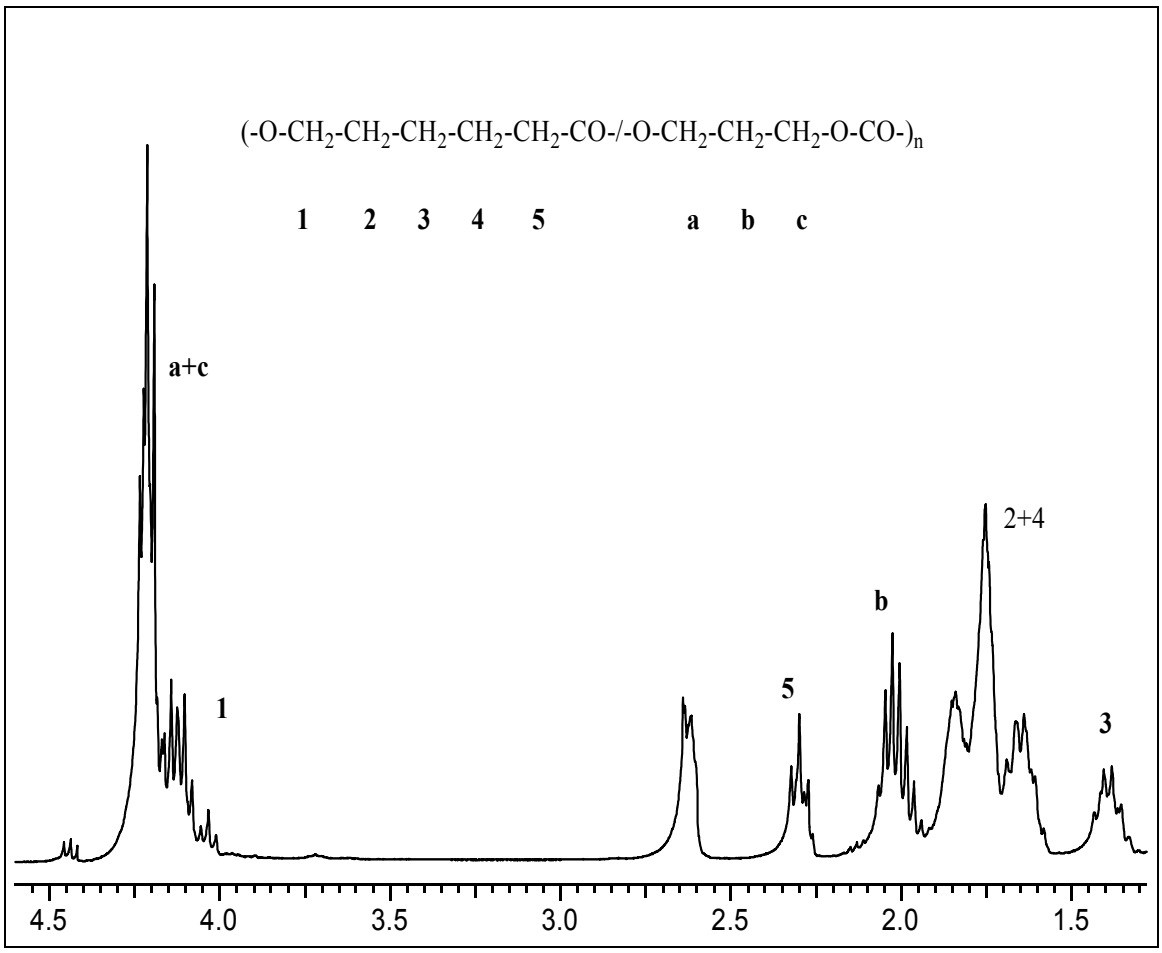

Figure 4.3: ^{1}HNMR spectrum of TMC-CL copolymer in $CDCl_3$

The peaks at 4.47 ppm and 2.60 ppm indicate the amount of monomer of TMC and CL left over after 2hrs of simultaneous copolymerization. As is evident from the spectra the rate of TMC polymerization is much faster than in the case of CL.

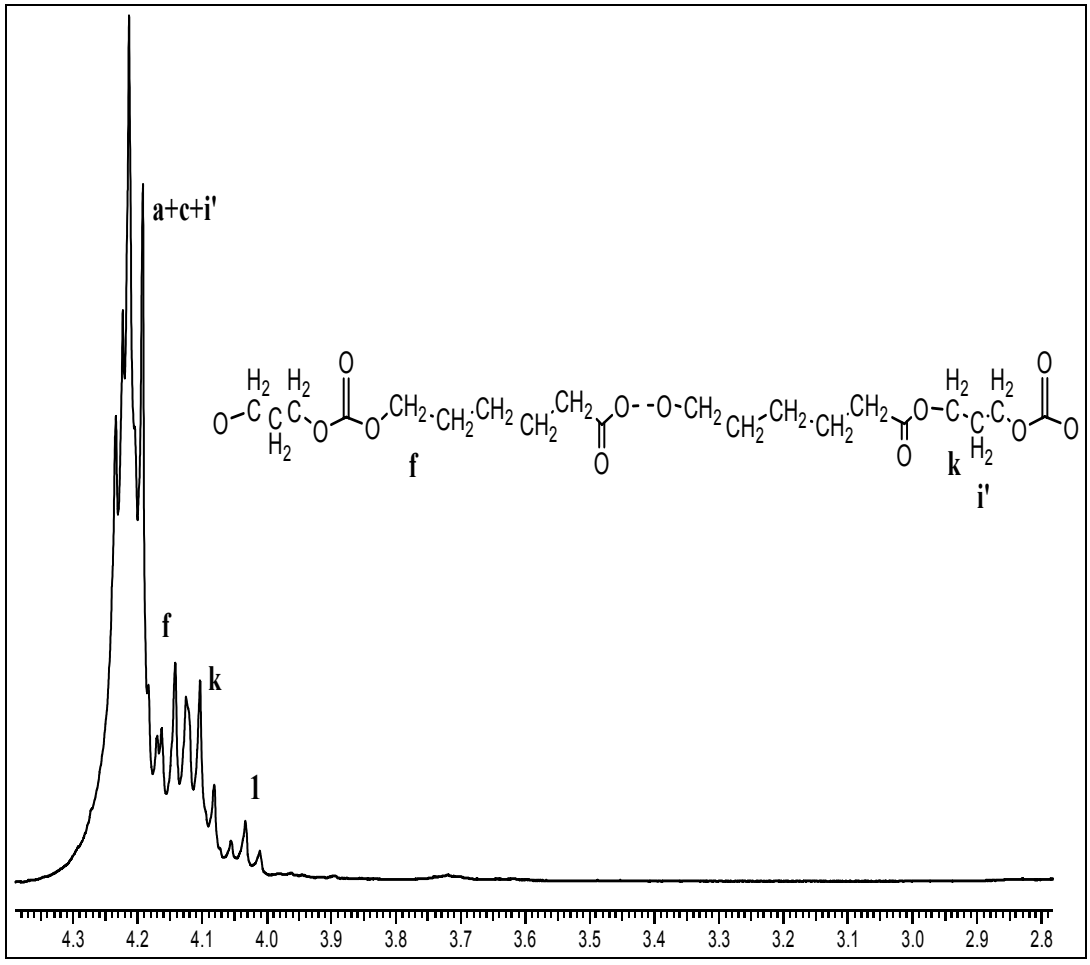

Figure 4.4: TMC-CL diads

Figure 4.4 is an evidence of the direct bonding of the TMC-CL units. It indicates the formation of a highly random copolymer X according the Shen and coworkers.[8] In conjunction with Table 4.1 it can be concluded that this copolymer has a high percentage of TMC-TMC units followed by TMC-CL and CL-TMC units. There is a very small amount of CL-CL units in this copolymer. As the initiator strength increases (Entry 2 & Entry 3, Table 4.1) there is an increase in the TMC-CL units is observed (17.71%) accompanied by a drop in the TMC-TMC units (20.34%)indicating a greater insertion of CL units into TMC units. A proportional increase in the CL-CL units is not observed (2.13%).

Apart from copolymers of structure X, where X is a random copolymer sample, we also attempted to synthesize a copolymer of structure XB, B being a homopolymer of CL. This was done by maintaining the TMC:CL ratio of 30:70. The reasoning given by Shen and coworkers is that since the polymerization rate of Cl is slower than that of TMC, a random polymer would be formed at the first stage of polymerization. After all the TMC monomers have inserted into the copolymer chain, the remaining CL would form a homopolymer.[9] However we were not been able to synthesize such a polymer in spite of allowing the reaction to run for both its usual 2hrs as well as 4hrs.. But, after a reaction time of 15hrs we did observe such a polymer. Figure 4.5 shows the ^{1}HNMR of the XB polymer in $CDCl_3$. The difference in the structure of the X and XB polymer can be clearly observed by comparing the peaks in the region 4.0 - 4.3ppm.. The prominent signal at 4.05ppm is that of homopolymer of caprolactone. Homopolymer of TMC appears at 4.21ppm. The signal between the two peaks is that

of the TMC-CL diad. On integrating the signals it was found that though the initial feed was 30:70 (TMC:CL) the resulting polymer had 22.51% TMC-TMC units, 65.93% CL-CL units and 11.56% TMC-CL units.

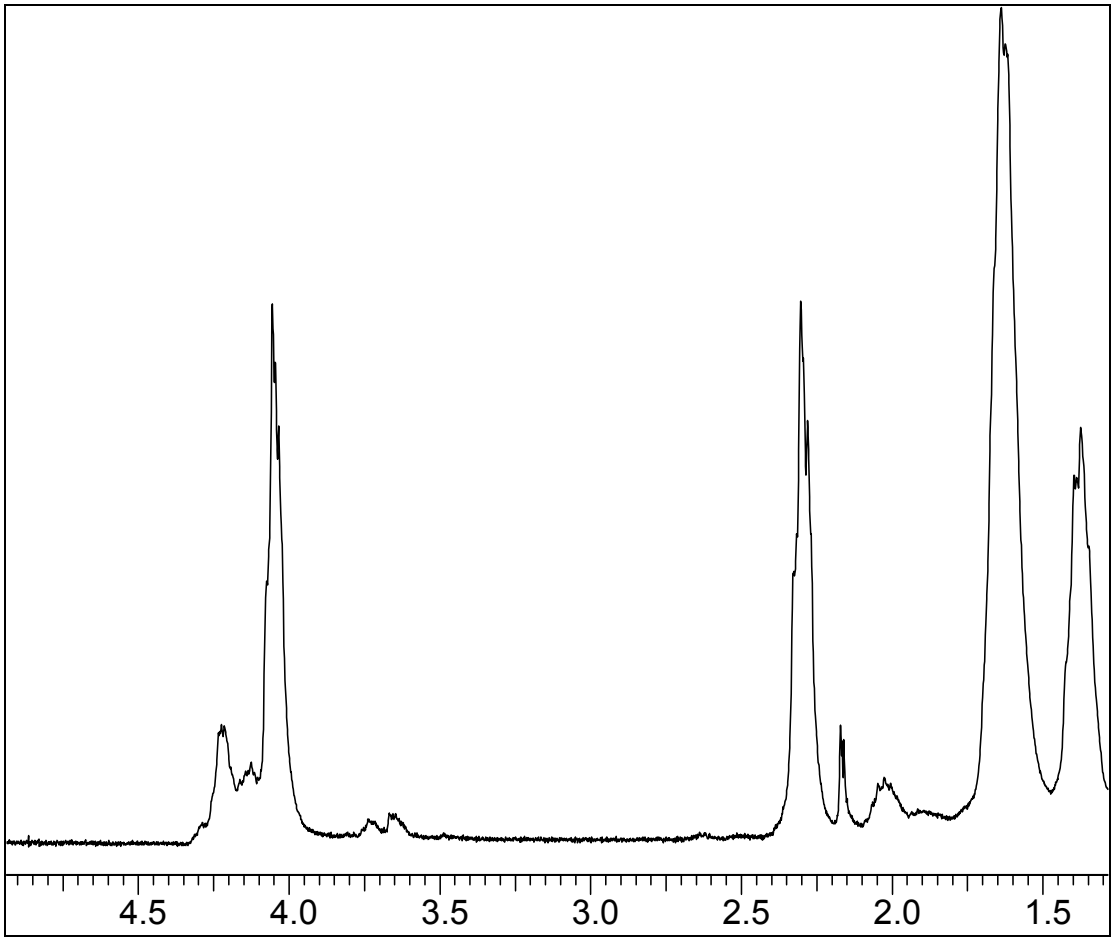

Figure 4.5: ^{1}HNMR of XB polymer in $CDCl_3$

Hence, from the copolymerization in melt conditions we concluded that the rate of polymerization of TMC was faster than the rate of polymerization of ε-CL. We have been able to obtain a copolymer of structure X and another copolymer of structure XB. The polymerization conditions were optimized by varying the cocatalyst, the temperature and the central metal atom.

In order to compare the rates of copolymerization of TMC and CL with respect to each other we decided to conduct a solution study where the rate of polymer formation was monitored by taking out an aliquot after regular intervals of time and taking an ^{1}HNMR of the sample. The reaction was conducted in a high boiling chlorinated solvent TCE (1,1,2,2 tetrachloroethane) in which both the monomer and the polymer are soluble at a temperature of 110°C. A 1:1 ratio of the two monomers were added to a Schlenk flask along with the catalyst {N,N-bis(3,5-di-*tert*-butyl-salicylidene)-ethylene diimine}Ca (II), 1eq of [Bu4N]Cl and 10ml of TCE (1,1,2,2,-tetrachloroethane). . The monomer: initiator ratio was maintained at 700:1.

Figure 4.6 shows the time conversion curve of TMC-CL copolymerization reaction. As is evident, the rate of conversion of TMC to PTMC is much faster than the rate of conversion of ε-CL to PCL. From the slope of semilograthmic plot it can be seen that rate of polymerization of TMC is ~ 2.3 times faster than the rate of polymerization of CL in TCE.

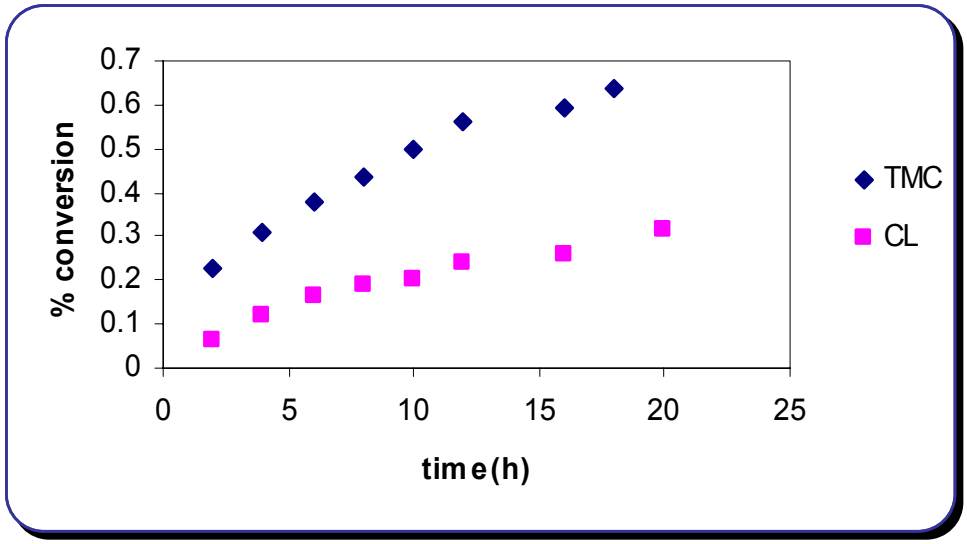

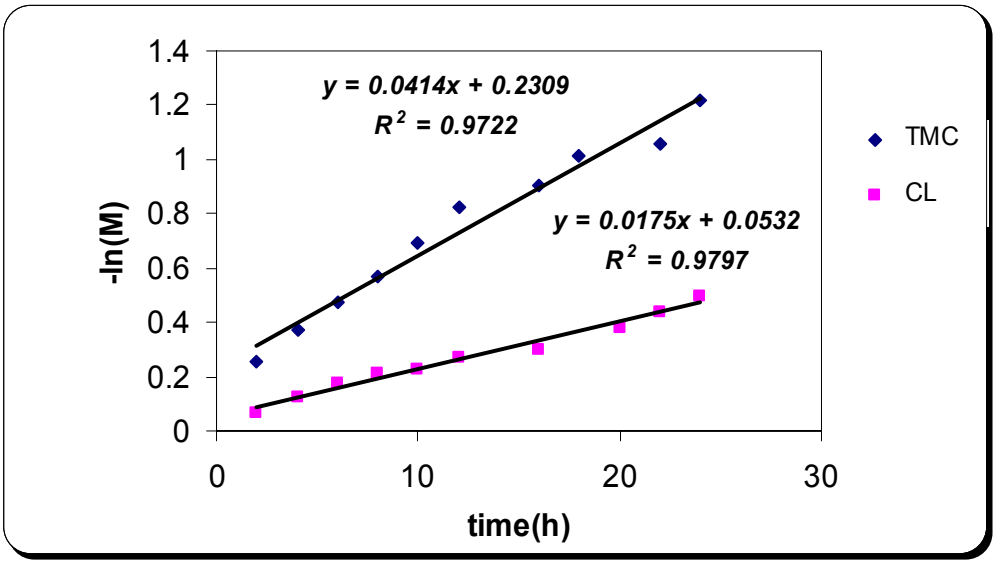

Figure 4.6: Plot of rate of polymerization vs. time

Sequential Polymerization of Trimethylene Carbonate and ε- Caprolactone

Block polymerization of trimethylene carbonate (TMC) and ε-caprolactone (CL) was attempted with the Ca catalyst {N,N-bis(3,5-di-*tert*-butyl- salicylidene)-phenylene diimine}Ca (II) as well. This catalyst with a phenylene backbone shows an enhanced activity for homopolymerization of TMC when compared to the ethylene backbone (TOF of 1175 vs TOF of 1123). 2 equivalents of n-butyl ammonium azide was used as the cocatalyst in all the runs.

For the block polymerization runs, the ratio of M_1:M_2 was maintained as 1:1. Two different approaches adopted by two separate research groups were followed. Since the homopolymerization of CL with Ca catalyst is extremely slow (20% conversion after 2days with {N,N-bis(3,5-di-*tert*-butyl- salicylidene)-ethylene diimine}Ca (II)), adding CL as the first monomer could not be considered an option. Hence, in our case we have restricted ourselves to the addition of CL as the second monomer to a polymerized sample of TMC. .Table 4.2 summarizes our results of block polymerization of TMC with CL.

Table 4.2. Block polymerization of TMC and CL using {N,N-bis(3,5-di-*tert*-butyl-salicylidene)-phenylene diimine}Ca (II) as the catalyst and 2eq of $[Bu_4N]^+N_3^-$ as co-initiator.

Entry	Time (h)	Temperature (°C)	% composition[a]	
			TMC	CL
1[b]	24	86	69.2	30.8
2[c]	1+24	86	59.9	40.1
3	1+48	86	52.26	47.74
4[d]	1+24	86	75.78	24.22

[a] % composition of each polymer in copolymer obtained by integrating signals corresponding to poly-TMC and poly CL in ^{1}HNMR spectra. [b] Feijan's technique of block polymerization [c] Entry 2,3 & 4 uses Shen's technique of block polymerization. The initial time of 1hr is time for which TMC was allowed to polymerize before addition of ε-CL. [d] {N,N-bis(3,5-di-*tert*-butyl- salicylidene)-ethylene diimine}Ca (II) and 2eq of $[Bu_4N]^+Cl^-$ used for entry 4

Entry 1 & 2 compares our results using the two techniques for block polymerization. According to the technique used by Feijan and coworkers, in a Schlenk flask to a prepolymerized sample of TMC, the required amount of CL was added along with the catalyst. Polymerization was terminated after desired time followed by precipitation from acidified methanol. The second technique used by Shen and coworkers (entry 2),1g of TMC was polymerized with the required amount of catalyst maintaining the M:I ratio of 350:1. After an hour during which the homopolymerization is complete, an equal equivalent of caprolactone was added to the same schlenk flask and the reaction allowed to continue for a desired time.

As is evident, there is substantial increase in the CL composition in the copolymer when Shen's procedure for block polymerization was used. The composition of the copolymer have been determined by integrating the PCL signal at

2.30 ppm and PTMC signal at 2.01ppm. Though theoretically, block polymerization should give a polymer of the structure poly A-b-B with no random units, we do observe random units in the ^{1}HNMR.. A plausible reason for this could be the difference in the polymerization rates of the two monomers. CL is activated by inserting into the TMC chains before homopolymerizing on its own resulting in the formation of the second block. On allowing the polymerization of CL to go on for 48 hrs (Entry 3) till completion, a copolymer containing almost an equal amount each monomer is produced which is in accordance to the initial feed ratio. Figure 4.7 is a typical block polymer obtained from run 3, Table 4.2.

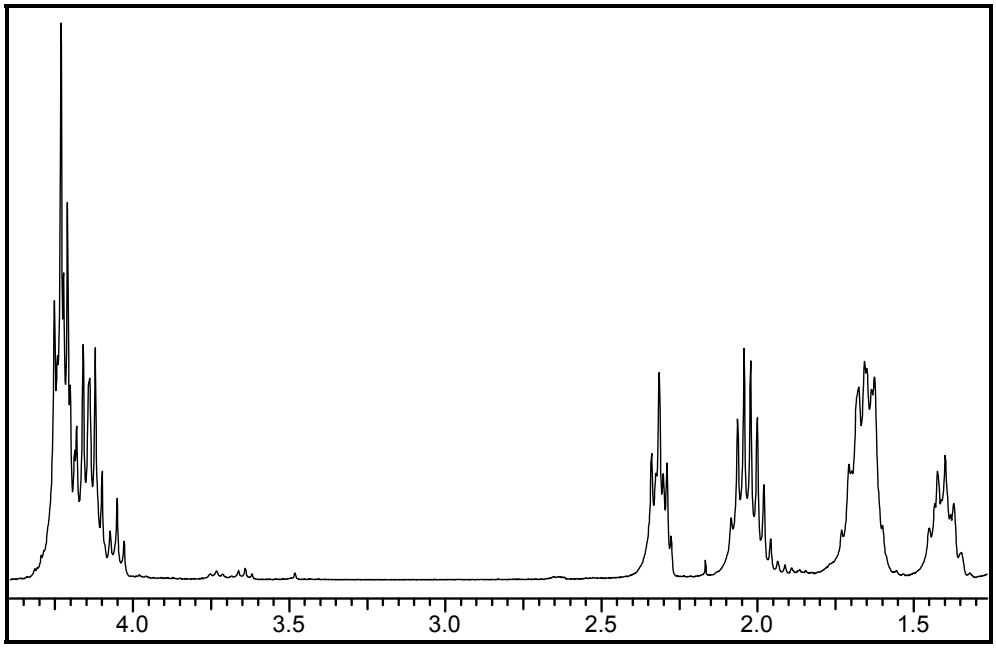

Figure 4.7: ^{1}HNMR of PTMC-b-PCL in $CDCL_3$

An increase in activity is also observed when a more sterically unencumbering catalyst system is used (Figure 4.8) along with a better nucleophile like an azide as a co initiator. The composition of polyCL in the copolymer increases by almost 16%

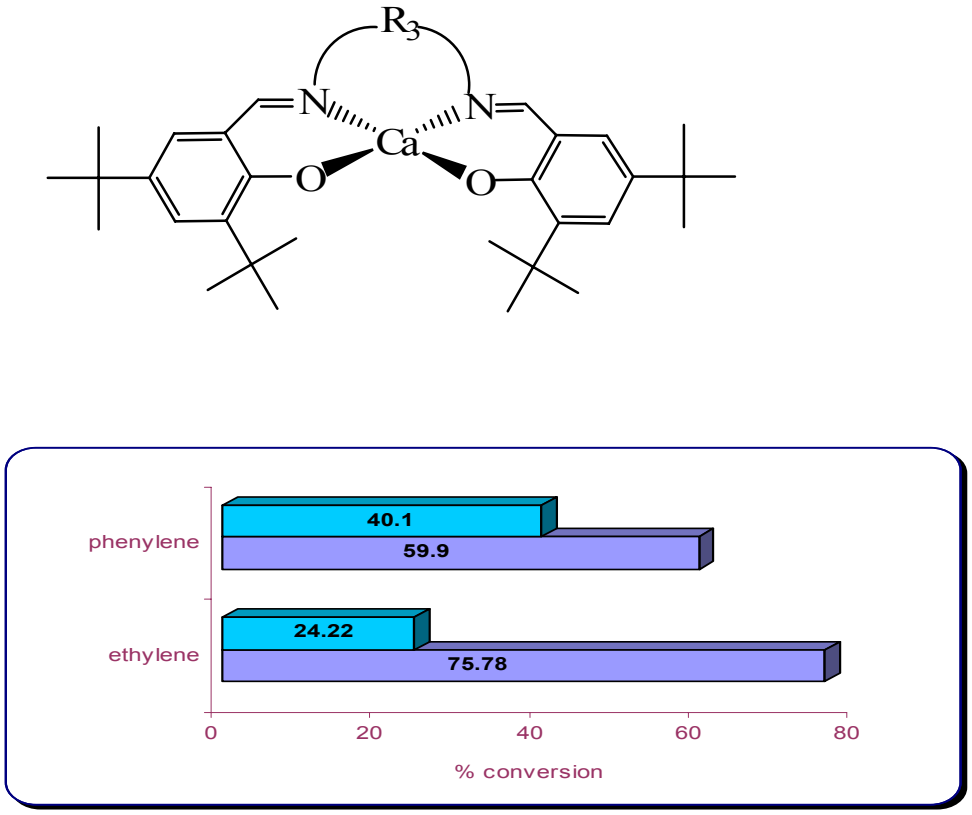

Figure 4.8: Change in individual polymer composition in copolymer as ligand architecture is changed

Conclusions

The synthesis of both random as well as block copolymers containing poly(TMC) and poly(CL) were carried out successfully using a Ca(II) salen system along with an anionic co initiator. We were encountered with an unprecedented situation where our catalyst system was extremely active with respect to one monomer (trimethylene carbonate) and equally inactive for the second monomer (ε-caprolactone).

In spite of this deficiency of our catalyst system, copolymers of structures X, XB and AXB (where X is a random sequence and A & B are pure polymers obtained from monomers TMC and CL) have been obtained. The monomer of superior activity was activating the inferior one. This is especially advantageous in the designing of random copolymers where both the monomers are added together in one pot. We have been able to optimize the reaction conditions by changing the cocatalyst, the central metal of the salen and the temperature of the reaction. By conducting solution studies we were able to see that the rate of polymerization of TMC was 2.3 time faster than the rate of polymerization of CL w.r.t to Ca(II) systems.

Two different techniques of block polymerization was followed. In case of block polymerization too, the presence of polyTMC activated the polymerization of CL. Due to the large difference in the homopolymerization rates, an ideal polymer of the structure AB was never obtained.

Presently, a coworker Wonsook Choi is synthesizing copolymers of TMC with lactides using similar catalyst systems. Unlike ε-caprolactone, lactides can be polymerized quite efficiently by Ca(II) salen systems.

Currently sutures made from homopolymers or copolymers of glycolide, lactide, caprolactone, p-dioxanone and trimethylene carbonate have been cleared for marketing by FDA. In the long run, we hope investigate the biodegradable polymers obtained from each of these monomers extensively using our biometal based catalyst systems.

CHAPTER V

METAL SALEN DERIVATIVES AS CATALYSTS FOR THE ALTERNATING COPOLYMERIZATION OF OXETANE AND CARBON DIOXIDE

Introduction

The alternating copolymerization of CO_2 and epoxides in the presence of heterogeneous metal catalysts to provide polycarbonates, along with cyclic carbonates, was pioneered by Inoue and coworkers in the later 1960s.[3] Since that time the development of discrete metal catalysts for this process has led to greatly enhanced catalytic activity and selectivity, for both *alicyclic* and *aliphatic* epoxides.[70] Nevertheless, the synthesis of polycarbonates from these latter epoxides has been a real challenge due to the propensity of aliphatic epoxides to couple with CO_2 to afford cyclic carbonates, either *via* a direct route or by copolymer degradation.[71] An alternative process for the synthesis of aliphatic polycarbonates is the ring-opening polymerization (ROP) of 6- and 7-membered cyclic carbonates. As we have seen in Chapters II & III, metal salen derivatives are effective homogeneous catalysts for the ROP of the six-membered cyclic carbonate, trimethylene carbonate (TMC or 1,3-dioxan-2-one), eq. (1).[53] This process was found to occur with complete retention of carbon dioxide in the polycarbonate, i.e., there were no ether linkages in the copolymer.

Since four-membered cyclic ethers have only slightly less ring-strain energy than epoxides, it might be anticipated that active catalysts for the CO_2/epoxide coupling process, such as (salen)MX complexes in the presence of a co catalyst, would be effective at coupling CO_2 and oxetanes (Figure 5.1). Importantly, in this instance the

byproduct, cyclic carbonate, unlike that in the epoxide process, can ultimately be transformed into the completely alternating copolymer.

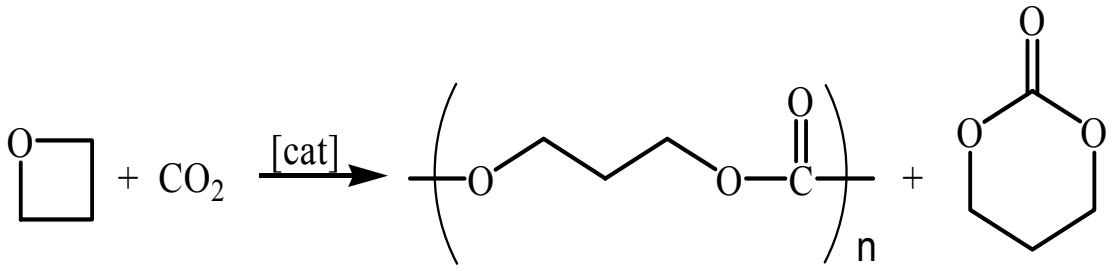

Figure 5.1: Copolymerization of CO_2 and Trimethylene Oxide

Surprisingly, the above reaction has received very limited attention. Organotin compounds were used as initiators for this reaction by Baba and coworkers.[72] However, very low molecular weight polymers were obtained along with polyoxetane units incorporated in the polycarbonate chain.

Experimental

All syntheses were carried out under argon atmosphere using standard Schlenk and glovebox techniques. Solvents were distilled from appropriate reagents before use. All reagents were commercially available and used without further purification unless otherwise indicated. Trimethylene oxide (Lancaster) was stirred under CaH_2 overnight, and then distilled over molecular sieves. The salen ligand {N,N'- bis (3,5-*tert*-butyl-salicylidene) – 1,2 ethylenediamine) was synthesized according to literature procedure.[12] Tetra-*n*-butylammonium halides (Aldrich) were recrystallized from acetone/ether twice before use. Tetra-*n*-butylammonium azide (TCI) was stored in the freezer of the glovebox immediately upon arrival. Bone dry CO_2 was purchased from

Scott Specialty Gases. ^{1}H NMR spectra were recorded on Unity+ 300MHz and VXR 300MHz superconducting NMR spectrometers. Infrared spectra were recorded on a Mattson 6021 FT-IR spectrometer with DTGS and MCT detectors. Molecular weight determinations (M_w and M_n) were carried out at the New Jersey Center for Biomaterials, Rutgers University.

Synthesis of {N,N'- bis (3,5-*tert*-butyl-salicylidene) – 1,2 ethylenediamine)} Aluminum (III) Chloride. The synthesis of {salen} AlCl compound was adapted from the procedure used by Rutherford and Atwood.[50] A 50ml Schlenck flask was charged with 1.0 mmol of the H_2salen ligand and dissolved in 40ml of toluene. A 100ml Schlenk flask was charged with 1.0mmol of a 1.9M toulene solution of Et_2AlCl, and an additional 10ml of toluene was added. The ligand was cannulated into the flask containing the metal, and the mixture was stirred for 12h at room temperature. A yellow precipitate was observed. The reaction mixture was concentrated to ~10ml and approximately 30ml of hexanes was added to precipitate the product. The precipitate was collected by filtration and dried under vacuum.

Synthesis of {N,N'- bis (3,5-*tert*-butyl-salicylidene) – 1,2 ethylenediamine)} Chromium (III) Chloride. One equivalent of the salen ligand and 1.1 equivalent of chromium (II) chloride were dissolved in THF. and stirred under an argon atmosphere for 24 hours. The reaction was then opened to the atmosphere and stirred for additional 24 hours. The reaction mixture was then washed with aqueous saturated NH_4Cl (3 x 100 ml) and aqueous saturated NaCl (3 x 100ml) and then dried over Na_2SO_4. After filtration the solvent was removed in *vacuo*, yielding a red or brown solid.

Polymerization Runs. Both bulk and solution runs were conducted. A typical solution run was carried out using the following protocol. 1 g of oxetane was dissolved in 10ml of toluene, along with the catalyst and cocatalyst and injected *via* inlet port into a Parr autoclave. The M/I ratio was maintained at 675/1 and 2eq of cocatalyst was used. The reactor was subsequently charged to 500 psi with bone dry CO_2. The reaction was allowed to run for at 110°C for a required amount of time. After this time the autoclave was cooled and the CO_2 vented in a fume hood. The reactor was opened, and the polymer was isolated by dissolution in small amounts of methylene chloride followed by precipitation from methanol. For the bulk runs, the catalyst and cocatalyst was dissolved in 4g of oxetane and injected into the Parr autoclave. The M/I ratio was maintained at 1292:1 along with 2eq of cocatalyst.

Characterization was accomplished by ^{1}H NMR and infrared spectroscopy. The amount of ether linkages was determined *via* ^{1}H NMR by integrating peaks corresponding to the methine protons of the polyether at ~3.45 ppm and the polyTMC ~4.21 ppm. An absorbance at 1750cm^{-1} indicated the formation of the polycarbonate. by infrared spectroscopy.

Results and Discussion

In this chapter our preliminary findings utilizing chromium(III) and aluminum(III) salen derivatives as catalysts for the coupling of oxetane(trimethylene oxide) and carbon dioxide to provide completely alternating copolymer and trimethylene carbonate will be reported. Three different studies have been performed involving both solution and bulk investigations. Due to the very high cost of the monomer, we did practice some austerity and restricted ourselves to solution studies unless absolutely necessary. Solution based studies were used to determine the polymer composition with respect to cyclic, polycarbonate and ether formation by varying the cocatalyst, the time and the temperature. Activities were obtained from bulk investigations by using both Cr and Al salen derivatives as catalysts.

Our initial foray at examining the copolymerization reaction of oxetanes and carbon dioxide involved the utilization of the metal salen derivatives shown in Figure 5,2 as catalysts. These particular metal complexes, along with anions as cocatalysts, were previously determined to be among the most active for selective coupling of cyclohexene oxide and CO_2 to poly(cyclohexylene)carbonate.[58,59] Table 5.1 contains data for the copolymerization reaction carried out in toluene at 110ºC. We employed as cocatalysts highly purified alkylammonium salts instead of the hydrophobic PPN(*bis*(triphenylphosphine)iminium) salts because these latter salts are only sparingly soluble in toluene. As is readily seen from Table 5.1, formation of poly(TMC) is favored using either one or two equivalents of the cocatalysts *n*-Bu_4NCl or *n*-Bu_4NN_3, with the latter salt being more selective towards formation of the copolymer. Indeed, in

this instance the utilization of two equivalents of nBu$_4$NN$_3$ afforded 100% copolymer under these conditions with the complete absence of the cyclic trimethylene carbonate (Figure 5.3).

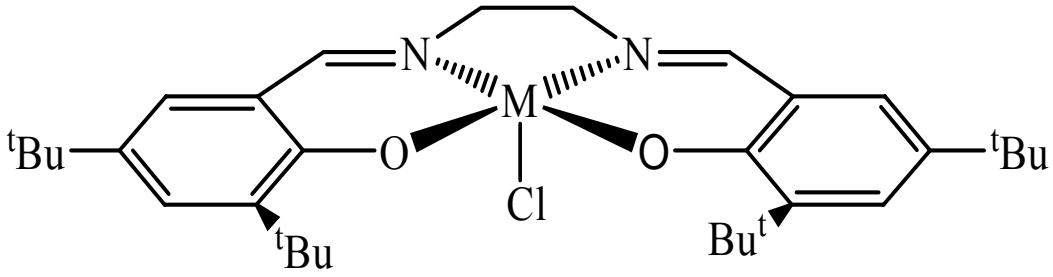

M = Cr(**1**) or Al(**2**)

Figure 5.2: Structure of metal salen catalysts utilized for the copolymerization reactions

Table 5.1. Copolymerization of trimethylene oxide and carbon dioxide in the presence of complex **1**.[a]

Cocatalyst	% TMC [b]	% poly (TMC) [b]
n-Bu$_4$NCl (1 eq)	22.4	77.6
n-Bu$_4$NCl (2 eq)	18.4	81.6
n-Bu$_4$NN$_3$ (1 eq)	6.6	93.4
n-Bu$_4$NN$_3$ (2 eq)	0	100

[a] Copolymerization conditions: 17 mg of catalyst 1 (0.15 mol %), M/I = 675:1, 10 mL of toluene, 35 bar CO_2, 110ºC, 24 hr reaction time.
[b] Based on ^{1}H NMR measurements at ~100% conversion.

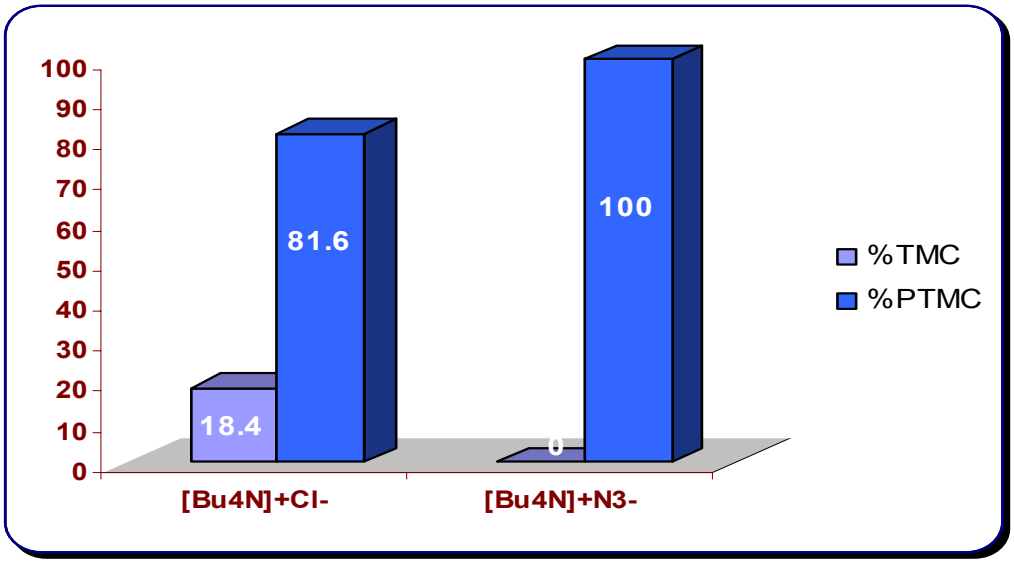

Figure 5.3: Effect of change in cocatalyst on the cyclic carbonate to polymer ratio

During investigations on the ring opening polymerization of trimethylene carbonate, we have been able to establish that complex 1 (Cr salen derivative) is a rather poor catalyst for the ring-opening polymerization of TMC to poly(TMC) resulting in a turnover frequency of 50 mol of TMC/ mole of catalyst–hr.. Al salen derivatives on the other hand show a far better activity (TOF = 82) for the same process under similar conditions. This trend is just reverse of the case of epoxide / CO_2 copolymerization were Cr(III) salen derivatives are by fare the more superior catalysts compared to their Al(III) counterparts.

Hence it became imperative to ascertain whether the copolymer produced originated from TMC or the formation of PTMC was the main reaction. For this purpose we carried out a series of time dependent studies in solution. In the past our efforts to understand the mechanistic aspects of the copolymerization of epoxides and

CO_2 have been greatly aided by the use of *in situ* infrared spectroscopy. Unfortunately, at this point we have been unable to resolve problems associated with this technique for this monomer, and hence have resorted to carrying out time dependent bulk polymerization reactions under identical reaction conditions. As shown Figure 5.4, ^{1}HNMR has been extensively to analyze the products and determine the composition of the polymer. The signal for polyTMC appears at 4.21 ppm, whereas the methane protons corresponding cyclic carbonate (TMC) is observed at 4.47ppm. The triplet between 3.4-3.5ppm is indicative of ether linkages formed by successive ring opening of oxetane with carbon dioxide insertion. The monomer appears as a triplet more downfield at 4.73ppm.

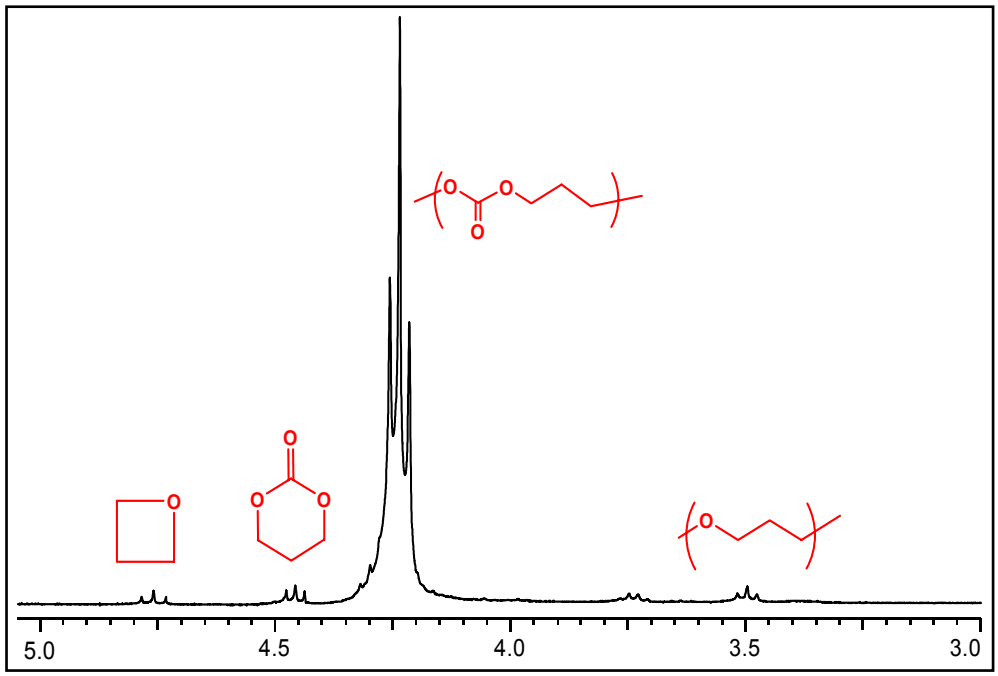

Figure 5.4: ^{1}HNMR spectra of the copolymerization reaction of CO_2\oxetane in $CDCl_3$

Table 5.2 contains the results of our time dependent study where, it is apparent that the selectivity of reaction catalyzed by complex 1 in the presence of 2 eq. of *n*-Bu_4NCl is independent of time. That is, examination of the copolymerization process over five time periods ranging from 4hrs to 24 hrs demonstrated that the ratio of poly(TMC) to TMC of 5.3 displayed no apparent time-dependence, as is evident from Figure 5.5. Hence, poly(TMC) is a primary product from the coupling of trimethylene oxide and CO_2, and *not* the byproduct of ring-opening polymerization of first formed TMC.

Secondly, when the run in entry 3 was conducted at the lower temperature of 90ºC the selectivity for completely alternating copolymer production was greatly enhanced (by 11.5%). Similar observations have been noted for the epoxide/CO_2 coupling process where we have observed that temperature elevation favors the formation of the cyclic carbonate.

Table 5.2. Time-dependent copolymerization runs of trimethylene oxide and CO_2 catalyzed by complex 1 in the presence of two equivalents of *n*-Bu_4NCl.[a]

entry	Time (hrs)	% TMC [b]	% poly(TMC) [b]	% CO_2 content of copolymer [b]
1	4	19.7	80.3	91.0
2	8	17.9	82.1	96.4
3	16	15.2 (3.7)[c]	84.8(96.3)[c]	88.9 (>99)[c]
4	18	11.2	88.8	90.1
5	24	16.2	83.8	93.7

Copolymerization conditions: 17 mg of 1, M/I = 675, 10 mL of toluene, 35 bar CO_2, 110ºC. [b] Respective average values with standard deviations for the five entries are 16.0 ± 2.3%, 84.0 ± 2.3%, 92.0 ± 3.0%. [c] Temperature lowered to 90ºC.

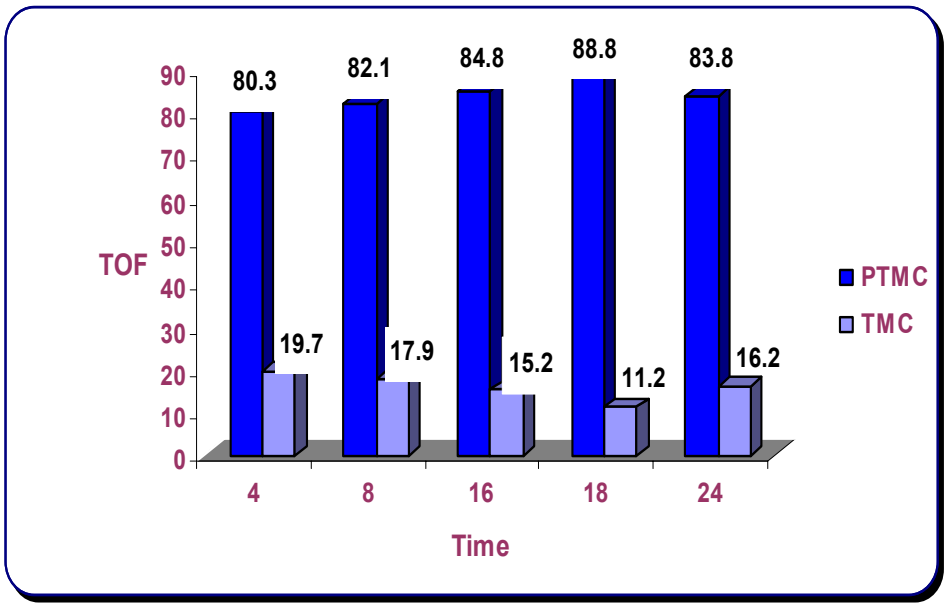

Figure 5.5: Time dependent studies of oxetane\CO_2 copolymerization

We have performed additional coupling reactions of trimethylene oxide and CO_2 in the absence of organic solvent, i.e., in CO_2-expanded TMO, for comparison with previously reported epoxide/CO_2 copolymerization reactions. Turnover frequencies could only be obtained from these bulk runs. . These results are provided in Table 5.3, where both complexes 1 and 2 were employed as catalysts in the presence of anionic cocatalysts. As is apparent from the data in Table 5.3, the chromium salen derivative is much more effective than its aluminum analog by almost 38% (Figure 5.6). This is consistent with observations for the epoxide/CO_2 copolymerization process.

Furthermore, the coupling of CO_2 and TMO occurs at a reduced rate compared to propylene oxide and cyclohexene oxide and CO_2. This latter observation is not

unanticipated based on the fact that ring-opening of three-membered cyclic ethers is energetically favored over their four-membered counterparts. What is extremely encouraging about these results is that the selectivity for copolymer formation from oxetane and CO_2 is very high (>97%) in all instances, even at 110ºC where the selectivity for propylene oxide and CO_2 is generally 100% in favor of monomeric propylene carbonate.

Table 5.3. Copolymerization of trimethylene oxide and CO_2 with (salen)MCl (M = Al, Cr) catalysts.[a]

Catalyst	Cocatalyst[b]	% TMC	% poly(TMC)	% CO_2 content	TOF[c]
1	*n*-Bu_4NCl	2.9	97.1	96.7	41.2[d]
1	*n*-Bu_4NN_3	1.7	98.3	95.9	38.8[e]
2	*n*-Bu_4NCl	1.7	98.3	94.2	8.59[d]

[a] Copolymerization conditions: Catalyst loading = 0.138 mol %, 4.0 g of TMO, 110ºC, M/I = 1292, 35 bar CO_2. [b] Two equivalents of cocatalyst. [c] Measured in mol TMO consumed/mol of metal•hr. [d] Reaction time = 7.5 hr. [e] Reaction time = 6.5 hr.

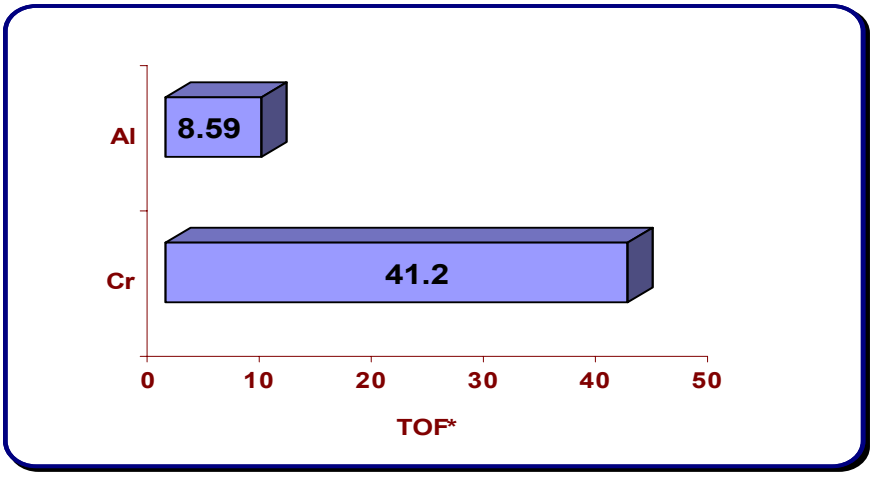

Figure 5.6: Effect of change of central metal atom on the rate of polymerization

The molecular weights of the copolymers reported in Table 5.3 produced from catalyst 1 in the presence of cocatalysts *n*-Bu_4NCl and *n*-Bu_4NN_3 were determined by GPC to be 10,100 and 7,400 with corresponding PDIs of 1.58 and 1.51, respectively. Furthermore, a low molecular weight copolymer produced from a reaction catalyzed by complex 1 and one equivalent of *n*-Bu_4NN_3 revealed *only* an azide end-group by MALDI-TOF-MS. Consistent with this observation this copolymer possessed a ν_{N3} vibrational frequencies at 2102 cm^{-1} in CH_2Cl_2 which is representative of an organic azide. Hence, in this instance for the initiation step (Figure 5.7) where X = N_3, monomer enchainment is occurring on one side of the metal(salen) plane. This may not be true here for X = Cl as proposed in other related cases for epoxide ring-opening processes. Studies to address this issue, as well as investigations into the mechanistic aspects of the oxetane/CO_2 coupling reaction for a variety of oxetane derivatives in the presence of optimized metal catalysts are currently underway in our laboratories.

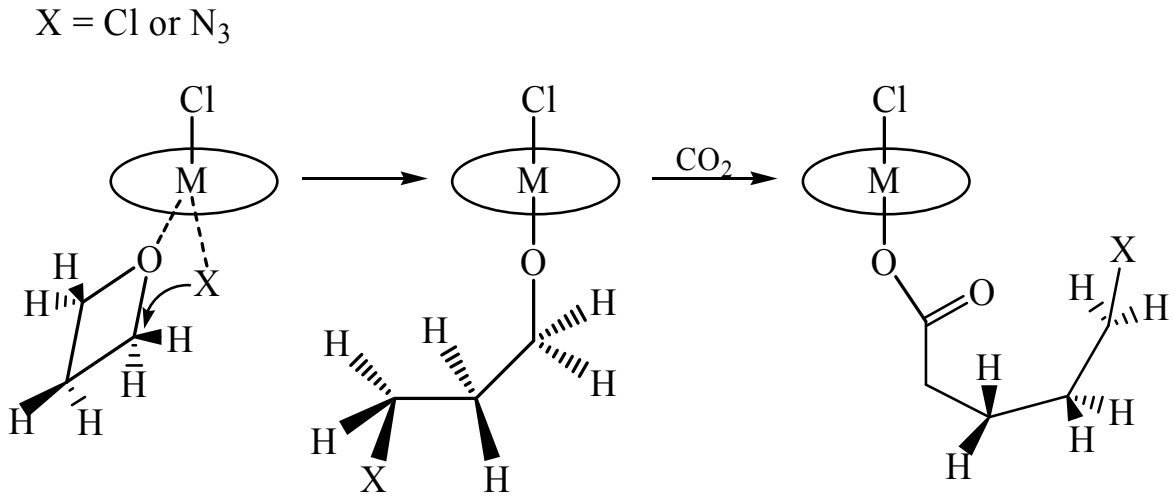

Figure 5.7: Plausible initiation step where X = N_3

Conclusions

Metal salen derivatives of chromium and aluminum, along with *n*-Bu_4NX (X = Cl or N_3) salts, were shown to be effective catalysts for the selective coupling of CO_2 and oxetane (trimethylene oxide) to provide the corresponding polycarbonate with only trace quantities of ether linkages. The catalyst needs for this system parallels those of the epoxide/CO_2 with Cr derivatives being more active than their Al counterparts. Polymers obtained with *n*-Bu_4NN_3 as the coinitiator showed a higher selectivity for the polymer, than *n*-Bu_4NCl. The formation of copolymer was demonstrated *not* to proceed *via* the intermediacy of trimethylene carbonate which was observed as a minor product of the coupling reaction, through our time dependent studies. It was further shown that formation of this latter six-membered cyclic carbonate could be retarded upon lowering the reaction temperature. For a reaction catalyzed by (salen)CrCl in the presence of *n*-Bu_4NN_3 as cocatalyst, both MALDI-TOF-MS and infrared spectroscopy revealed an azide end group in the copolymer

Future efforts in this area will focus on optimizing this reaction by modifying the sterics and electronics of the salen ligands, along with the use of different metal salen derivatives. Though right now, we have been conducting our time dependent studies in solution and then monitoring the product by ^{1}HNMR on completion, we hope to find a suitable spectroscopic technique for constant monitoring, to get mechanistic information regarding this process..

The research presented in this chapter is just the tip of the iceberg for this route of making polytrimethylene carbonate. Though the activities obtained by the use of

these metal salen derivative are far better than those in the previously published literature, they still pale in comparison to the alternate route of making polytrimethylene carbonate- by the ring opening polymerization of trimethylene carbonate. We hope that through proper catalyst design, this novel and green route of making the biodegradable polymer poly trimethylene carbonatepolit will receive the same visibility and commercial viability as ROP of cyclic carbonates.

CHAPTER VI

THE STRUCTURAL CHARACTERIZATION OF SEVERAL $(CO)_3(DPPP)MNX$ DERIVATIVES, DPPP = DIPHENYLPHOSPHINOPROPANE AND X = H, OTS, OC_2H_5, CL, BR OR N_3. AN ASSESSMENT OF THEIR EFFICACY FOR CATALYZING THE COUPLING OF CARBON DIOXIDE AND EPOXIDES

Introduction

The coupling reaction of carbon dioxide and epoxides to provide polycarbonates or cyclic organic carbonate represents one of the most promising reactions for the large scale utilization of this low cost C1 feedstock (eq. 1).[73] These CO_2 derived products are extremely useful materials, and this synthetic route affords an environmentally benign alternative pathway to their production than that commonly employed. That is, polycarbonates are a class of thermoplastics highly regarded for their optical clarity, exceptional impact resistance, and ductility.[1] Similarly, cyclic organic carbonates are of interest for use in a variety of applications, including high-boiling solvents,[74] additives for hydraulic fluids,[75] and the curing of phenol-formaldehyde resins,[76] plus many more.[77] The catalytic coupling of CO_2 and epoxides was first reported by Inoue and coworkers in 1969, employing a heterogeneous catalyst derived from $Zn(CH_2CH_3)_2$ and H_2O. More recently, this process has received a great deal of attention utilizing well defined, more active, homogeneous catalysts. .

---

* Reprinted with permission from "The Structural Characterization of Several $(CO)_3$(dppp)MnX Derivatives, dppp = diphenylphosphinopropane and X = H, OTs, OC_2H_5, Cl, Br or N_3. An Assessment of Their Efficacy for Catalyzing the Coupling of Carbon Dioxide and Epoxides" by D.J.Darensbourg, 2004. *Organometallics, 23*, 6025-6030. © 2004 by American Chemical Society.

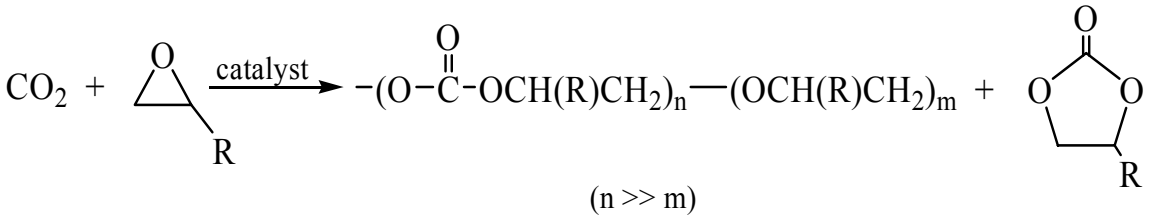

Figure 6.1: Scheme of CO_2\ epoxide copolymerization

As shown in Figure 6.1, successive ether enchainment leading to polyethers linkages in the copolymer is an undesirable reaction which accompanies the completely alternating copolymerization process.

A fundamental step in the CO_2/epoxide coupling reaction is insertion of carbon dioxide into the metal-alkoxide bond subsequent to the epoxide ring-opening process. Indeed, in some instances this insertion reaction can be rate-limiting. Hence, transition metal alkoxides are of particular interest as models in this regard since they undergo insertion of small molecules like CO_2 or CS_2 into the metal-oxygen bond.[78] For example, Orchin and coworkers have reported the synthesis of octahedral manganese alkoxide complexes of the general formula, $(CO)_3$(dppp)MnOR, and have examined their ability to reversibly insert CO_2 into the Mn-OR bond to give the corresponding carbonate complexes.[79] *In situ* infrared spectroscopic kinetic studies by our group showed that the insertion of carbon dioxide into the Mn-OR bond occurred instantaneously at -78ºC *via* a concerted mechanism, Figure 6.2.[80] Because of the rapidity of this process, only a lower limit for the second-order constant could be established of $2.0 \times 10^{-3} M^{-1}$-$sec^{-1}$ at -78ºC.

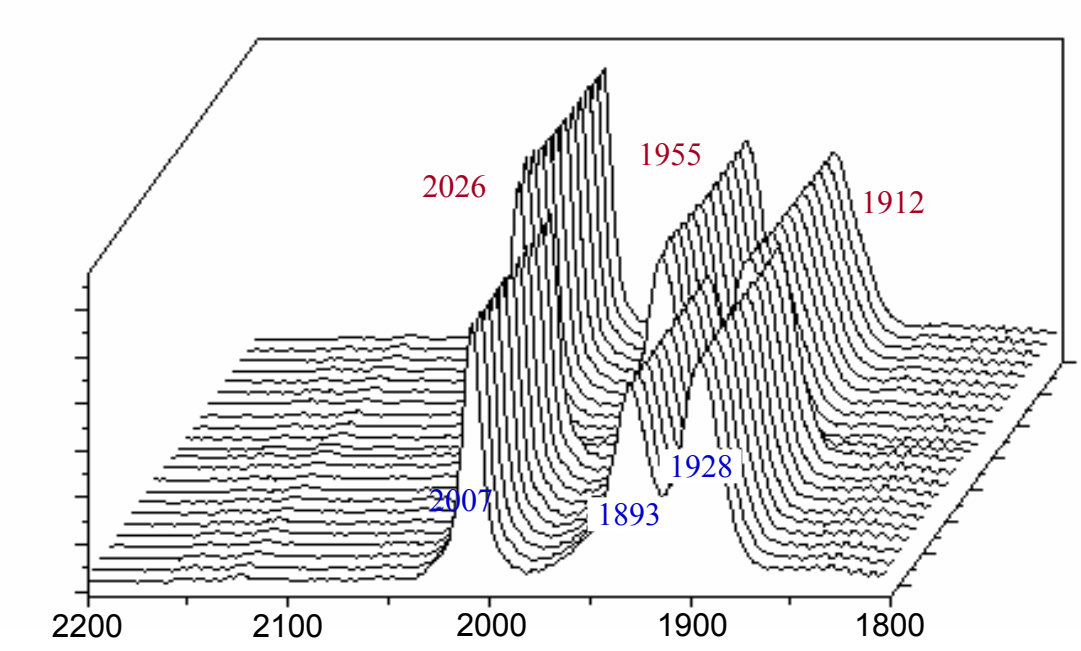

Figure 6.2: Monitoring the insertion of CO_2 in the Mn-OR complex by *in situ* Infrared spectroscopy

This finding prompted us to wonder whether these and other $(CO)_3$(dppp)MnX derivatives could serve as catalysts or catalyst precursors for the CO_2 epoxide coupling reaction. In this report we will present our observations on the subject along with mechanistic implications. Included in this study are the X-ray crystallographically defined structures of these $(CO)_3$(dppp)MnX (X = H, OTs, OC_2H_5, Cl, Br, and N_3) derivatives.

Experimental

All syntheses were carried out under argon atmosphere using standard Schlenk and glovebox techniques. Solvents were distilled from appropriate reagents before use. All reagents were commercially available and used without further purification unless otherwise indicated. The synthetic precursors $Mn_2(CO)_{10}$ and diphenylphosphinopropane were purchased from Aldrich Chemical Company. Bone dry CO_2 was purchased from Scott Specialty Gases. Infrared spectroscopy was recorded using a Mattson 6021 FTIR spectrometer. ^1H NMR spectra were recorded on a 300 MHz Varian Unity Plus spectrometer.

Preparation of *fac*-$(CO)_3$(dppp)MnH (1). The methodology employed in this synthesis was identical to that reported by Orchin and coworkers.[79] X-ray quality crystals were grown by the slow diffusion of hexane to a benzene solution of **1**.

Preparation of *fac*-$(CO)_3$(dppp)MnOTs (2). 2 was synthesized by a previously published procedure.[79] Yellow-orange crystals were obtained from the diffusion of hexane to a concentrated solution of **2** in CH_2Cl_2.

Preparation of *fac*-$(CO)_3$(dppp)MnOC_2H_5 (3). 1.0g (1.72 mmol) of *fac*-$(CO)_3$(dppp)MnOCH_3 **(3a)**, the synthesis of which has already been reported, was slurried with 25 mL of dry ethanol and stirred for 2 h. After 2 h the yellow solid was collected by filtration and washed with 5 mL of hexane.[79] X-ray quality crystals were obtained by slow diffusion of hexane into a concentrated benzene solution of **3**.

Preparation of *fac*-$(CO)_3$(dppp)MnCl (4) and *fac*-$(CO)_3$(dppp)MnBr (5). The syntheses of **4** and **5** have been reported in literature previously.[81,82] Crystals were

grown by slow evaporation of a concentrated CH_2Cl_2 solution of the respective complex into toluene.

Preparation of *fac*-$(CO)_3$(dppp)MnN_3 (6). *fac*-[$(CO)_3$(dppp)$Mn(OH_2)$]BF_4 **(6a)** was synthesized by a previously published procedure.[83] **6a** (0.05 g, 0.1107 mmol) was added with 30 mL of CH_3CN to a suspension of excess NaN_3 in CH_3CN. The mixture was stirred overnight, filtered and the solvent removed under reduced pressure. The spectroscopic data agreed with those previously reported.[13] X-ray quality crystals were grown by a slow diffusion of hexane to a CH_2Cl_2 solution of **(6)**.

X-ray Diffraction Studies. A Bausch and Lomb 10x microscope was used to identify suitable crystals from a representative sample of crystals of the same habit. Crystals were coated with mineral oil, placed on a glass fiber, and mounted on a Bruker SMART 1000 CCD diffractometer. X-ray data were collected covering more than a hemisphere of reciprocal space by a combination of three sets of exposures. Each exposure had a different φ angle for the crystal orientation and each exposure covered 0.3º in ω. The crystal to detector distance was 4.9 cm. Decay was monitored by repeating collection of the initial 50 frames collected and analyzing the duplicate reflections. Crystal decay was negligible. The space group was determined on the basis of systematic absences and intensity statistics. The structure was solved by direct methods and refined by full-matrix least squares on F^2. All non-hydrogen atoms were refined with anisotropic displacement parameters. All H atoms were placed in idealized positions with fixed isotropic displacement parameters equal to 1.5 times (1.2 for methyl

protons) the equivalent isotropic displacement parameters of the atom to which they are attached.

The following programs were used: data collection and cell refinement, SMART[16]; data reduction, SAINTPLUSS (Bruker[84]); programs used to solve structures, SHELXS-97 (Sheldrick[85]); programs used to refine structures, SHELXL-99 (Sheldrick[86]) ; molecular graphics and publication materials, SHELXTL-Plus version 5.0 (Bruker[87]).

Copolymerization of CO_2 and Epoxides. A typical reaction was carried out using the following protocol. 50 mg of the catalyst was dissolved in 20 mL of cyclohexene oxide and injected *via* inlet port into a Parr autoclave. The reactor was subsequently charged to 500 psi with bone dry CO_2 and stirred at 80º for 24 h. After this time the autoclave was cooled and the CO_2 vented in a fume hood. The reactor was opened, and the polymer was isolated by dissolution in small amounts of methylene chloride followed by precipitation from methanol.

Characterization was accomplished by ^{1}H NMR and IR spectroscopy. The amount of ether linkages was determined *via* ^{1}H NMR by integrating peaks corresponding to the methane protons of the polyether at ~3.45 ppm and the polycarbonate at ~4.6 ppm.

Results and Discussion

The syntheses of all of the $(CO)_3$(dppp)MnX complexes utilized in this study have been previously reported in the literature. Most of these complexes originate from the hydride derivative, $(CO)_3$(dppp)MnH (**1**), which is synthesized by refluxing manganese decacarbonyl and the ligand, 1,3-bis(diphenylphosphinopropane) in propanol as shown in Figure 6.3. The routes to making the other Mn(I) complexes of interest are shown in Figure 6.3. In all instances we were able to find suitable conditions to obtain crystalline samples for carrying out X-ray crystallographic studies of these derivatives.

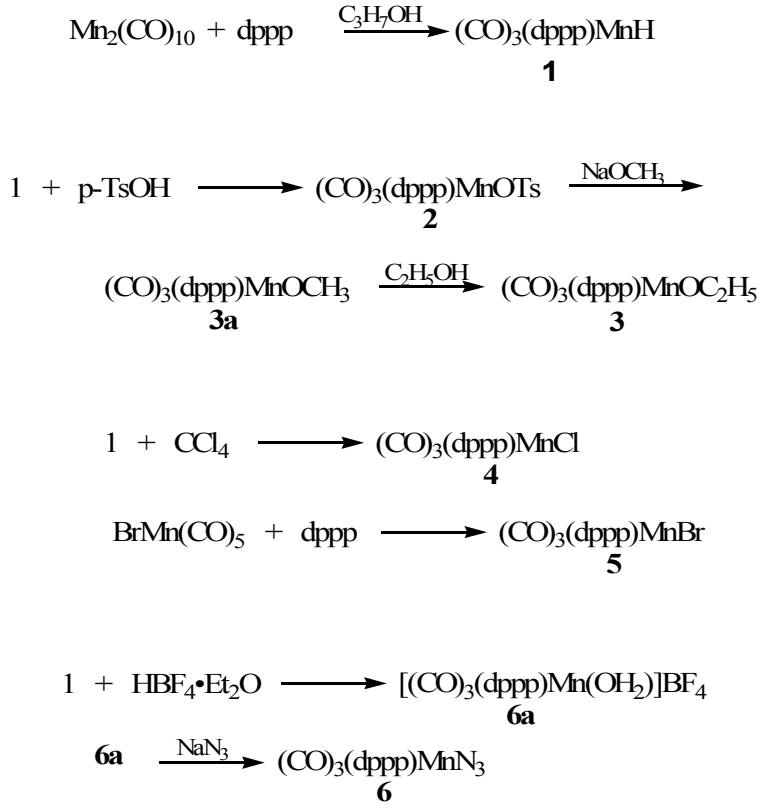

Figure 6.3: Syntheses of $(CO)_3$(P-P)Mn(I) complexes

The structures of molecules **1-6** are indicative of a manganese atom octahedrally coordinated to three (*facial*) terminal carbonyl groups, a chelating diphenylphosphino-propane (dppp) ligand, and a nucleophile (X). The latter group is *trans* to one carbonyl and has a *cis* orientation to the remaining two carbonyls as well as the chelating ligand as has been observed by Orchin and coworkers for one such derivative.[79] Table 6.1 contains crystallographic and structure refinement data for complexes **1-6**. All thermal ellipsoid drawings are at 50% probability and the hydrogen atoms have been omitted for clarity with the exception of the hydride in complex **1**. The relevant bond distances and bond angles based on the atomic numbering scheme in these figures are listed in Table 6.2.

The molecular structure of **1** is provided in Figure 6.4. Complex **1** crystallized in the space group P-1 with two molecules in the asymmetric unit. The position of the hydrogen atom was located by a difference map to define the average Mn–H bond length of 1.72 Å.

Table 6.1. Crystallographic data and data collection parameters for complexes **1**-**6**.

	1	**2**	**3**	**4**	**5**	**6**
Empirical formula	$C_{30}H_{27}MnO_3P_2$	$C_{37}H_{33}MnO_6P_2S$	$C_{32}H_{31}MnO_4P_2$	$C_{30}H_{26}ClMnO_3P_2$	$C_{30}H_{26}BrMnO_3P_2$	$C_{30}H_{26}N_3MnO_3P_2$
Crystal system	Triclinic	Monoclinic	Triclinic	Monoclinic	Monoclinic	Monoclinic
Space group	P-1	P2(1)/n	P-1	P2(1)/n	P2(1)/n	P2(1)/c
Volume ($Å^3$)	2634.3(15)	3385.7(17)	1443.7(12)	2696.8(8)	2739.4(19)	3208.7(12)
a(Å)	11.017(4)	10.539(3)	7.921(4)	9.9382(18)	10.073(4)	12.826(3)
b(Å)	15.451(5)	14.793(4)	10.031(5)	20.643(3)	20.612(8)	17.209(4)
c(Å)	15.773(5)	21.716(6)	18.271(9)	13.666(3)	13.765(6)	15.102(3)
α(°)	95.888(6)	90	94.634(8)	90	90	90
β(°)	90.886(6)	90.534(5)	93.541(9)	105.871(3)	106.551(7)	105.727(4)
γ(°)	99.3047(7)	90	91.340(9)	90	90	90
Temperature (K)	110(2)	110(2)	110(2)	110(2)	273(2)	110(2)
$d_{calc}(g/cm^3)$	1.393	1.418	1.372	1.445	1.531	1.39
Z	4	4	2	4	4	4
$\mu(mm^{-1})$	0.653	0.592	0.604	0.738	2.088	0.552
Reflections collected	11907	14890	6428	12136	12140	14172
Independent Reflections	7558	4885	4098	3879	3954	4611
Parameters	657	425	353	334	334	406
Goodness-of-Fit on F^2	1.051	1.094	1.043	0.968	1.159	1.08
Final R indices [I>2sigma(I)]	R_1= 0.0798	R_1= 0.0382	R_1= 0.0726	R_1= 0.0730	R_1= 0.0598	R_1= 0.0623
R indices (all data)	wR_2= 0.1078	wR_2= 0.0437	wR_2= 0.1017	wR_2=0.1430	wR_2= 0.0737	wR_2= 0.0875

[a] $R_1 = \Sigma||F_o|-|F_c||/\Sigma|F_o|$ [b] $wR_2 = \{[\Sigma w(F_o^2-F_c^2)^2]/[\Sigma w(F_o^2)^2]\}^{1/2}$.

Table 6.2. Selected bond lengths (Å) and angles(deg) for complexes **1**-**6**.

Complex 1			
Mn(1A)-H(1A)	1.735(19)	Mn(1A)-C(1A)	1.8120(6)
Mn(1A)-P(1A)	2.2881(18)	Mn(1A)-C(2A)	1.837(6)
Mn(1A)-P(2A)	2.2927(17)	Mn(1)-C(3A)	1.814(7)
P(2A)-Mn-P(1A)	89.42		
C(2A)-Mn-H(1A)	175.4(19)		
Mn(1B)-H(1B)	1.71(6)	Mn(1B)-C(1B)	1.814(7)
Mn(1B)-P(1B)	2.3047(16)	Mn(1)-C(2B)	1.809(5)
Mn(1B)-P(2B)	2.2828(18)	Mn(1)-C(3B)	1.812(6)
P(2B)-Mn-P(1B)	89.42		
C(2B)-Mn-H(1B)	175.4(19)		
Complex 2			
Mn(1)-O(1)	2.092(2)	Mn(1)-C(27)	1.774(3)
O(1)-S(1)	1.495(2)	Mn(1)-C(26)	1.833(3)
S(1)-O(2)	1.439(2)	Mn(1)-C(36)	1.834(3)
S(1)-O(3)	1.431(2)		
S(1)-C(28)	1.769(3)		
C(26)-Mn(1)-O(1)	178.27(11)	O(1)-S(1)-C(28)	102.78(12)
O(3)-S(1)-O(2)	115.42(14)		
Complex 3			
Mn(1)-O(4)	2.037(3)	Mn(1)-C(1)	1.841(7)
O(4)-C(31)	1.394(7)	Mn(1)-C(2)	1.832(6)
C(31)-C(32)	1.534(8)	Mn(1)-C(3)	1.789(6)
C(31)-O(4)-Mn(1)	117.7(3)		
P(1)-Mn(1)-P(2)	90.54(6)		
Complex 4			
Mn(1)-Cl(1)	2.379(2)	Mn(1)-C(3)	1.802(9)
Mn(1)-C(1)	1.814(9)		
Mn(1)-C(2)	1.754(9)		
C(2)-Mn-Cl(1)	174.9(3)		
Complex 5			
Mn(1)-Br(1)	2.5189(11)	Mn(1)-C(3)	1.821(6)
Mn(1)-C(1)	1.816(6)		
Mn(1)-C(2)	1.783(6)		
C(2)-Mn-Br(1)	174.02(17)		
Complex 6			
Mn(1)-N(1)	2.126(3)	Mn(1)-C(1)	1.816(5)
N(1)-N(2)	1.164(5)	Mn(1)-C(2)	1.832(5)
N(2)-N(3)	1.200(6)	Mn(1)-C(3)	1.799(5)
N(2)-N(1)-Mn(1)	117.2(3)	N(1)-N(2)-N(3)	175.4(4)

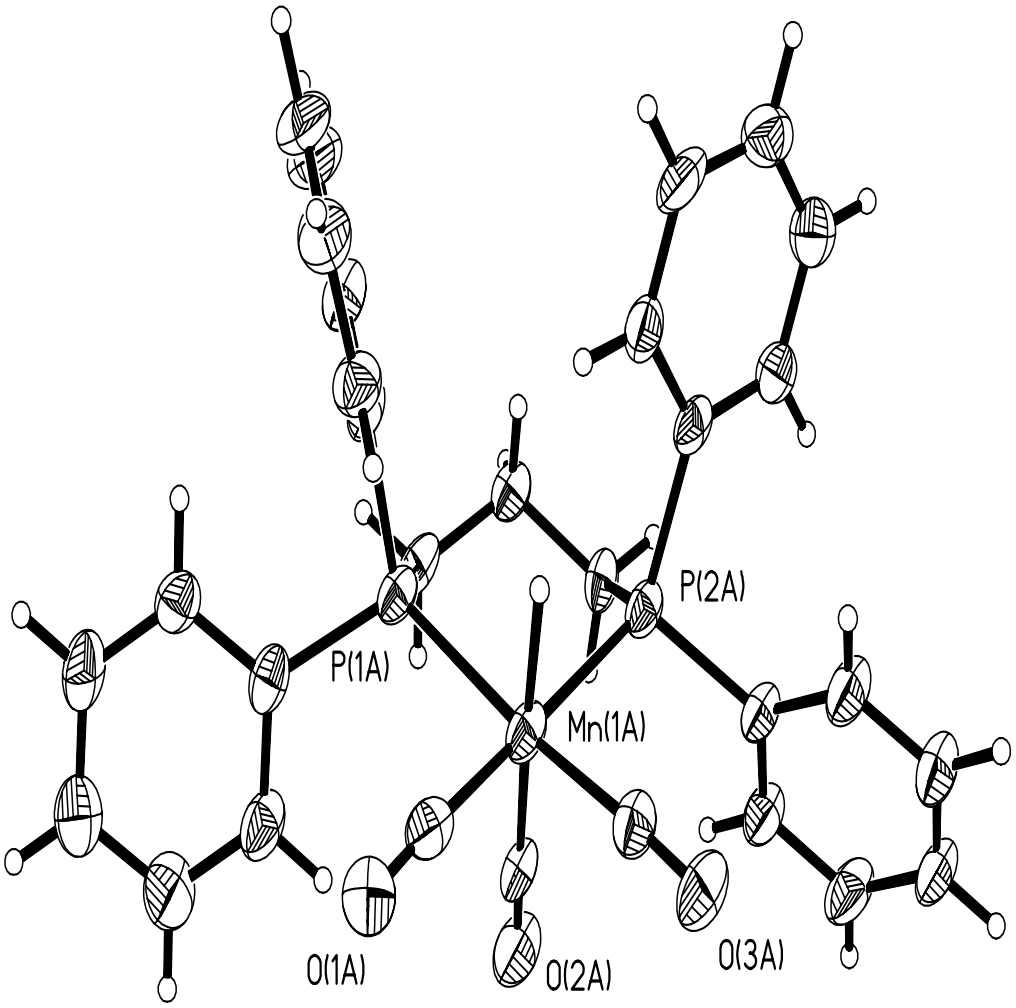

Figure 6.4: Thermal ellipsoid representation of *fac*-$(CO)_3$(dppp)MnH, **1**

Complex **2**, $(CO)_3$(dppp)MnOTs, crystallized in the space group $P2_1/n$. A thermal ellipsoid representation is shown in Figure 6.5. Selected bond distances and bond angles are tabulated in Table 6.2. Notably, the Mn–tosylate bond length was found to be 2.092(2) Å, with the tosylate S(1)–O(1) bond distance of 1.495(2)Å being slightly longer than the S(1)–O(2) and S(1)–O(3) distances which average 1.435 Å. The sulfur-phenyl ring (S(1)–C(28)) bond length was determined to be 1.769(3) Å. As expected the two types of carbonyl ligands have different Mn–C distances, with the *Mn–C*O_{axial} bond length of 1.774(3) Å shorter than the *Mn–C*O_{eq} average distance of 1.833(3) Å.

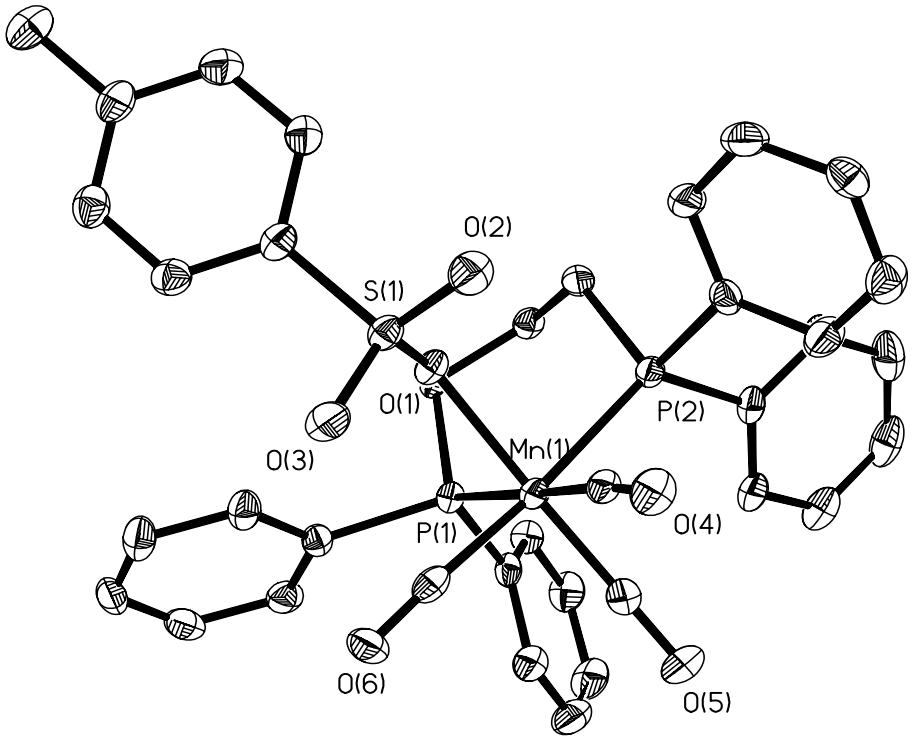

Figure 6.5: Thermal ellipsoid representation of *fac*-$(CO)_3$(dppp)MnOTs, **2**

We were extremely fortunate to isolate in crystalline form and characterize *via* X-ray crystallography the $(CO)_3$(dppp)MnX derivative where X = ethoxide, Figure 6.6. In general the alkoxide group in the absence of electron-withdrawing substituents affords complexes which are extremely reactive towards trace quantities of CO_2 in the atmosphere even in the solid-state. Typically, these derivatives are characterized in the solid-state as their CO_2 inserted product. For example, the structure of the methoxide analog of **3** was reported as its alkoxycarbonate derivative, $(CO)_3$(dppp)MnOC(O)OCH_3. Complex **3** crystallized in the triclinic space group P-1. The Mn–O bond distance of 2.037(3) Å compares favorably to the Mn–O bond distance of 2.029(3) Å observed in the *fac*-$(CO)_3$(dppp)MnOC(O)OCH_3 derivative.[79] As was observed in complex **2**, the *Mn–C*O_{axial} bond length of 1.789(6) Å is significantly shorter than the *Mn–C*$O_{eq.}$ distance of 1.841(7) Å. A thermal ellipsoid representation of **3** is provided in Figure 6.6.

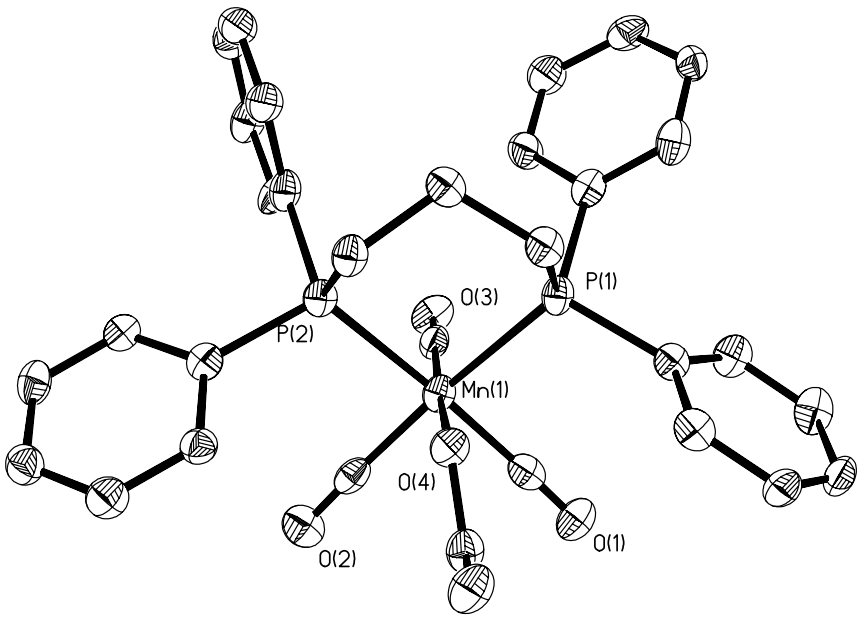

Figure 6.6: Thermal ellipsoid representation of *fac*-$(CO)_3$(dppp)MnOC_2H_5, **3**

The halide derivatives, complexes **4** and **5**, crystallized in the monoclinic space group $P2_1/n$. The Mn–Cl bond length in **4** of 2.379(2) Å is comparable to that seen in the closely related derivative, *fac*-$(CO)_3$(depe)MnCl, of 2.406(2) Å. The Mn–Br bond length in complex **5** of 2.518(9) Å, is as expected based on the difference in the covalent radii of 0.15 Å of the two halogen atoms. Unlike complex **3**, these manganese derivatives are very air stable. Figures 6.7 and 6.8 depict the thermal ellipsoid representations of complexes **4** and **5**.

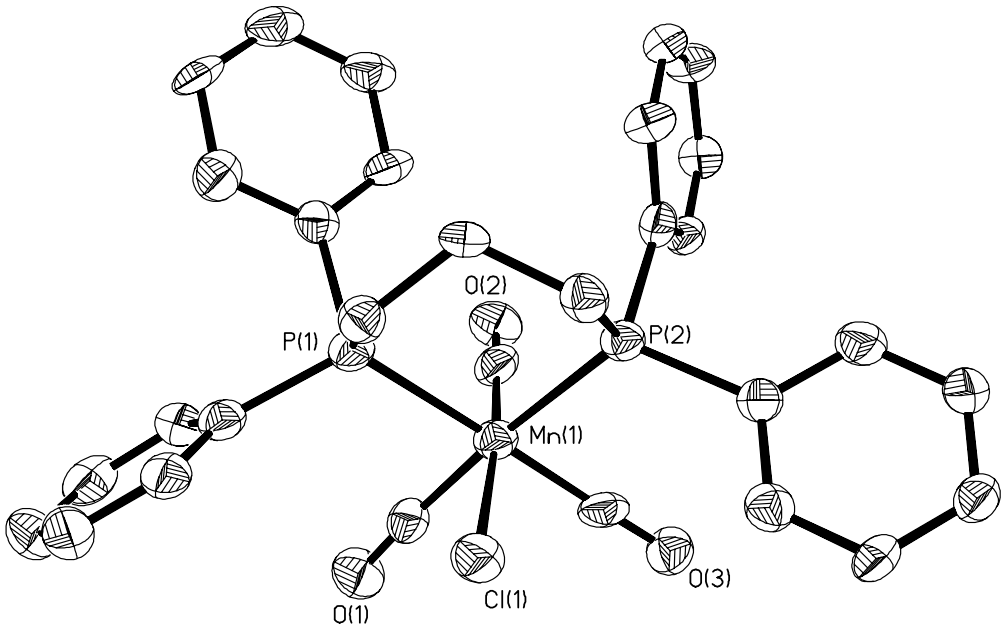

Figure 6.7: Thermal ellipsoid representation of *fac*-$(CO)_3$(dppp)MnCl, **4**.

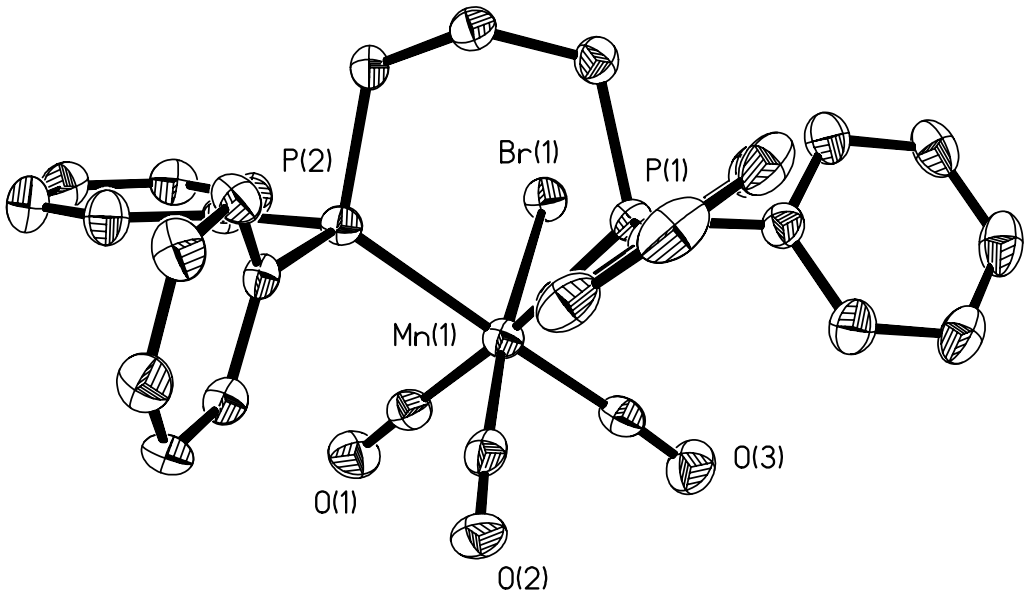

Figure 6.8: Thermal ellipsoid representation of *fac*-$(CO)_3$(dppp)MnBr, **5**.

In our studies involving the use of (salen)$Cr^{III}X$ (X = Cl or N_3) complexes as catalysts for the effective coupling of CO_2 and epoxides to afford polycarbonates, the azide derivatives were found to be better initiators than their chloride analogs.[88] Hence, it was of importance to obtain a well-characterized sample of $(CO)_3$(dppp)MnN_3 for our current studies. This was achieved *via* reaction of the aquo complex, $[(CO)_3(dppp)Mn(OH_2)][BF_4]$, with an aqueous solution of NaN_3. $(CO)_3$(dppp)MnN_3 (**6**) crystallized in the space group $P2_1/c$ as a benzene solvate. A thermal ellipsoid drawing of complex **6** is found in Figure 6.9, along with the atomic number scheme for selected atoms. The Mn–azide bond distance was found to be 2.126(3) Å, and the nearly linear N_3 unit (175.4(4)º) formed an angle with the Mn–N(1) bond of 117.2(2)º. Bond distances within the azide ligand are N(1)–N(2) = 1.164(5) and N(2)–N(3) = 1.200(6) Å.

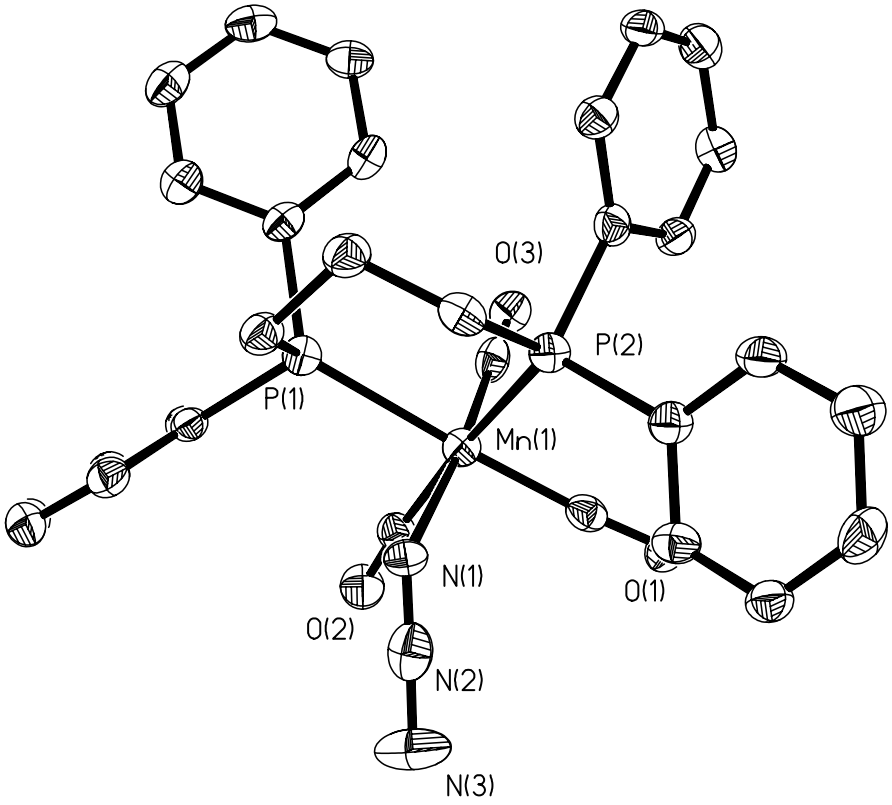

Figure 6.9: Thermal ellipsoid representation of *fac*-$(CO)_3$(dppp)MnN_3, **6**

An interesting feature of the Mn^{I}–azide linkage in complex **6** as compared to that in (salen)Cr^{III}azides is the internal nitrogen–nitrogen bond distances. Considering the $:N\equiv\overset{+1}{N}-\overset{-2}{\underset{\cdot\cdot}{\overset{\cdot\cdot}{N}}}:$ resonance form for the free azide moiety, in the low-valent manganese derivative the azide ligand binds *via* the triply bonded terminal nitrogen, whereas, in the chromium(III) salen derivative is binds through the terminal single bonded nitrogen atom. That is, in the six-coordinate chromium salen complex, N(1)–N(2) = 1.210(9) and N(2)–N(3) = 1.144(8) Å. This difference in binding modes might be anticipated based on hard/soft arguments. On the other hand, the ν_{asym} mode for complex **6** is observed at

2056 cm^{-1}, whereas, that of the chromium(III) azide complex is similarly found at 2054 cm^{-1}.

Table 6.3 lists the ν_{CO} values for the manganese derivatives described in this report. These ν_{CO} stretching vibrations reflect the electron density available at the metal center for backbonding to the carbonyl ligands. Therefore, it is possible from the average ν_{CO} frequency for these six derivatives to order the electron rich character of the metal centers as **1** ≥ **3** > **6** > **4** = **5** > **2**. This will be useful information when considering these complexes as catalysts for the coupling of CO_2 and epoxides.

Table 6.3. ν_{CO} stretching vibrations in $(CO)_3$(dppp)MnX complexes.[a]

X	ν_{CO}, cm^{-1}	average ν_{CO}, cm^{-1}
H (**1**)	1998, 1926, 1902	1942
OTs (**2**)	2037, 1969, 1911	1972
OC_2H_5 (**3**)	2009, 1936, 1891	1945
Cl (**4**)[b]	2027, 1957, 1905	1963
Br (**5**)	2028, 1963, 1908	1966
N_3 (**6**)	2014, 1956, 1912	1960

[a] Spectra determined in benzene solution. [b] Spectrum determined in dichloromethane.

The following complexes, $(CO)_3$(dppp)MnX (X = OCH_3, OC_2H_5 (**3**), Cl (**4**), Br (**5**), and N_3 (**6**)) were examined for their efficacy for catalyzing the coupling of cyclohexene oxide and carbon monoxide. Reaction conditions were consistent with

those we routinely employ for the very effective (salen)Cr X/cocatalyst systems, i.e., catalyst loading 0.040 mol %, 500 psi CO_2 pressure, and 80ºC. Subsequent to a polymer run the crude reaction mixture was dissolved in methylene chloride and examined by infrared spectroscopy for product identification. Importantly, in these instances the highly informative metal carbonyl absorbances in the infrared also provide a probe of the resting state of the catalytically active species. Figure 6.10 represents the infrared spectra in the carbonyl region of the before and after reaction solutions for the copolymerization process involving the most effective catalyst examined here, complex **3** whereas Figure 6.11 depicts the ^{1}HNMR spectra of poly(cyclohexylene carbonate). As is evident in Figure 6.10, the major reaction product is the poly(cyclohexylene)carbonate, with a minor quantity of the *trans*-cyclohexylcarbonate also afforded. That is, the ν_{CO_2} bond at 1750 cm^{-1} corresponds to the copolymer carbonate function, with the weak absorbances at 1802 and 1818 cm^{-1} to that of the *trans* cyclic carbonate.[89] The ν_{CO} absorbances at 2029, 1962, and 1903 cm^{-1} are readily assigned to the CO stretching vibrations of the $(CO)_3$(dppp)Mn–OC(O)OR species, where R represents the growing polymer chain. This assignment is greatly aided by comparison with the fully characterized $(CO)_3$(dppe)MnOC(O)OMe derivative previously reported.[79, 80] As expected, a similar spectrum in the ν_{CO} region is observed at the end of the copolymerization reaction for all of the manganese catalysts employed in Table 6.4. Furthermore, this species would be expected to be the resting state of the catalyst based on the very facile insertion of CO_2 into the Mn–OMe bond of $(CO)_3$(dppe)MnOMe.

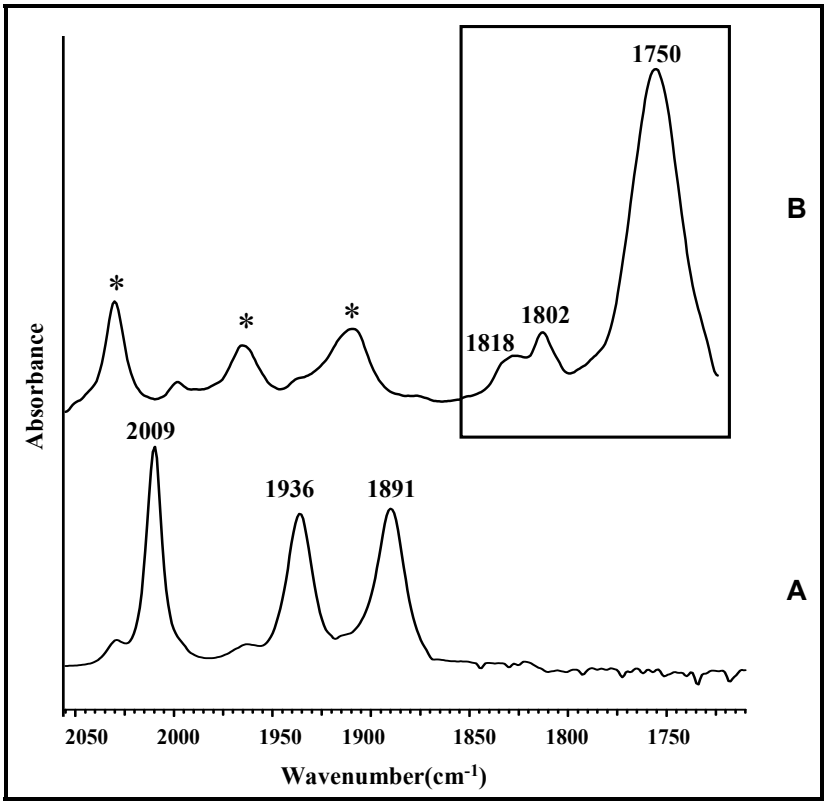

Figure 6.10: Infrared spectra in the ν_{CO} and ν_{CO_2} regions before and after CO_2/cyclohexene oxide coupling reaction. **A.** ν_{CO} of $(CO)_3(dppp)MnOC_2H_5$. **B.** ν_{CO} and ν_{CO_2} of $(*)(CO)_3(dppp)MnOC(O)OC_2H_5$, (1818, 1802) *trans*-cyclic carbonate and (1750 cm^{-1}) poly(cyclohexylene)carbonate.

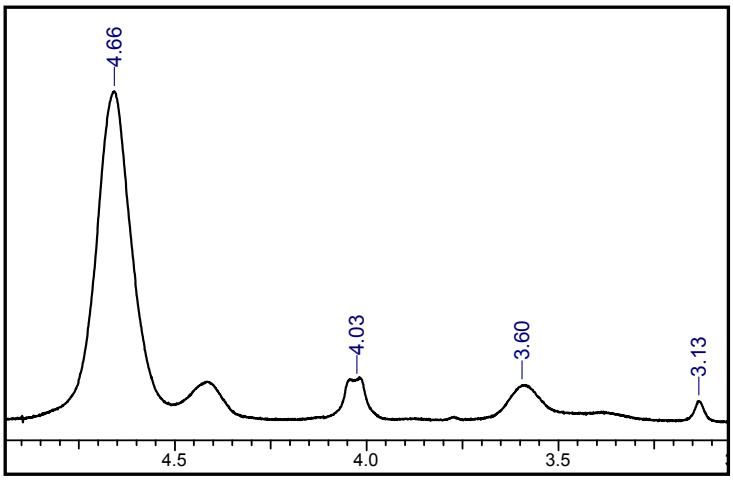

Figure 6.11: ^{1}HNMR spectrum of poly(cyclohexylene carbonate) in $CDCl_3$

Table 6.4. Results of Mn^I complexes catalyzed coupling reactions of cyclohexene oxide and CO_2.[a]

Catalyst	TON[b]		% Carbonate
	copolymer	cyclic carbonate	
$(CO)_3(dppp)MnOCH_3$	42	11	66
$(CO)_3(dppp)MnOC_2H_5$	40 (48)[c]	10 (25)[c]	70 (83)[c]
$(CO)_3(dppp)MnCl$	30 (44)[c]	10(28)[c]	56 (72)[c]
$(CO)_3(dppp)MnN_3$	24	10	47
$(CO)_3(dppp)MnBr$	12	8	25

[a] Reactions carried out for 24 hrs at 80ºC. [b] mol. of epoxide consumed / mol. of Mn. [c] Reactions carried out at 100ºC.

Table 6.4 and Figure 6.12 summarizes the results of the CO_2/cyclohexene oxide coupling reaction catalyzed by the Mn^I derivatives reported herein. Although these organometallic complexes do serve as catalysts for this process, the TON's for 24 hr runs are not very impressive relative to other catalysts for this reaction. For example, the best catalysts found in this study were those containing alkoxide initiators, yet these only exhibited TON's around 50 mol. epoxide consumed/mol. Mn with 70% carbonate linkages at 80ºC. Concomitantly, the selectivity for copolymer production was only 80%, i.e., the minor product *trans*-cyclohexylcarbonate accounts for 20% of the coupling product. As anticipated, an increase in reaction temperature to 100ºC increased the percentage of cyclic carbonate formation to about 34%, however, the higher temperature favorably enhanced both the TON and % carbonate linkages in the copolymer.

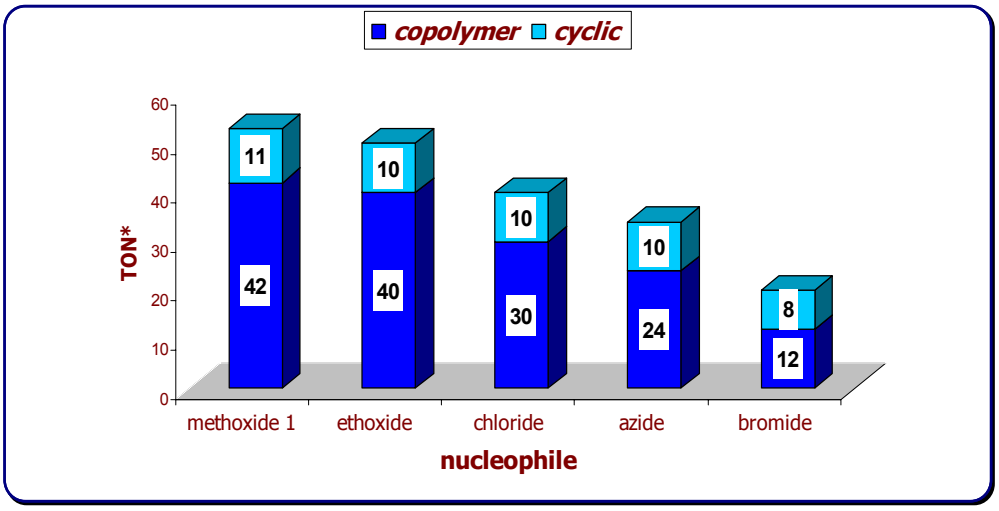

Figure 6.12: Ratio of copolymer: cyclic carbonate in Mn(I) catalyzed copolymerization of CO_2 and cyclochexene oxide

Conclusions

Herein we have structurally characterized a series of closely related 18-electron derivatives of $(CO)_3$(dppp)MnX which differ only in the nature of the X group. Although these complexes were found not to be very effective catalysts for the coupling of CO_2 and epoxides, findings from these studies contribute significantly to our understanding of this important process. Furthermore, these complexes have previously been shown *via* ^{13}CO exchange studies to be thermally inert to ligand dissociation.[80] Hence, upon utilizing these derivatives as catalysts for the CO_2/epoxide coupling reaction, ring-opening of the epoxide must be taking place *via* an associative interchange mechanism. Because CO_2 insertion into the Mn^I–OR bond in the absence of electron-withdrawing substituents on R has been shown to be rapid even at -78ºC, in the presence of CO_2 the $(CO)_3$(dppp)MnOR (R = Me, Et) complexes will exist as $(CO)_3$(dppp)MnOC(O)OR (R = Me, Et).[12]

As the data in Table 6.4 indicates, the order of epoxide ring-opening by the X group (initiator) is: –OC(O)OR > Cl ≥ N_3 > Br. This trend roughly parallels what's observed in the (salen)CrX catalyzed processes, as well as the electron donating abilities of the X groups as revealed by their effect on the ν_{CO} values of the Mn^I carbonyl derivatives. The observation that *trans*-cyclohexylcarbonate is selectively produced is consistent with it being formed by copolymer degradation. Consequently, cyclic carbonate production should be independent of the initiator which is borne out by the data in Table 6.4. The somewhat reduced cyclic carbonate production in the case of X = Br is undoubtedly due to the significant reduction in copolymer production in this instance. Furthermore, the enhanced production of cyclic carbonate over copolymer at higher reaction temperatures is consistent with a unimolecular degradation of the growing polymer chain. In our previous studies involving (salen)CrX derivatives as catalysts for this process we have noted that at the onset of the copolymerization process larger amounts of polyethers linkages are seen in the copolymer which upon longer reaction times afford copolymers with > 99% carbonate content. This observation would account for the large degree of polyethers linkages i.e., the small degree of carbonate linkages in the slowly initiating bromide derivative.

Hence, these studies reinforce the proposed mechanistic features of the more complex (salen)CrX/cocatalyst systems. However, in this instance unlike in the (salen)CrX/cocatalyst system, CO_2 insertion into the alkoxide intermediate under all reaction conditions is faster than epoxide ring-opening by the transient carbonate moiety of the growing polymer chain, Figure 6.13. That is, the rate-limiting step in the

propagation process of the copolymerization reaction is epoxide ring-opening and not CO_2 insertion.

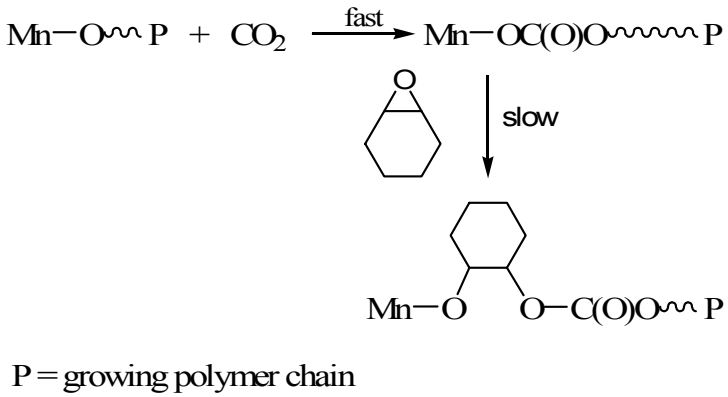

Figure 6.13: Plausible propagation of the copolymerization reaction

CHAPTER VII

CONCLUSIONS

The focus of this dissertation has been designing catalysts for the efficient production of polytrimethylene carbonate. Though different from our group's traditional research area, the polymer still falls under the broad class of polycarbonates. One of the key commercial applications of polytrimethylene carbonate is in the suture industry. This industry today is a 1.45 billion dollar industry with 319 million sutures produced industry. However, a search of the literature and available patents revealed to us, that research and development efforts on designing catalysts to enhance the efficiency of this process has been minimal. Even, academically the catalysts have been restricted to simple metal based Lewis acidic initiators.

Our group has been a dynamic player and witness to the process of homogeneous catalyst development for the copolymerization of epoxide and carbon dioxide. We have observed exponential increase in the efficacy of this process by the design and development of better catalysts. Hence, we wondered if we could lead a similar trend for the synthesis of polytrimethylene carbonate by the use of well defined and characterized catalysts.

The salen ligand gave us the perfect arsenal to attack this problem. Endless volumes of literature has been devoted to the advantages of salen ligands and its utility in organometallic and coordination chemistry, more specifically as catalysts. Hence our decision to use salen based metal complexes. Just to emphasize on the popularity of this ligand system, in this dissertation itself six different metal based salens have been

utilized as catalyst – not a very big number considering 2,500 salen complexes have been synthesized till date.

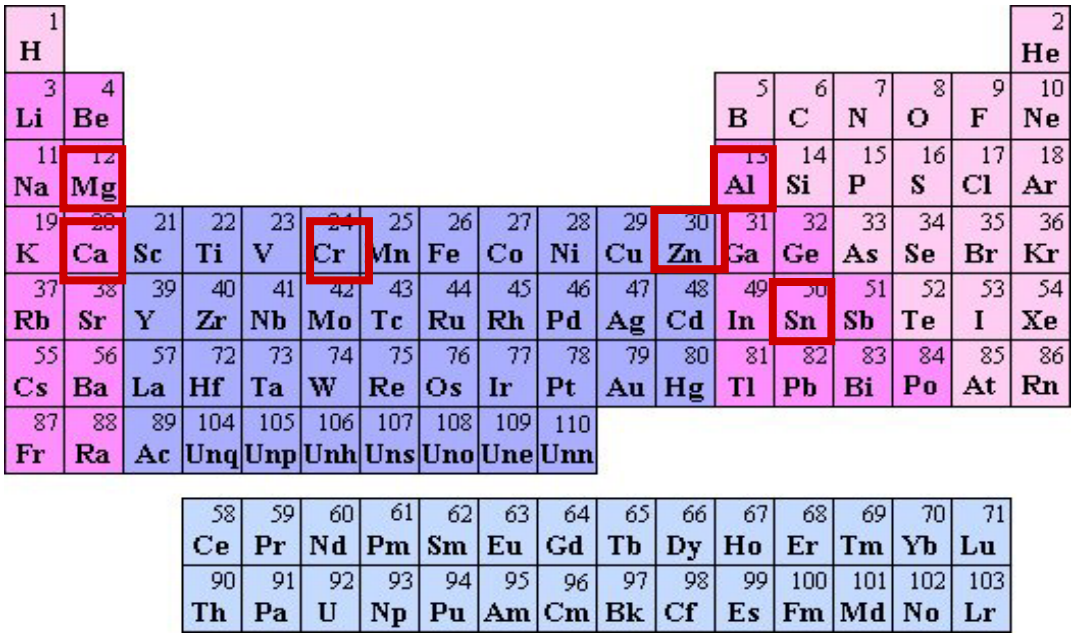

Figure 7.1: Periodic table indicating the metal salen catalysts utilized in the studies for producing polytrimethylene carbonate

One of the greatest advantages of salen catalysts is the ease of modification of the electronic and steric environment around the metal center to influence the activity. A series of studies in Chapters II & III have been devoted to this attribute to obtain our most optimal catalyst. A similar trend was also observed in Chapter IV in our investigation of the copolymerization trimethylene carbonate with ε- caprolactone.

Chapters II & III summarizes the various metal salen complexes, Figure 7.1, (Al, Sn, Zn, Mg and Ca) that we have used for the ring opening polymerization of trimethylene carbonate. All these metals were shown to effectively catalyze the process,

though our most active derivative was calcium based. Importantly, the resultant polycarbonate was shown to be completely void of ether linkages by ^{1}HNMR, even when the reaction was conducted at a high temperature of 140°C. Though rare earth initiators have shown very good reactivity for these systems, their high cost and long term toxicity should be taken into consideration while making a comparison over the choice of a catalyst for commercial use, especially biomedical applications.

The use of these calcium catalysts for copolymerization of trimethylene carbonate and ε-caprolactone have been discussed in Chapter IV. Both random and block copolymers of structure X, XB and AXB have been synthesized where A is a random unit of copolymer whereas A and B are two blocks of polymers. The thermal and mechanical properties of these copolymers can be adjusted by varying the composition of each monomer. Currently, Dr. Hong Liang's group, Mechanical Engineering Department, Texas A&M University, are studying the applications of these copolymers synthesized by us for joint replacement materials.

Chapter V probes into our efforts to obtain polytrimethylene carbonate by the copolymerization of oxetane (trimethylene oxide) and carbon dioxide. Surprisingly this process has not received much attention with the most recent literature dating back to the 1980s by the group Akio Baba in Japan. Metal salen derivatives of chromium and aluminum, along with *n*-Bu_4NX (X = Cl or N_3) salts, were observed by us as effective catalysts for the selective coupling of CO_2 and oxetane (trimethylene oxide) to provide the corresponding polycarbonate with only trace quantities of ether linkages. The

formation of copolymer was demonstrated *not* to proceed *via* the intermediacy of trimethylene carbonate which was observed as a minor product of the coupling reaction.

In Chapter VI, the X-ray structures of a series of $(CO)_3$(dppp)MnX complexes, X = H, OTs, OEt, Cl, Br, and N_3, and dppp = diphenylphosphinopropane, prepared by literature methods are reported, Figure 7.2. Several of these derivatives were examined for their ability to serve as catalysts for the coupling of cyclohexene oxide and carbon dioxide. Although, these organometallic complexes do catalyze the formation of polycarbonate, their activity is not competitive with other very effective catalysts for this coupling reaction. Nevertheless, findings from these studies contribute significantly to our understanding of this important process. The complex containing the alkoxide ligand is the most active, yet it possesses a TON (mol. epoxide consumed/mol. Mn) of only 50 for a 24 hr reaction. In this instance the $(CO)_3$(dppp)MnOEt complex exists as the carbonate species, $(CO)_3$(dppp)MnOC(O)OEt, because of rapid CO_2 insertion into the Mn–OEt bond. The order of epoxide ring-opening by the X group (initiator) was found to be: –OC(O)OR > Cl ≥ N_3 > Br.

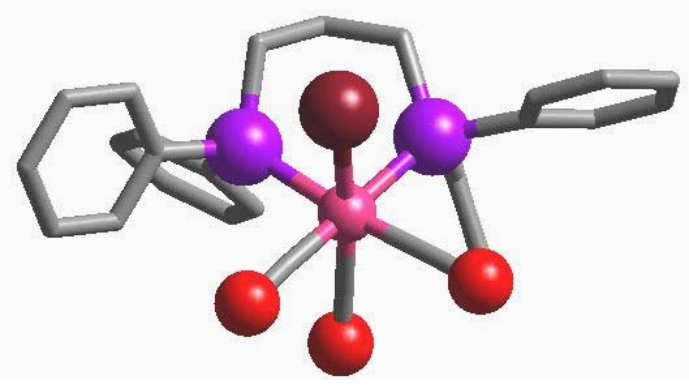

Figure 7.2: Ball and stick representation of a $(CO)_3$(dppp)MnX complex

In retrospect, the major part of this dissertation focuses on two processes for synthesizing polytrimethylene carbonate, Figure 7.3. In the initial part, the more conventional route of ring opening polymerization of trimethylene carbonate is discussed, with chapter V being devoted to the novel method of copolymerization of trimethylene oxide (oxetane) and carbon dioxide. We have observed that even though the end product is the same the needs for each of these systems catalytically could not be more different. Just to emphasize the point in question are following two charts comparing the efficacy of the chromium salen and aluminum salen derivative for each of the processes. Though, current turnover frequencies obtained from the novel process of oxetane/CO_2 do pale in front of those obtained from the conventional ring opening polymerization process, our initial positive results make us very optimistic regarding the future applicability of this process as an alternate greener route for making this biodegradable polymer.

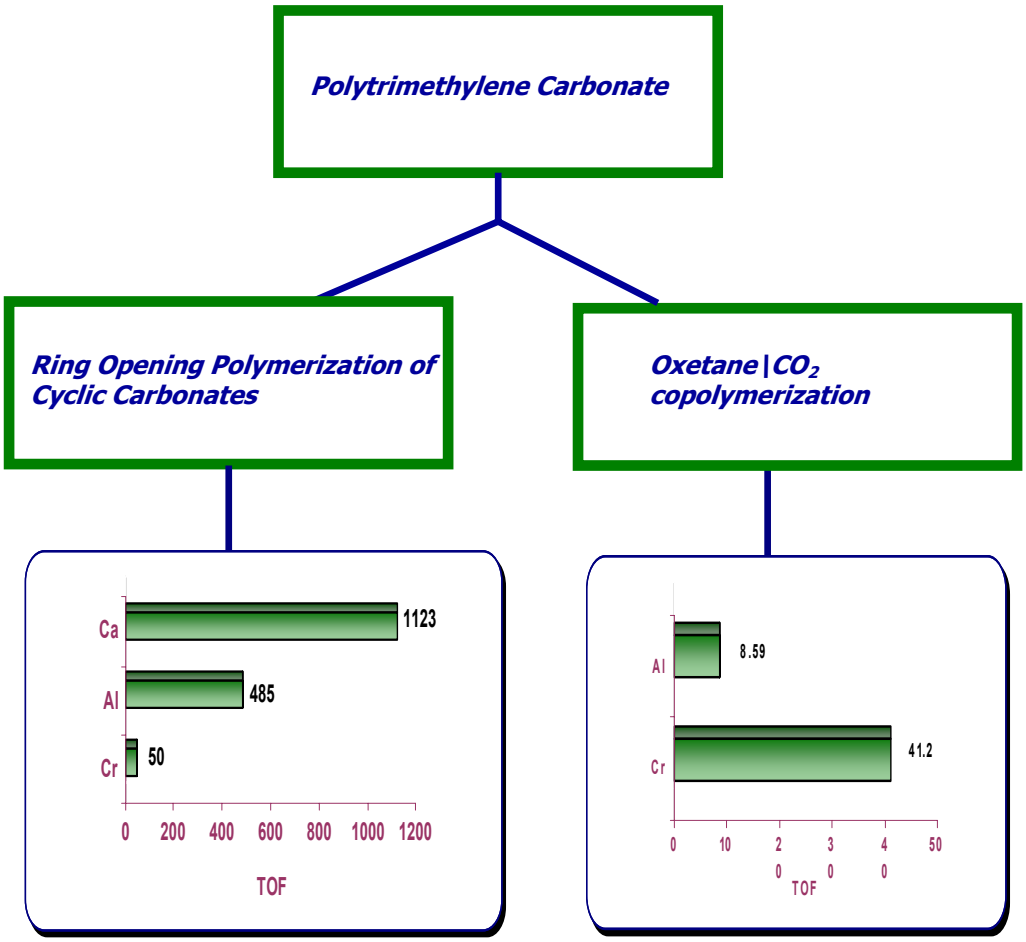

Figure 7.3: Comparing the efficacy of Chromium and Aluminum catalysts for the two processes for synthesizing polytrimethylene carbonate

Hence, this dissertation represents our first step towards catalyst development for a commercially available polymer - polytrimethylene carbonate. The positive results we have obtained, definitely makes us optimistic that some of our biometal based catalysts will find applications in the industry for the production of this biodegradable polymer and copolymers associated with it. To conclude, I feel very fortunate to have been given the opportunity to initiate a new project in our research group with far reaching commercial applications.

REFERENCES AND NOTES

1. Bottenbruch, L. *Engineering Thermoplastics: Polycarbonates, Polyacetals, Polyesters, Cellulose Esters*; Hanser Pub.: New York: 1996. p. 112
2. Brunnelle, D. *Advances in Polycarbonates: ACS Symposium Series 898*: American Chemical Society. 2005. p. 13.
3. Inoue, S.; Koinuma, H.; Tsuruta, T. *J. Polym. Sci., Part B: Polym. Phys.* **1969**, *7*, 287.
4. Darensbourg, D. J.; Holtcamp, M. W.; Struck. G.E.; Zimmer, M.S.; Niezgoda, S.A.; Rainey, P.R.; Robertson, J.B.; Draper, J. D.; Reibenspies, J. H. *J. Am. Chem. Soc.* **1999**, *121*, 107.
5. (a) Darensbourg, D. J.; Yarbrough, J. C.; Ortiz, C. G.; Fang, C. C. *J. Am. Chem. Soc.* **2003**, *125*, 7586-7591. (b) Darensbourg, D. J.; Mackiewicz, R. M.; Phelps, A. L.; Billodeaux D. R. *Acc. Chem. Res.* **2004**, *37*, 836-844.
6. Darensbourg, D. J.; Holtcamp, M. W. *Coord. Chem. Rev.* **1996**, *153*, 155-174.
7. (a)Albertsson, A. C.; Eklund, M. *J. Polym. Sci. Part A: Polym. Chem.* **1994**, *32*, 265. (b) Pego, A. P.; Zhong, Z.; Dijkstra, P.J.; Gripjma, D.W.; Feijen, J. *Macromol. Chem. Phys.* **2003**, *204*, 747.
8. Pego, A. P.; Poot, A. A.; Gripjma, D.W.; Feijen, *J. Biomater. Sci. Polym. Edn.* **2001**, *12*, 35.
9. Zhu, K.J.; Hendren, R.W.; Pitt, C. G. *Macromolecules* **1991**, 24, 1736.
10. Rokicki, G.; *Prog. Polym. Sci.* **2000**, 25, 259.

11. Carothers, W. H.; Van Natta, F. J. *J. Am. Chem. Soc.* **1930**, *52*, 314. (b) Carothers, W. H.; Van Natta, F. J. *J. Am. Chem. Soc.* **1932**, *54*, 761.

12. Kricheldorf, H. R.; Jensen, J. *J. Makromol. Sci. Pure Appl. Chem.* **1989**, A26, 631.

13. Kricheldorf, H. R.; Weegen-Schulz, B. *Macromolecules* **1993**, *26*, 5991.

14. Albertsson, A. C.; Sjoling, M. *J. Macrom. Sci. Pure & Applied Chemistry* **1991**, *29*, 43.

15. Kricheldorf, H. R.; Weegan-Schulz, B. *Polymer* **1995**, *36*, 4997.

16. Kricheldorf, H. R.; Weegan-Schulz, B. *J. Polym. Sci. A, Polym. Chem.* **1995**, *33*, 2193.

17. Kricheldorf, H. R.; Stricker, A. *Macromol. Chem. Phys.* **2000**, *17*, 201.

18. Kricheldorf, H. R.; Stricker, A. *Polymer* **2000**, *41*, 7311

19. Kricheldorf, H. R.; Stricker, A.; Lossin, M. *J. Polym. Sci. A, Polym. Chem.* **2000**, *37*, 2179.

20. . Kricheldorf, H. R.; Stricker, A.; Gomurashvili, Z. *Macromol. Chem. Phys.* **2001**, *3*, 202.

21. Shen, Y.; Shen, Z.; Zhang, Y.; Hang, Q. *J. Polym. Sci. A, Polym. Chem.* **1997**, *35*, 1339.

22. Ling, J.; Shen, Z. *Macromol. Chem. Phys.* **2002**, *4*, 203.

23. Ling, J.; Shen, Z.; Hang, Q. *Macromolecules* **2001**, *34*, 7613.

24. Ling, G.; Shen, Z.; Zhang, Y.; Hang, Q. *Chinese Journal of Polym. Sci.* **2000**, *18*, 77.

25. Zhu, W.; Ling, J.; Xu, H.; Shen, Z. *Chinese Journal of Polym. Sci.* **2005**, *23*, 407.

26. Aggarwal, S.; Puchner, M. *European Polymer Journal* **2002**, *38*, 2365.

27. Aggarwal, S.; Puchner, M.; Greiner, A.; Wendroff, J. *Polym. Int.* **2005**, *54*, 1422.

28. Yasuda, H.; Aludin, M.; Kitamaru, N.; Tanabe, M.; Sirahama, H. *Macromolecules* **1999**, *32*, 6047.

29. Zhou, L.; Yao, Y.; Sun, H.; Chen, J.; Shen, Q. *J. Polym. Sci. A, Polym. Chem.* **2005**, *43*, 1778.

30. Hovestadt, W.; Keul, H.; Hocker, H. *Polymer* **1992***, 33,* 1941.

31. Kricheldorf, H. R.; Weegan-Schulz, B. *J. Makromol. Sci. Pure Appl. Chem.* **1995**, A32, 1847.

32. Takeuchi, D.; Aida, T.; Endo, T.*Macromol. Rapid Commun*. **1999,** *20*, 182.

33. Ling, J.; Zhu, W.; Shen, Z.; *Macromolecules* **2004**, *37*, 758.

34. Dobrzynski, P.; Malgorzata P.; Bero, M. *J. Polym. Sci. A, Polym. Chem.* **2005**, *43*, 1913.

35. Matsumura, S.; Tsukada, K.; Toshima, K. *Macromolecules* **1997**, *30*, 3122.

36. Bisht, K.; Svirkin, Y.; Henderson, L.; Gross, R. *Macromolecules* **1997**, *30*, 7735.

37. Azemi, T.; Harmon, J.; Bisht, K. *Biomacromolecules* **2000**, *1*, 493.

38. For excellent recent reviews in this area, see: (a) Coates, G. W.; Moore, D. R. *Angew. Chem. Int. Ed.* **2004**, *43*, 6618-6639. (b) Chisholm, M. H.; Zhou, Z. *J. Materials Chemistry* **2004**, *14*, 3081-3092.

39. (a) Chisholm, M. H.; DaVarro-Llobet, D.; Zhou, Z. *Macromolecules* **2002**, *35*, 6494-6504. (b) Eberhardt, R.; Allendinger, M.; Rieger, B. *Macromol. Rapid Commun.* **2003**, *24*, 194-196. (c) Qin, Z.; Thomas, C. M.; Lee, S.; Coates, G. W. *Angew.*

Chem., Int. Ed. **2003**, *42*, 5484-5487. (d) Lu, X.-B.; Wang, Y. *Angew. Chem., Int. Ed.* **2004**, *43*, 3574-3577

40. (a) Soga, K.; Hosoda, S.; Tazuke, Y.; Ikeda, S. *J. Polym. Sci. A, Polym. Chem.* **1976**, *14*, 161. (b) Soga, K.; Tazuke, Y.; Hosoda, S.; Ikeda, S. *J. Polym. Sci. A, Polym. Chem.* **1977**, *15*, 219. (c) Harris, R. F. *J. Appl. Polym. Sci*. **1989**, *37*, 183. (d) Harris, R. F.; McDonald, L. A. *J. Appl. Polym. Sci*. **1989**, *37*, 1491. (e) Vogdanis, L.; Heitz, W. *Makromol. Chem., Rapid Commun*. **1986**, *7*, 543. (f) Storey, R. F.; Hoffman, D. C. *Macromolecules* **1992**, *25*, 5369. (e) Vogdanis, L.; Martens, B.; Uchtmann, H.; Hensel, F.; Heitz, W. *Makromol. Chem.* **1990**, *191*, 465. (f) Lee, J. C.; Litt, M. H. *Macromolecules* **2000**, *33*, 1618-1627. (h) Kéki, S.; Török, J.; György, D.; Zsuga, M. *Macromolecules*, **2001**, *34*, 6850-6857.
41. Albertsson, A. C.; Eklund, M. *J. Polym. Sci. Part A: Polym. Chem.* **1994**, *32*, 265.
42. Ariga, T.; Takata, T.; Endo, T. *Macromolecules* **1997**, *30*, 737.
43. (a) Darensbourg, D. J.; Mackiewicz, R. M.; Billodeaux, D. R. *Organometallics* **2005**, *24*, 144-148. (b) Darensbourg, D. J.; Billodeaux,D. R. *Inorg. Chem*. **2005**, *44*, 1433-1442.
44. Pfeiffer, E.; Lubbe, E.; Tsumaki, T. *Liebigs Ann.* **1933**, *503*, 84.
45. Dalton, C.T.; Ryan, K.M.; Wall, V.M.; Bousquet, C.; Gilheany, D.G.; *Top. Catal.* **1998**, *5*, 75.
46. (a) Jacobosen, E.N.; Zhang, W.; Muci, A.R.; Ecker, J.R.; Deng, L. *J. Am. Chem. Soc.* **1991**, *113*, 7063.(b) Katsuki, T. *Chem. Soc. Rev.* **2004**, *33*, 437.

47. Haikarainen, A. *Metal–Salen Catalysts in the Oxidation of Lignin Model Compounds,* Ph.D. Dissertation, University of Helsinki, Finland, June 2005.

48. (a) Yang, J.; Yu,Y.; Li, Q.; Li, Y.; Cao, A. *J. Polym. Sci. Part A: Polym. Chem.* **2004**, 30, 737. (b) Chisholm, M. H.; Patmore, N. J.; Zhou, Z. *Chem. Commun.* **2005**, 127-129.

49. TMC was prepared from 1,3-propanediol and ethylchloroformate as described by Endo and coworkers (*Macromolecules*, **1997**, *30*, 737).

50. (a) Atwood, D. A.; Jegier, J. A.; Martin, K. J.; Rutherford, D. *Inorg. Chem.* **1996**, *35*, 63. (b) Darensbourg, D. J.; Billodeaux, D. R. *Inorg. Chem.* **2005**, *44*, 1433. Bhaw-Luximon, A.; Jhurry, D.; Spassky, N. *Polym. Bull.*, **2000**, 44, 31.

51. Cameron, P. A.; Jhurry, D.; Gibson, V. C.; White, A. J. P.; Williams, D. J.; Williams, S. *Macrolmol. Rapid. Commun.* **1999**, *20*, 616.

52. Takata, T.; Matsuoka, H.; Endo, T. *Chem. Lett.* **1991**, 2091.

53. Darensbourg, D. J.; Ganguly, P.; Billodeaux, D. R. *Macromolecules* **2005**, *38*, 5406.

54. Chamberlain, B. M.; Cheng, M.; Moore, D. R.; Ovitt, T. M.; Lobkovsky, E. B.; Coates, G. W. *J. Am. Chem. Soc.* **2001**, *123*, 3229-3238.

55. Chisholm, M. H.; Gallucci, J. C.; Phomphrai, K. *Inorg. Chem.* **2004**, *43*, 6717-6725.

56. Zhong, Z.; Schneiderbauer, S.; Djikstra, P.J.; Westerhausen, M.; Feijan, J. *J. Polym. & Env*. **2001**, *9*, 31.

57. Wurm, B.; Keul, H.; Hocker, H. *Makromol. Chem. Rapid Commun.* **1992**, *13*, 9.

58. Darensbourg, D. J.; Mackiewicz, R. *J. Am. Chem. Soc.* **2005**, *127*, 14026.

59. Darensbourg, D. J.; Mackiewicz, R.; Rodgers, J. L.; Billodeaux, D. R. *Inorg. Chem.* **2004**, *23*, 6024.

60. (a) Lu, X. B.; Feng, X. J.; He, R. *Applied Catalysis A: General* **2002**, *234*, 25. (b) Singer, A. L.; Atwood, D. A. *Inorg. Chim. Acta* **1998**, *277*, 157.

61. Demadis, K. D.; Meyer, T. J.; White, P. S. *Inorg Chem.***1998**, *37*, 3610.

62. Kumar, A.; Garg, K.; Gross, R. A. *Macromolecules* **2001***, 34,* 3527.

63. Hu, Y.; Zhu, K. J.; *J. Biomater. Sci. Polym. Edn*. **2003**, *14*, 1363.

64. Albertsson, A. C.; Eklund, M. *J. Appl. Polym. Sci., Part A: Polym. Chem.* **1995**, *57*, 87.

65. Polymers and Liquid Crystals Virtual Laboratory. Case Western Reserve University. http://plc.cwru.edu/ (accessed on 10/09/05).

66. Kricheldorf, H. R.; Ahrensdorf, K.; Rost, S. *Macromolecular Chemistry and Physics* **2004**, 205, 1602.

67. Chen, X.; Gross, R. A. *Macromolecules* **1999***, 32,* 308.

68. Shen, Y.; Shen, Z.; Zhang, Y.; Yao, K. *Macromolecules* **1996***, 29,* 8289.

69. In't Veld, P. J. A.; Velner, E. M.; Van De Witte, P.; Hamhuis, J.; Dijkstra, P.J.; Feijan, J. *J. Appl. Polym. Sci., Part A: Polym. Chem.* **1997***, 35,* 219.

70. For reviews and recent contributions to this area see: (a) Moore, D. R.; Coates, G. W. *Angew. Chem. Int. Ed.* **2004**, *43*, 6618. (b) Darensbourg, D. J.; Mackiewicz, R. M.; Phelps, A. L.; Billodeaux, D. R. *Acc. Chem. Res.* **2004**, *37*, 836. (c) Sugimoto, H.; Inoue, S. *J. Polym. Sci., Part A: Polym. Chem.* **2004**, *42*, 5561. (d) Chisholm, M. H.; Zhou, Z. *J. Materials Chemistry* **2004**, *14*, 3081. (e) Super, M. S.; Beckman, E.

J. *Trends Polym. Sci.* **1997**, *5*, 236. (f) Kuran, W. *Prog. Polym. Sci.* **1998**, *23*, 919. (g) Paddock, R. L.; Nguyen, S. T. *Macromolecules* **2005**, *38*, 6251. (h) Cohen, C. T.; Chu, T.; Coates, G. W. *J. Am. Chem. Soc.* **2005**, *127*, 10869.

71. (a) Kruper, W. J.; Dellar, D. V. *J. Org. Chem.* 1995, *60*, 725. (b) Kuran, W.; Listós, T. *Macromol. Chem. Phys.* **1994**, *195*, 1011.
72. (a) Koinuma, H.; Hirai, H. *Makromol. Chem.* **1977**, *178*, 241. (b) Baba, A.; Kashiwagi, H.; Matsuda, H. *Tetrahedron Lett.* **1985**, *26*, 1323. (c) Baba, A.; Meishou, H.; Matsuda, H. *Makromol. Chem., Rapid Commun.* **1984**, *5*, 665. (d) Baba, A.; Kashiwagi, H.; Matsuda, H. *Organometallics* **1987**, *6*, 137.
73. (a) Inoue, S. *Carbon Dioxide as a Source of Carbon;* Aresta, M., Forti, G., Eds.; Reidel Publishing Co.: Dordrecht, 1987; p. 331. (c) Rokicki, A.; Kuran, W. *J. Macromol. Sci., Rev. Macromol. Chem.* **1981**, *C21*, 135. (d) Super, M. S.; Beckman, E. J. *Trends in Polymer Science* **1997**, *5*, 236.
74. Behr, A. *Carbon Dioxide Activation by Metal Complexes;* VCH: Weinheim, 1988; p. 7.
75. Nankee, R. J.; Avery, J. R.; Schrems, J. E. Dow Chem. Patent FR. 15,72,282,1967; *Chem. Abstr.* **1970**, *72*, 69016.
76. Pizzi, H.; Stephanou, A. *J. Appl. Polym. Sci.* **1993**, *49*, 2157.
77. Shaikh, A.-A. G.; Sivaram, S. *Chem. Rev.* **1996**, *96*, 951.
78. (a) Darensbourg, D. J.; Sanchez, K. M.; Reibenspies, J. H.; Rheingold, A. L. *J. Am. Chem. Soc.* **1989**, *111*, 7094. (b) Simpson, R. D.; Bergman, R. G. *Angew. Chem.,*

Int. Ed. Engl. **1992**, *31*, 220. (c) Darensbourg, D. J.; Mueller, B. L.; Bischoff, C. J.; Chojnacki, S. S.; Reibenspies, J. H. *Inorg. Chem.* **1991**, *30*, 2418.

79. Mandal, S. K.; Ho, D. M.; Orchin, M. *Organometallics* **1993**, *12*, 1714.
80. Darensbourg, D. J.; Lee, W-Z.; Phelps, A. L.; Guidry, E. *Organometallics* **2003**, *22*, 5585.
81. Li, G.Q.; Feldman, J. *Polyhedron* **1997**, *16*, 2041.
82. Riera; V. *J. Organomet. Chem.* **1981**, *205*, 371.
83. Becker, T.M.; Orchin, M. *Polyhedron* **1999**, *18*, 2563.
84. SMART 1000 CCD, Bruker Analytical X-ray Systems: Madison, WI, **1999**.
85. Sheldrick, G. *SHELXS-97: Program for Crystal Structure Solution*, Institut fur Anorganische Chemie der Universitat: Gottingen, Germany, 1997.
86. Sheldrick, G. *SHELXL-99: Program for Crystal Structure Refinement*, Institut fur Anorganische Chemie der Universitat: Gottingen, Germany, 1999.
87. *SHELXTL, version 5.0;* Bruker: Madison, WI, 1999.
88. Darensbourg, D. J.; Mackiewicz, R. M.; Rodgers, J. L.; Fang, C. C.; Billodeaux, D. R.; Reibenspies, J. H. *Inorg. Chem.* **2004**, *43*, 6024-6034.
89. Darensbourg, D. J.; Lewis, S. J.; Rodgers, J. L. Yarbrough, J. C. *Inorg. Chem.* **2003**, *42*, 581-589.

APPENDIX A

SUPPLEMENTARY MATERIAL FOR CRYSTAL STRUCTURES IN CHAPTER VI

Table A-1. Atomic coordinates (x 10^4) and equivalent isotropic displacement parameters (Å^{2}x 10^3) for **6.4**. U(eq) is defined as one third of the trace of the orthogonalized U^{ij} tensor.

	x	y	z	U(eq)
Mn(1A)	4748(1)	7441(1)	8380(1)	30(1)
Mn(1B)	1299(1)	7440(1)	3379(1)	28(1)
P(1A)	4694(1)	7786(1)	7005(1)	28(1)
P(2A)	2967(1)	6444(1)	8129(1)	29(1)
P(1B)	2618(1)	6428(1)	3164(1)	28(1)
P(2B)	1649(1)	7819(1)	2033(1)	29(1)
O(1A)	6787(4)	8918(3)	8847(3)	44(1)
O(2A)	6330(4)	6120(3)	7841(3)	50(1)
O(3A)	4805(4)	7163(3)	10199(3)	41(1)
O(1B)	1169(4)	7290(3)	5230(3)	42(1)
O(2B)	-865(4)	6114(3)	2786(3)	41(1)
O(3B)	-151(4)	8873(3)	3739(3)	44(1)
C(1A)	5997(5)	8353(4)	8637(4)	33(1)
C(2A)	5721(5)	6615(4)	8050(4)	31(1)
C(3A)	4754(5)	7256(3)	9497(4)	32(1)
C(4A)	4238(5)	6830(3)	6204(3)	30(1)
C(5A)	2935(5)	6341(3)	6330(3)	31(1)
C(6A)	2854(5)	5787(3)	7079(3)	34(1)
C(7A)	3712(5)	8544(3)	6654(4)	30(1)
C(8A)	2739(5)	8764(3)	7143(4)	36(1)
C(9A)	1977(5)	9317(4)	6853(4)	46(2)
C(10A)	2184(6)	9643(4)	6072(4)	44(2)

C(11A)	3130(5)	9431(4)	5574(4)	42(2)
C(12A)	3889(5)	8885(3)	5865(4)	34(1)
C(13A)	6212(5)	8262(3)	6654(3)	31(1)
C(14A)	6566(5)	9172(4)	6733(4)	40(2)
C(15A)	7694(5)	9546(4)	6491(4)	41(2)
C(16A)	8539(5)	9021(4)	6181(4)	42(2)
C(17A)	8208(5)	8112(4)	6114(4)	47(2)
C(18A)	7049(5)	7735(4)	6354(4)	37(1)
C(19A)	1492(5)	6852(4)	8207(4)	33(1)
C(20A)	1370(5)	7473(4)	8894(4)	36(1)
C(21A)	250(6)	7764(4)	9022(4)	45(2)
C(22A)	-728(6)	7447(4)	8476(5)	52(2)
C(23A)	-614(6)	6827(4)	7789(4)	48(2)
C(24A)	488(5)	6531(4)	7661(4)	40(2)
C(25A)	2723(5)	5544(3)	8819(3)	33(1)
C(26A)	3708(5)	5140(4)	9014(4)	42(2)
C(27A)	3561(6)	4434(4)	9497(4)	52(2)
C(28A)	2432(6)	4127(4)	9820(4)	46(2)
C(29A)	1458(6)	4535(4)	9630(4)	43(2)
C(30A)	1591(5)	5225(4)	9135(4)	36(1)
C(1B)	1236(5)	7313(3)	4509(4)	33(1)
C(2B)	-19(5)	6619(3)	3017(3)	27(1)
C(3B)	413(5)	8326(4)	3582(4)	34(1)
C(4B)	2390(5)	5766(3)	2125(3)	33(1)
C(5B)	2580(5)	6311(3)	1360(4)	35(1)
C(6B)	1583(5)	6867(3)	1223(3)	32(1)
C(7B)	2449(5)	5542(3)	3866(3)	30(1)
C(8B)	3453(5)	5217(3)	4198(4)	34(1)
C(9B)	3289(6)	4540(4)	4708(4)	39(2)
C(10B)	2109(6)	4149(4)	4895(4)	40(2)
C(11B)	1127(6)	4443(4)	4560(4)	41(2)
C(12B)	1284(5)	5128(4)	4057(4)	36(1)
C(13B)	4277(5)	6812(3)	3251(3)	30(1)
C(14B)	5111(5)	6483(4)	2707(4)	38(1)

C(15B)	6358(5)	6791(4)	2824(4)	47(2)
C(16B)	6805(5)	7433(4)	3479(4)	47(2)
C(17B)	5989(5)	7762(4)	4039(4)	42(2)
C(18B)	4727(5)	7460(3)	3917(4)	34(1)
C(19B)	3108(5)	8487(3)	1790(4)	33(1)
C(20B)	3291(6)	8714(4)	959(4)	45(2)
C(21B)	4421(7)	9175(4)	746(5)	56(2)
C(22B)	5348(6)	9406(4)	1375(5)	56(2)
C(23B)	5186(6)	9192(4)	2169(5)	51(2)
C(24B)	4055(5)	8727(3)	2393(4)	38(2)
C(25B)	492(5)	8399(4)	1592(3)	34(1)
C(26B)	743(6)	9292(4)	1493(4)	42(2)
C(27B)	-137(6)	9706(4)	1145(4)	52(2)
C(28B)	-1293(6)	9238(5)	914(4)	58(2)
C(29B)	-1566(6)	8368(5)	1060(4)	53(2)
C(30B)	-694(5)	7953(4)	1383(4)	41(2)

Table A-2. Bond lengths [Å] and angles [°] for **6.4**

Mn(1A)-C(1A)	1.812(6)	C(4A)-H(4A2)	0.9900
Mn(1A)-C(3A)	1.814(7)	C(5A)-C(6A)	1.523(8)
Mn(1A)-C(2A)	1.837(6)	C(5A)-H(5A1)	0.9900
Mn(1A)-P(1A)	2.2881(18)	C(5A)-H(5A2)	0.9900
Mn(1A)-P(2A)	2.2927(17)	C(6A)-H(6A1)	0.9900
Mn(1A)-H(1A)	1.735(19)	C(6A)-H(6A2)	0.9900
Mn(1B)-C(2B)	1.809(5)	C(7A)-C(8A)	1.396(7)
Mn(1B)-C(3B)	1.812(6)	C(7A)-C(12A)	1.404(8)
Mn(1B)-C(1B)	1.814(7)	C(8A)-C(9A)	1.395(8)
Mn(1B)-P(2B)	2.2828(18)	C(8A)-H(8A)	0.9500
Mn(1B)-P(1B)	2.3047(16)	C(9A)-C(10A)	1.387(9)
Mn(1B)-H(1B)	1.71(6)	C(9A)-H(9A)	0.9500
P(1A)-C(13A)	1.833(5)	C(10A)-C(11A)	1.376(8)
P(1A)-C(7A)	1.836(5)	C(10A)-H(10A)	0.9500
P(1A)-C(4A)	1.841(5)	C(11A)-C(12A)	1.385(8)
P(2A)-C(19A)	1.838(5)	C(11A)-H(11A)	0.9500
P(2A)-C(25A)	1.841(6)	C(12A)-H(12A)	0.9500
P(2A)-C(6A)	1.843(5)	C(13A)-C(18A)	1.384(7)
P(1B)-C(13B)	1.826(5)	C(13A)-C(14A)	1.389(7)
P(1B)-C(4B)	1.832(5)	C(14A)-C(15A)	1.360(8)
P(1B)-C(7B)	1.836(6)	C(14A)-H(14A)	0.9500
P(2B)-C(19B)	1.832(6)	C(15A)-C(16A)	1.393(8)
P(2B)-C(6B)	1.838(5)	C(15A)-H(15A)	0.9500
P(2B)-C(25B)	1.838(6)	C(16A)-C(17A)	1.385(8)
O(1A)-C(1A)	1.146(6)	C(16A)-H(16A)	0.9500
O(2A)-C(2A)	1.125(6)	C(17A)-C(18A)	1.390(8)
O(3A)-C(3A)	1.133(7)	C(17A)-H(17A)	0.9500
O(1B)-C(1B)	1.144(7)	C(18A)-H(18A)	0.9500
O(2B)-C(2B)	1.144(6)	C(19A)-C(24A)	1.384(8)
O(3B)-C(3B)	1.137(6)	C(19A)-C(20A)	1.395(7)
C(4A)-C(5A)	1.535(7)	C(20A)-C(21A)	1.391(8)
C(4A)-H(4A1)	0.9900	C(20A)-H(20A)	0.9500

C(21A)-C(22A)	1.362(9)	C(11B)-H(11B)	0.9500
C(21A)-H(21A)	0.9500	C(12B)-H(12B)	0.9500
C(22A)-C(23A)	1.392(9)	C(13B)-C(14B)	1.388(8)
C(22A)-H(22A)	0.9500	C(13B)-C(18B)	1.400(7)
C(23A)-C(24A)	1.375(8)	C(14B)-C(15B)	1.383(8)
C(23A)-H(23A)	0.9500	C(14B)-H(14B)	0.9500
C(24A)-H(24A)	0.9500	C(15B)-C(16B)	1.382(8)
C(25A)-C(26A)	1.382(8)	C(15B)-H(15B)	0.9500
C(25A)-C(30A)	1.384(8)	C(16B)-C(17B)	1.387(8)
C(26A)-C(27A)	1.384(8)	C(16B)-H(16B)	0.9500
C(26A)-H(26A)	0.9500	C(17B)-C(18B)	1.397(8)
C(27A)-C(28A)	1.382(9)	C(17B)-H(17B)	0.9500
C(27A)-H(27A)	0.9500	C(18B)-H(18B)	0.9500
C(28A)-C(29A)	1.373(8)	C(19B)-C(24B)	1.379(8)
C(28A)-H(28A)	0.9500	C(19B)-C(20B)	1.402(8)
C(29A)-C(30A)	1.376(8)	C(20B)-C(21B)	1.395(9)
C(29A)-H(29A)	0.9500	C(20B)-H(20B)	0.9500
C(30A)-H(30A)	0.9500	C(21B)-C(22B)	1.390(10)
C(4B)-C(5B)	1.538(8)	C(21B)-H(21B)	0.9500
C(4B)-H(4B1)	0.9900	C(22B)-C(23B)	1.335(10)
C(4B)-H(4B2)	0.9900	C(22B)-H(22B)	0.9500
C(5B)-C(6B)	1.526(7)	C(23B)-C(24B)	1.404(8)
C(5B)-H(5B1)	0.9900	C(23B)-H(23B)	0.9500
C(5B)-H(5B2)	0.9900	C(24B)-H(24B)	0.9500
C(6B)-H(6B1)	0.9900	C(25B)-C(26B)	1.389(7)
C(6B)-H(6B2)	0.9900	C(25B)-C(30B)	1.393(8)
C(7B)-C(12B)	1.390(7)	C(26B)-C(27B)	1.381(8)
C(7B)-C(8B)	1.402(7)	C(26B)-H(26B)	0.9500
C(8B)-C(9B)	1.376(8)	C(27B)-C(28B)	1.382(10)
C(8B)-H(8B)	0.9500	C(27B)-H(27B)	0.9500
C(9B)-C(10B)	1.391(8)	C(28B)-C(29B)	1.373(9)
C(9B)-H(9B)	0.9500	C(28B)-H(28B)	0.9500
C(10B)-C(11B)	1.359(8)	C(29B)-C(30B)	1.359(8)
C(10B)-H(10B)	0.9500	C(29B)-H(29B)	0.9500
C(11B)-C(12B)	1.378(8)	C(30B)-H(30B)	0.9500

C(1A)-Mn(1A)-C(3A)	88.2(2)	C(4A)-P(1A)-Mn(1A)	114.28(18)
C(1A)-Mn(1A)-C(2A)	96.2(2)	C(19A)-P(2A)-C(25A)	101.4(3)
C(3A)-Mn(1A)-C(2A)	95.2(2)	C(19A)-P(2A)-C(6A)	104.0(3)
C(1A)-Mn(1A)-P(1A)	89.70(18)	C(25A)-P(2A)-C(6A)	99.5(2)
C(3A)-Mn(1A)-P(1A)	175.28(17)	C(19A)-P(2A)-Mn(1A)	118.34(19)
C(2A)-Mn(1A)-P(1A)	89.19(18)	C(25A)-P(2A)-Mn(1A)	116.42(18)
C(1A)-Mn(1A)-P(2A)	170.90(17)	C(6A)-P(2A)-Mn(1A)	114.59(18)
C(3A)-Mn(1A)-P(2A)	90.54(18)	C(13B)-P(1B)-C(4B)	103.9(2)
C(2A)-Mn(1A)-P(2A)	92.87(17)	C(13B)-P(1B)-C(7B)	101.3(2)
P(1A)-Mn(1A)-P(2A)	90.85(6)	C(4B)-P(1B)-C(7B)	99.7(2)
C(1A)-Mn(1A)-H(1A)	82.4(15)	C(13B)-P(1B)-Mn(1B)	119.23(18)
C(3A)-Mn(1A)-H(1A)	87.1(14)	C(4B)-P(1B)-Mn(1B)	113.79(18)
C(2A)-Mn(1A)-H(1A)	177.3(15)	C(7B)-P(1B)-Mn(1B)	116.26(17)
P(1A)-Mn(1A)-H(1A)	88.5(14)	C(19B)-P(2B)-C(6B)	101.0(2)
P(2A)-Mn(1A)-H(1A)	88.5(15)	C(19B)-P(2B)-C(25B)	103.1(3)
C(2B)-Mn(1B)-C(3B)	94.6(2)	C(6B)-P(2B)-C(25B)	101.0(2)
C(2B)-Mn(1B)-C(1B)	98.2(2)	C(19B)-P(2B)-Mn(1B)	120.5(2)
C(3B)-Mn(1B)-C(1B)	87.6(2)	C(6B)-P(2B)-Mn(1B)	113.65(19)
C(2B)-Mn(1B)-P(2B)	92.24(17)	C(25B)-P(2B)-Mn(1B)	115.01(19)
C(3B)-Mn(1B)-P(2B)	90.01(19)	O(1A)-C(1A)-Mn(1A)	176.1(5)
C(1B)-Mn(1B)-P(2B)	169.46(17)	O(2A)-C(2A)-Mn(1A)	178.8(5)
C(2B)-Mn(1B)-P(1B)	91.83(16)	O(3A)-C(3A)-Mn(1A)	177.1(5)
C(3B)-Mn(1B)-P(1B)	173.59(17)	C(5A)-C(4A)-P(1A)	112.6(4)
C(1B)-Mn(1B)-P(1B)	91.81(17)	C(5A)-C(4A)-H(4A1)	109.1
P(2B)-Mn(1B)-P(1B)	89.42(6)	P(1A)-C(4A)-H(4A1)	109.1
C(2B)-Mn(1B)-H(1B)	175.4(19)	C(5A)-C(4A)-H(4A2)	109.1
C(3B)-Mn(1B)-H(1B)	85.3(18)	P(1A)-C(4A)-H(4A2)	109.1
C(1B)-Mn(1B)-H(1B)	86.4(19)	H(4A1)-C(4A)-H(4A2)	107.8
P(2B)-Mn(1B)-H(1B)	83.2(19)	C(6A)-C(5A)-C(4A)	113.6(4)
P(1B)-Mn(1B)-H(1B)	88.3(18)	C(6A)-C(5A)-H(5A1)	108.9
C(13A)-P(1A)-C(7A)	102.3(2)	C(4A)-C(5A)-H(5A1)	108.9
C(13A)-P(1A)-C(4A)	102.4(2)	C(6A)-C(5A)-H(5A2)	108.9
C(7A)-P(1A)-C(4A)	100.4(2)	C(4A)-C(5A)-H(5A2)	108.9
C(13A)-P(1A)-Mn(1A)	112.51(18)	H(5A1)-C(5A)-H(5A2)	107.7
C(7A)-P(1A)-Mn(1A)	122.35(19)	C(5A)-C(6A)-P(2A)	113.7(4)

C(5A)-C(6A)-H(6A1)	108.8	C(16A)-C(17A)-C(18A)	120.2(5)
P(2A)-C(6A)-H(6A1)	108.8	C(16A)-C(17A)-H(17A)	119.9
C(5A)-C(6A)-H(6A2)	108.8	C(18A)-C(17A)-H(17A)	119.9
P(2A)-C(6A)-H(6A2)	108.8	C(13A)-C(18A)-C(17A)	120.4(5)
H(6A1)-C(6A)-H(6A2)	107.7	C(13A)-C(18A)-H(18A)	119.8
C(8A)-C(7A)-C(12A)	118.4(5)	C(17A)-C(18A)-H(18A)	119.8
C(8A)-C(7A)-P(1A)	121.0(4)	C(24A)-C(19A)-C(20A)	119.3(5)
C(12A)-C(7A)-P(1A)	120.5(4)	C(24A)-C(19A)-P(2A)	123.4(4)
C(9A)-C(8A)-C(7A)	120.3(6)	C(20A)-C(19A)-P(2A)	117.1(4)
C(9A)-C(8A)-H(8A)	119.9	C(21A)-C(20A)-C(19A)	119.9(6)
C(7A)-C(8A)-H(8A)	119.9	C(21A)-C(20A)-H(20A)	120.0
C(10A)-C(9A)-C(8A)	119.7(6)	C(19A)-C(20A)-H(20A)	120.0
C(10A)-C(9A)-H(9A)	120.2	C(22A)-C(21A)-C(20A)	120.2(6)
C(8A)-C(9A)-H(9A)	120.2	C(22A)-C(21A)-H(21A)	119.9
C(11A)-C(10A)-C(9A)	121.2(6)	C(20A)-C(21A)-H(21A)	119.9
C(11A)-C(10A)-H(10A)	119.4	C(21A)-C(22A)-C(23A)	120.2(6)
C(9A)-C(10A)-H(10A)	119.4	C(21A)-C(22A)-H(22A)	119.9
C(10A)-C(11A)-C(12A)	119.1(6)	C(23A)-C(22A)-H(22A)	119.9
C(10A)-C(11A)-H(11A)	120.5	C(24A)-C(23A)-C(22A)	120.0(6)
C(12A)-C(11A)-H(11A)	120.5	C(24A)-C(23A)-H(23A)	120.0
C(11A)-C(12A)-C(7A)	121.4(6)	C(22A)-C(23A)-H(23A)	120.0
C(11A)-C(12A)-H(12A)	119.3	C(23A)-C(24A)-C(19A)	120.4(6)
C(7A)-C(12A)-H(12A)	119.3	C(23A)-C(24A)-H(24A)	119.8
C(18A)-C(13A)-C(14A)	118.6(5)	C(19A)-C(24A)-H(24A)	119.8
C(18A)-C(13A)-P(1A)	121.6(4)	C(26A)-C(25A)-C(30A)	117.7(5)
C(14A)-C(13A)-P(1A)	119.7(4)	C(26A)-C(25A)-P(2A)	118.7(4)
C(15A)-C(14A)-C(13A)	121.2(5)	C(30A)-C(25A)-P(2A)	123.6(4)
C(15A)-C(14A)-H(14A)	119.4	C(25A)-C(26A)-C(27A)	121.0(6)
C(13A)-C(14A)-H(14A)	119.4	C(25A)-C(26A)-H(26A)	119.5
C(14A)-C(15A)-C(16A)	120.5(6)	C(27A)-C(26A)-H(26A)	119.5
C(14A)-C(15A)-H(15A)	119.8	C(28A)-C(27A)-C(26A)	121.0(6)
C(16A)-C(15A)-H(15A)	119.8	C(28A)-C(27A)-H(27A)	119.5
C(17A)-C(16A)-C(15A)	119.0(5)	C(26A)-C(27A)-H(27A)	119.5
C(17A)-C(16A)-H(16A)	120.5	C(29A)-C(28A)-C(27A)	117.7(6)
C(15A)-C(16A)-H(16A)	120.5	C(29A)-C(28A)-H(28A)	121.2

C(27A)-C(28A)-H(28A)	121.2	C(8B)-C(9B)-H(9B)	119.8
C(28A)-C(29A)-C(30A)	121.6(6)	C(10B)-C(9B)-H(9B)	119.8
C(28A)-C(29A)-H(29A)	119.2	C(11B)-C(10B)-C(9B)	118.9(6)
C(30A)-C(29A)-H(29A)	119.2	C(11B)-C(10B)-H(10B)	120.6
C(29A)-C(30A)-C(25A)	120.9(5)	C(9B)-C(10B)-H(10B)	120.6
C(29A)-C(30A)-H(30A)	119.5	C(10B)-C(11B)-C(12B)	121.2(6)
C(25A)-C(30A)-H(30A)	119.5	C(10B)-C(11B)-H(11B)	119.4
O(1B)-C(1B)-Mn(1B)	175.1(5)	C(12B)-C(11B)-H(11B)	119.4
O(2B)-C(2B)-Mn(1B)	178.6(5)	C(11B)-C(12B)-C(7B)	121.5(5)
O(3B)-C(3B)-Mn(1B)	177.4(5)	C(11B)-C(12B)-H(12B)	119.3
C(5B)-C(4B)-P(1B)	114.0(4)	C(7B)-C(12B)-H(12B)	119.3
C(5B)-C(4B)-H(4B1)	108.7	C(14B)-C(13B)-C(18B)	118.6(5)
P(1B)-C(4B)-H(4B1)	108.7	C(14B)-C(13B)-P(1B)	123.6(4)
C(5B)-C(4B)-H(4B2)	108.7	C(18B)-C(13B)-P(1B)	117.8(4)
P(1B)-C(4B)-H(4B2)	108.7	C(15B)-C(14B)-C(13B)	120.4(5)
H(4B1)-C(4B)-H(4B2)	107.6	C(15B)-C(14B)-H(14B)	119.8
C(6B)-C(5B)-C(4B)	114.7(5)	C(13B)-C(14B)-H(14B)	119.8
C(6B)-C(5B)-H(5B1)	108.6	C(16B)-C(15B)-C(14B)	121.2(6)
C(4B)-C(5B)-H(5B1)	108.6	C(16B)-C(15B)-H(15B)	119.4
C(6B)-C(5B)-H(5B2)	108.6	C(14B)-C(15B)-H(15B)	119.4
C(4B)-C(5B)-H(5B2)	108.6	C(15B)-C(16B)-C(17B)	119.4(5)
H(5B1)-C(5B)-H(5B2)	107.6	C(15B)-C(16B)-H(16B)	120.3
C(5B)-C(6B)-P(2B)	113.1(4)	C(17B)-C(16B)-H(16B)	120.3
C(5B)-C(6B)-H(6B1)	109.0	C(16B)-C(17B)-C(18B)	119.7(6)
P(2B)-C(6B)-H(6B1)	109.0	C(16B)-C(17B)-H(17B)	120.2
C(5B)-C(6B)-H(6B2)	109.0	C(18B)-C(17B)-H(17B)	120.2
P(2B)-C(6B)-H(6B2)	109.0	C(17B)-C(18B)-C(13B)	120.8(5)
H(6B1)-C(6B)-H(6B2)	107.8	C(17B)-C(18B)-H(18B)	119.6
C(12B)-C(7B)-C(8B)	116.8(5)	C(13B)-C(18B)-H(18B)	119.6
C(12B)-C(7B)-P(1B)	120.2(4)	C(24B)-C(19B)-C(20B)	119.2(5)
C(8B)-C(7B)-P(1B)	123.0(4)	C(24B)-C(19B)-P(2B)	121.6(5)
C(9B)-C(8B)-C(7B)	121.3(5)	C(20B)-C(19B)-P(2B)	119.1(4)
C(9B)-C(8B)-H(8B)	119.3	C(19B)-C(20B)-C(21B)	120.2(6)
C(7B)-C(8B)-H(8B)	119.3	C(19B)-C(20B)-H(20B)	119.9
C(8B)-C(9B)-C(10B)	120.3(5)	C(21B)-C(20B)-H(20B)	119.9

C(22B)-C(21B)-C(20B)	118.6(7)	C(27B)-C(26B)-H(26B)	119.7
C(22B)-C(21B)-H(21B)	120.7	C(25B)-C(26B)-H(26B)	119.7
C(20B)-C(21B)-H(21B)	120.7	C(26B)-C(27B)-C(28B)	120.1(6)
C(23B)-C(22B)-C(21B)	121.8(6)	C(26B)-C(27B)-H(27B)	119.9
C(23B)-C(22B)-H(22B)	119.1	C(28B)-C(27B)-H(27B)	119.9
C(21B)-C(22B)-H(22B)	119.1	C(29B)-C(28B)-C(27B)	119.3(6)
C(22B)-C(23B)-C(24B)	120.3(7)	C(29B)-C(28B)-H(28B)	120.3
C(22B)-C(23B)-H(23B)	119.8	C(27B)-C(28B)-H(28B)	120.3
C(24B)-C(23B)-H(23B)	119.8	C(30B)-C(29B)-C(28B)	120.7(6)
C(19B)-C(24B)-C(23B)	119.9(6)	C(30B)-C(29B)-H(29B)	119.7
C(19B)-C(24B)-H(24B)	120.0	C(28B)-C(29B)-H(29B)	119.7
C(23B)-C(24B)-H(24B)	120.0	C(29B)-C(30B)-C(25B)	121.2(6)
C(26B)-C(25B)-C(30B)	117.9(5)	C(29B)-C(30B)-H(30B)	119.4
C(26B)-C(25B)-P(2B)	121.9(4)	C(25B)-C(30B)-H(30B)	119.4
C(30B)-C(25B)-P(2B)	120.1(4)		
C(27B)-C(26B)-C(25B)	120.6(6)		

Table A-3. Atomic coordinates (x 10^4) and equivalent isotropic displacement parameters (Å^{2}x 10^3) for **6-6** . U(eq) is defined as one third of the trace of the orthogonalized U^{ij} tensor.

	x	y	z	U(eq)
Mn(1)	5681(1)	6771(1)	7770(1)	24(1)
P(1)	5618(2)	5493(1)	6646(1)	24(1)
P(2)	3240(2)	5611(1)	8091(1)	23(1)
O(1)	8538(5)	8456(4)	7340(2)	34(1)
O(4)	3891(5)	7716(4)	7170(2)	27(1)
C(3)	7204(7)	5810(5)	8246(3)	26(1)
O(3)	8240(5)	5230(4)	8557(2)	35(1)
C(11)	7512(7)	1925(5)	5812(3)	29(1)
C(7)	6531(7)	3819(5)	6555(3)	25(1)
C(4)	3510(7)	5153(5)	6189(3)	25(1)
C(14)	8379(7)	6175(6)	5825(3)	31(1)
C(15)	9246(7)	6939(6)	5353(3)	34(2)
C(18)	5892(7)	7439(5)	5632(3)	28(1)
C(10)	7802(7)	1233(6)	6428(3)	34(2)
C(13)	6709(7)	6403(5)	5970(3)	24(1)
C(5)	2283(7)	4432(5)	6651(3)	26(1)
C(6)	1670(7)	5334(5)	7306(3)	25(1)
C(17)	6759(7)	8193(5)	5156(3)	30(1)
C(16)	8404(8)	7943(6)	5019(3)	31(1)
C(8)	6775(8)	3087(6)	7174(3)	33(1)
C(9)	7410(8)	1801(6)	7107(3)	39(2)
C(12)	6886(7)	3208(6)	5877(3)	31(1)
O(2)	5712(5)	8633(4)	9125(2)	37(1)
C(25)	2033(7)	6555(5)	8773(3)	24(1)
C(30)	1376(7)	7779(5)	8596(3)	26(1)
C(26)	1700(7)	6101(5)	9454(3)	25(1)
C(19)	3383(7)	3972(6)	8449(3)	27(1)
C(28)	88(7)	8043(6)	9754(3)	31(1)

C(1)	7425(8)	7811(6)	7480(3)	28(1)
C(27)	751(7)	6850(6)	9949(3)	31(1)
C(24)	2205(8)	2921(5)	8229(3)	31(1)
C(2)	5619(7)	7919(6)	8600(3)	26(1)
C(22)	3611(8)	1475(6)	9044(3)	37(2)
C(31)	4103(7)	9091(6)	7133(3)	30(1)
C(29)	400(7)	8499(6)	9082(3)	32(1)
C(20)	4660(7)	3731(6)	8984(3)	30(1)
C(32)	2625(8)	9630(6)	6673(3)	36(2)
C(21)	4757(8)	2491(6)	9279(3)	36(2)
C(23)	2327(8)	1690(6)	8519(3)	36(2)

Table A-4. Bond lengths [Å] and angles [°] for **6.6**

Mn(1)-C(3)	1.789(6)	C(30)-C(29)	1.383(7)
Mn(1)-C(2)	1.832(6)	C(26)-C(27)	1.394(8)
Mn(1)-C(1)	1.841(7)	C(19)-C(20)	1.402(8)
Mn(1)-O(4)	2.037(3)	C(19)-C(24)	1.408(8)
Mn(1)-P(1)	2.3299(18)	C(28)-C(29)	1.378(8)
Mn(1)-P(2)	2.3624(19)	C(28)-C(27)	1.382(8)
P(1)-C(4)	1.832(6)	C(24)-C(23)	1.385(8)
P(1)-C(13)	1.838(6)	C(22)-C(21)	1.373(9)
P(1)-C(7)	1.843(5)	C(22)-C(23)	1.387(8)
P(2)-C(19)	1.821(6)	C(31)-C(32)	1.534(8)
P(2)-C(25)	1.834(5)	C(20)-C(21)	1.396(8)
P(2)-C(6)	1.839(5)	C(3)-Mn(1)-C(2)	89.3(2)
O(1)-C(1)	1.136(7)	C(3)-Mn(1)-C(1)	89.1(2)
O(4)-C(31)	1.394(7)	C(2)-Mn(1)-C(1)	88.6(2)
C(3)-O(3)	1.163(6)	C(3)-Mn(1)-O(4)	174.9(2)
C(11)-C(10)	1.379(8)	C(2)-Mn(1)-O(4)	95.37(19)
C(11)-C(12)	1.389(8)	C(1)-Mn(1)-O(4)	93.1(2)
C(7)-C(12)	1.385(8)	C(3)-Mn(1)-P(1)	96.74(18)
C(7)-C(8)	1.403(7)	C(2)-Mn(1)-P(1)	173.76(16)
C(4)-C(5)	1.533(8)	C(1)-Mn(1)-P(1)	89.78(17)
C(14)-C(13)	1.386(8)	O(4)-Mn(1)-P(1)	78.71(11)
C(14)-C(15)	1.399(8)	C(3)-Mn(1)-P(2)	97.11(18)
C(15)-C(16)	1.383(8)	C(2)-Mn(1)-P(2)	90.44(18)
C(18)-C(17)	1.399(8)	C(1)-Mn(1)-P(2)	173.70(17)
C(18)-C(13)	1.403(7)	O(4)-Mn(1)-P(2)	80.77(12)
C(10)-C(9)	1.379(8)	P(1)-Mn(1)-P(2)	90.54(6)
C(5)-C(6)	1.551(7)	C(4)-P(1)-C(13)	102.6(2)
C(17)-C(16)	1.367(8)	C(4)-P(1)-C(7)	101.2(2)
C(8)-C(9)	1.395(8)	C(13)-P(1)-C(7)	103.3(2)
O(2)-C(2)	1.148(7)	C(4)-P(1)-Mn(1)	115.34(18)
C(25)-C(26)	1.398(7)	C(13)-P(1)-Mn(1)	110.19(18)
C(25)-C(30)	1.399(7)	C(7)-P(1)-Mn(1)	121.95(18)

C(19)-P(2)-C(25)	102.9(2)	C(17)-C(16)-C(15)	120.4(5)
C(19)-P(2)-C(6)	103.6(3)	C(9)-C(8)-C(7)	120.6(5)
C(25)-P(2)-C(6)	101.8(2)	C(10)-C(9)-C(8)	120.1(5)
C(19)-P(2)-Mn(1)	121.06(19)	C(7)-C(12)-C(11)	121.2(5)
C(25)-P(2)-Mn(1)	113.83(19)	C(26)-C(25)-C(30)	118.1(5)
C(6)-P(2)-Mn(1)	111.52(19)	C(26)-C(25)-P(2)	123.5(4)
C(31)-O(4)-Mn(1)	117.7(3)	C(30)-C(25)-P(2)	118.4(4)
O(3)-C(3)-Mn(1)	177.2(5)	C(29)-C(30)-C(25)	120.3(5)
C(10)-C(11)-C(12)	120.2(5)	C(27)-C(26)-C(25)	121.1(5)
C(12)-C(7)-C(8)	118.0(5)	C(20)-C(19)-C(24)	117.3(5)
C(12)-C(7)-P(1)	121.7(4)	C(20)-C(19)-P(2)	120.3(4)
C(8)-C(7)-P(1)	120.2(4)	C(24)-C(19)-P(2)	122.4(4)
C(5)-C(4)-P(1)	114.0(4)	C(29)-C(28)-C(27)	120.0(5)
C(13)-C(14)-C(15)	121.9(5)	O(1)-C(1)-Mn(1)	176.3(5)
C(16)-C(15)-C(14)	118.9(6)	C(28)-C(27)-C(26)	119.5(5)
C(17)-C(18)-C(13)	119.9(5)	C(23)-C(24)-C(19)	121.3(6)
C(9)-C(10)-C(11)	119.8(5)	O(2)-C(2)-Mn(1)	174.8(5)
C(14)-C(13)-C(18)	118.0(5)	C(21)-C(22)-C(23)	119.7(6)
C(14)-C(13)-P(1)	122.1(4)	O(4)-C(31)-C(32)	110.3(5)
C(18)-C(13)-P(1)	119.7(4)	C(28)-C(29)-C(30)	120.9(5)
C(4)-C(5)-C(6)	113.5(5)	C(21)-C(20)-C(19)	120.9(6)
C(5)-C(6)-P(2)	114.0(4)	C(22)-C(21)-C(20)	120.5(6)
C(16)-C(17)-C(18)	120.9(5)	C(24)-C(23)-C(22)	120.2(6)

Table A-5. Atomic coordinates (x 10^4) and equivalent isotropic displacement parameters (Å^{2}x 10^3) for **6.7**. U(eq) is defined as one third of the trace of the orthogonalized U^{ij} tensor.

	x	y	z	U(eq)
Mn(1)	318(1)	1115(1)	2662(1)	32(1)
P(1)	1861(2)	1345(1)	4251(2)	32(1)
P(2)	1321(2)	80(1)	2703(1)	30(1)
Cl(1)	-1117(2)	692(1)	3646(2)	42(1)
O(1)	-1242(6)	2342(3)	2606(4)	53(2)
O(2)	1991(6)	1773(3)	1509(4)	48(2)
O(3)	-1717(6)	751(3)	728(4)	43(1)
C(1)	-604(8)	1876(4)	2639(5)	36(2)
C(2)	1363(8)	1495(4)	1983(6)	39(2)
C(3)	-942(8)	887(4)	1493(7)	37(2)
C(4)	3694(8)	1564(3)	4387(6)	32(2)
C(5)	4347(8)	1434(4)	3637(6)	36(2)
C(6)	5768(8)	1521(4)	3790(7)	44(2)
C(7)	6559(9)	1744(4)	4725(7)	45(2)
C(8)	5938(8)	1877(3)	5490(6)	39(2)
C(9)	4508(8)	1799(4)	5322(6)	43(2)
C(10)	1255(7)	1992(4)	4929(6)	35(2)
C(11)	1325(8)	2630(4)	4605(6)	44(2)
C(12)	780(8)	3132(4)	5044(7)	47(2)
C(13)	213(9)	3002(4)	5857(7)	51(2)
C(14)	158(9)	2380(5)	6179(6)	50(2)
C(15)	657(8)	1878(4)	5724(6)	38(2)
C(16)	2143(8)	672(3)	5154(5)	33(2)
C(17)	2878(7)	91(3)	4818(5)	32(2)
C(18)	1894(8)	-300(4)	3958(5)	34(2)
C(19)	2818(8)	51(3)	2186(5)	33(2)
C(20)	2690(8)	313(3)	1226(5)	30(2)
C(21)	3830(8)	353(4)	848(5)	33(2)
C(22)	5134(8)	145(4)	1407(6)	37(2)

C(23)	5273(8)	-119(4)	2342(6)	36(2)
C(24)	4139(8)	-184(4)	2738(6)	34(2)
C(25)	220(8)	-573(3)	2018(5)	31(2)
C(26)	-1145(8)	-646(4)	2093(6)	37(2)
C(27)	-1990(8)	-1154(4)	1646(5)	34(2)
C(28)	-1486(8)	-1601(4)	1076(6)	37(2)
C(29)	-140(8)	-1541(4)	985(6)	42(2)
C(30)	709(8)	-1043(4)	1445(6)	39(2)

Table A-6. Bond lengths [Å] and angles [°] for **6.7**

Mn(1)-C(2)	1.754(9)	C(23)-C(24)	1.383(10)
Mn(1)-C(3)	1.802(9)	C(25)-C(26)	1.396(10)
Mn(1)-C(1)	1.814(9)	C(25)-C(30)	1.414(10)
Mn(1)-P(1)	2.339(2)	C(26)-C(27)	1.377(10)
Mn(1)-P(2)	2.352(2)	C(27)-C(28)	1.387(10)
Mn(1)-Cl(1)	2.379(2)	C(28)-C(29)	1.383(10)
P(1)-C(10)	1.820(8)	C(29)-C(30)	1.368(10)
P(1)-C(16)	1.828(7)	C(2)-Mn(1)-C(3)	91.0(3)
P(1)-C(4)	1.837(8)	C(2)-Mn(1)-C(1)	88.5(4)
P(2)-C(19)	1.815(8)	C(3)-Mn(1)-C(1)	89.2(3)
P(2)-C(25)	1.826(7)	C(2)-Mn(1)-P(1)	93.9(2)
P(2)-C(18)	1.830(7)	C(3)-Mn(1)-P(1)	174.9(2)
O(1)-C(1)	1.146(8)	C(1)-Mn(1)-P(1)	92.3(2)
O(2)-C(2)	1.166(9)	C(2)-Mn(1)-P(2)	96.3(3)
O(3)-C(3)	1.150(8)	C(3)-Mn(1)-P(2)	88.3(3)
C(4)-C(5)	1.381(10)	C(1)-Mn(1)-P(2)	174.6(3)
C(4)-C(9)	1.399(10)	P(1)-Mn(1)-P(2)	89.75(8)
C(5)-C(6)	1.382(10)	C(2)-Mn(1)-Cl(1)	174.9(3)
C(6)-C(7)	1.383(11)	C(3)-Mn(1)-Cl(1)	91.5(2)
C(7)-C(8)	1.379(11)	C(1)-Mn(1)-Cl(1)	87.1(3)
C(8)-C(9)	1.386(10)	P(1)-Mn(1)-Cl(1)	83.75(8)
C(10)-C(15)	1.393(10)	P(2)-Mn(1)-Cl(1)	88.17(8)
C(10)-C(11)	1.397(10)	C(10)-P(1)-C(16)	103.0(3)
C(11)-C(12)	1.381(11)	C(10)-P(1)-C(4)	103.0(3)
C(12)-C(13)	1.403(11)	C(16)-P(1)-C(4)	98.8(3)
C(13)-C(14)	1.364(11)	C(10)-P(1)-Mn(1)	113.4(2)
C(14)-C(15)	1.369(10)	C(16)-P(1)-Mn(1)	114.5(2)
C(16)-C(17)	1.539(9)	C(4)-P(1)-Mn(1)	121.6(3)
C(17)-C(18)	1.537(9)	C(19)-P(2)-C(25)	102.5(3)
C(19)-C(20)	1.391(9)	C(19)-P(2)-C(18)	105.8(3)
C(19)-C(24)	1.410(10)	C(25)-P(2)-C(18)	98.8(3)
C(20)-C(21)	1.370(9)	C(19)-P(2)-Mn(1)	114.1(2)
C(21)-C(22)	1.380(10)	C(25)-P(2)-Mn(1)	117.9(2)
C(22)-C(23)	1.361(10)	C(18)-P(2)-Mn(1)	115.7(2)

O(1)-C(1)-Mn(1)	176.9(7)	C(29)-C(28)-C(27)	119.8(7)
O(2)-C(2)-Mn(1)	175.8(7)	C(30)-C(29)-C(28)	121.1(7)
O(3)-C(3)-Mn(1)	177.5(7)	C(29)-C(30)-C(25)	120.5(7)
C(5)-C(4)-C(9)	118.2(7)		
C(5)-C(4)-P(1)	122.1(6)		
C(9)-C(4)-P(1)	119.2(6)		
C(4)-C(5)-C(6)	122.0(8)		
C(5)-C(6)-C(7)	118.9(8)		
C(8)-C(7)-C(6)	120.5(8)		
C(7)-C(8)-C(9)	120.2(8)		
C(8)-C(9)-C(4)	120.2(8)		
C(15)-C(10)-C(11)	118.3(7)		
C(15)-C(10)-P(1)	123.0(6)		
C(11)-C(10)-P(1)	118.6(6)		
C(12)-C(11)-C(10)	120.8(8)		
C(11)-C(12)-C(13)	119.4(8)		
C(14)-C(13)-C(12)	119.7(8)		
C(13)-C(14)-C(15)	120.9(9)		
C(14)-C(15)-C(10)	120.8(8)		
C(17)-C(16)-P(1)	112.9(5)		
C(18)-C(17)-C(16)	112.5(6)		
C(17)-C(18)-P(2)	117.5(5)		
C(20)-C(19)-C(24)	118.0(7)		
C(20)-C(19)-P(2)	118.7(6)		
C(24)-C(19)-P(2)	123.1(6)		
C(21)-C(20)-C(19)	120.5(7)		
C(20)-C(21)-C(22)	121.3(7)		
C(23)-C(22)-C(21)	118.9(7)		
C(22)-C(23)-C(24)	121.4(7)		
C(23)-C(24)-C(19)	119.8(7)		
C(26)-C(25)-C(30)	117.1(7)		
C(26)-C(25)-P(2)	120.0(6)		
C(30)-C(25)-P(2)	122.8(6)		
C(27)-C(26)-C(25)	122.4(7)		
C(26)-C(27)-C(28)	119.1(7)		

Table A-7. Atomic coordinates (x 10^4) and equivalent isotropic displacement parameters (Å^{2}x 10^3) for **6.8**. U(eq) is defined as one third of the trace of the orthogonalized U^{ij} tensor.

	x	y	z	U(eq)
Mn(1)	4617(1)	1130(1)	2363(1)	23(1)
Br(1)	6187(1)	722(1)	1364(1)	27(1)
P(1)	3101(1)	1348(1)	755(1)	23(1)
P(2)	3645(1)	86(1)	2319(1)	22(1)
O(1)	6681(4)	762(2)	4279(3)	37(1)
O(2)	2939(4)	1776(2)	3501(3)	33(1)
O(3)	6107(4)	2378(2)	2441(3)	41(1)
C(1)	5892(6)	896(3)	3534(4)	27(1)
C(2)	3556(5)	1502(2)	3044(4)	27(1)
C(3)	5512(5)	1900(3)	2384(4)	28(1)
C(4)	3058(5)	-297(2)	1071(4)	25(1)
C(5)	2088(5)	95(2)	215(4)	27(1)
C(6)	2805(6)	668(2)	-141(4)	27(1)
C(7)	1289(5)	1574(2)	587(4)	24(1)
C(8)	643(5)	1449(2)	1336(4)	29(1)
C(9)	-762(5)	1547(3)	1150(5)	34(1)
C(10)	-1548(6)	1756(3)	201(5)	38(2)
C(11)	-921(5)	1879(2)	-538(5)	34(1)
C(12)	494(5)	1797(2)	-352(4)	32(1)
C(13)	3696(5)	1992(2)	74(4)	27(1)
C(14)	4280(5)	1864(3)	-711(4)	32(1)
C(15)	4786(6)	2364(3)	-1182(4)	38(2)
C(16)	4734(6)	2992(3)	-868(5)	42(2)
C(17)	4169(6)	3129(3)	-74(5)	37(2)
C(18)	3648(6)	2636(3)	388(4)	34(1)
C(19)	4751(5)	-568(2)	3016(4)	24(1)
C(20)	6086(6)	-645(3)	2941(4)	31(1)
C(21)	6901(6)	-1157(3)	3399(4)	32(1)
C(22)	6413(6)	-1603(3)	3958(4)	37(1)

C(23)	5095(6)	-1534(3)	4051(5)	38(1)
C(24)	4265(6)	-1030(3)	3579(4)	34(1)
C(25)	2164(5)	57(2)	2826(4)	22(1)
C(26)	2290(5)	318(2)	3791(4)	25(1)
C(27)	1165(5)	352(3)	4166(4)	29(1)
C(28)	-116(6)	148(3)	3599(4)	32(1)
C(29)	-251(5)	-129(3)	2663(4)	32(1)
C(30)	860(5)	-180(3)	2272(4)	29(1)

Table A-8. Bond lengths [Å] and angles [°] for **6.8**.

Mn(1)-C(2)	1.783(6)	C(23)-C(24)	1.375(8)
Mn(1)-C(1)	1.816(6)	C(25)-C(30)	1.405(7)
Mn(1)-C(3)	1.821(6)	C(25)-C(26)	1.406(7)
Mn(1)-P(1)	2.3471(17)	C(26)-C(27)	1.374(7)
Mn(1)-P(2)	2.3563(17)	C(27)-C(28)	1.370(7)
Mn(1)-Br(1)	2.5189(11)	C(28)-C(29)	1.381(8)
P(1)-C(13)	1.822(5)	C(29)-C(30)	1.377(7)
P(1)-C(7)	1.833(5)	C(2)-Mn(1)-C(1)	91.5(2)
P(1)-C(6)	1.835(5)	C(2)-Mn(1)-C(3)	89.2(2)
P(2)-C(25)	1.819(5)	C(1)-Mn(1)-C(3)	89.7(2)
P(2)-C(4)	1.829(5)	C(2)-Mn(1)-P(1)	94.99(17)
P(2)-C(19)	1.836(5)	C(1)-Mn(1)-P(1)	173.33(17)
O(1)-C(1)	1.138(6)	C(3)-Mn(1)-P(1)	91.91(16)
O(2)-C(2)	1.151(6)	C(2)-Mn(1)-P(2)	95.71(17)
O(3)-C(3)	1.146(6)	C(1)-Mn(1)-P(2)	87.97(17)
C(4)-C(5)	1.530(7)	C(3)-Mn(1)-P(2)	174.66(17)
C(5)-C(6)	1.536(7)	P(1)-Mn(1)-P(2)	89.84(5)
C(7)-C(12)	1.391(7)	C(2)-Mn(1)-Br(1)	174.02(17)
C(7)-C(8)	1.391(7)	C(1)-Mn(1)-Br(1)	90.02(17)
C(8)-C(9)	1.379(7)	C(3)-Mn(1)-Br(1)	85.06(17)
C(9)-C(10)	1.389(8)	P(1)-Mn(1)-Br(1)	83.68(5)
C(10)-C(11)	1.366(8)	P(2)-Mn(1)-Br(1)	90.13(5)
C(11)-C(12)	1.385(7)	C(13)-P(1)-C(7)	102.3(2)
C(13)-C(14)	1.394(8)	C(13)-P(1)-C(6)	103.0(2)
C(13)-C(18)	1.400(7)	C(7)-P(1)-C(6)	98.3(2)
C(14)-C(15)	1.388(8)	C(13)-P(1)-Mn(1)	113.85(17)
C(15)-C(16)	1.370(8)	C(7)-P(1)-Mn(1)	121.62(18)
C(16)-C(17)	1.398(8)	C(6)-P(1)-Mn(1)	115.13(17)
C(17)-C(18)	1.380(8)	C(25)-P(2)-C(4)	105.3(2)
C(19)-C(20)	1.388(8)	C(25)-P(2)-C(19)	102.5(2)
C(19)-C(24)	1.400(8)	C(4)-P(2)-C(19)	99.1(2)
C(20)-C(21)	1.375(7)	C(25)-P(2)-Mn(1)	113.63(16)
C(21)-C(22)	1.377(8)	C(4)-P(2)-Mn(1)	116.06(17)
C(22)-C(23)	1.377(8)	C(19)-P(2)-Mn(1)	118.14(17)

O(1)-C(1)-Mn(1)	178.3(5)	C(27)-C(28)-C(29)	119.0(5)
O(2)-C(2)-Mn(1)	175.2(4)	C(30)-C(29)-C(28)	121.4(5)
O(3)-C(3)-Mn(1)	176.9(5)	C(29)-C(30)-C(25)	120.0(5)
C(5)-C(4)-P(2)	117.4(4)		
C(4)-C(5)-C(6)	113.4(4)		
C(5)-C(6)-P(1)	112.0(4)		
C(12)-C(7)-C(8)	118.9(5)		
C(12)-C(7)-P(1)	119.3(4)		
C(8)-C(7)-P(1)	121.3(4)		
C(9)-C(8)-C(7)	120.4(5)		
C(8)-C(9)-C(10)	120.0(6)		
C(11)-C(10)-C(9)	119.9(5)		
C(10)-C(11)-C(12)	120.6(5)		
C(11)-C(12)-C(7)	120.2(5)		
C(14)-C(13)-C(18)	118.5(5)		
C(14)-C(13)-P(1)	122.3(4)		
C(18)-C(13)-P(1)	119.0(4)		
C(15)-C(14)-C(13)	120.9(5)		
C(16)-C(15)-C(14)	120.1(6)		
C(15)-C(16)-C(17)	119.9(5)		
C(18)-C(17)-C(16)	120.2(6)		
C(17)-C(18)-C(13)	120.4(5)		
C(20)-C(19)-C(24)	117.6(5)		
C(20)-C(19)-P(2)	120.1(4)		
C(24)-C(19)-P(2)	122.2(4)		
C(21)-C(20)-C(19)	121.2(5)		
C(20)-C(21)-C(22)	120.5(5)		
C(21)-C(22)-C(23)	119.4(5)		
C(24)-C(23)-C(22)	120.4(5)		
C(23)-C(24)-C(19)	120.9(5)		
C(30)-C(25)-C(26)	117.7(5)		
C(30)-C(25)-P(2)	123.1(4)		
C(26)-C(25)-P(2)	119.1(4)		
C(27)-C(26)-C(25)	120.8(5)		
C(28)-C(27)-C(26)	121.0(5)		

Table A-9. Atomic coordinates (x 10^4) and equivalent isotropic displacement parameters (Å^{2}x 10^3) for **6.9**. U(eq) is defined as one third of the trace of the orthogonalized U^{ij} tensor.

	x	y	z	U(eq)
Mn(1)	1753(1)	315(1)	9440(1)	24(1)
P(1)	2983(1)	1340(1)	9900(1)	25(1)
P(2)	1877(1)	443(1)	7929(1)	24(1)
O(1)	146(2)	-933(2)	8731(2)	34(1)
O(2)	1830(2)	-102(2)	11368(2)	35(1)
O(3)	-116(2)	1340(2)	9351(2)	30(1)
N(1)	3176(3)	-373(2)	9637(2)	25(1)
N(2)	3214(3)	-947(3)	10052(3)	36(1)
N(3)	3317(4)	-1552(2)	10462(3)	55(1)
C(1)	801(4)	-470(2)	9020(3)	26(1)
C(2)	1806(3)	85(2)	10636(3)	28(1)
C(3)	620(4)	953(2)	9359(3)	28(1)
C(4)	4113(3)	1331(2)	9375(3)	28(1)
C(5)	3747(4)	1443(2)	8326(3)	30(1)
C(6)	3206(3)	734(2)	7795(3)	26(1)
C(7)	3641(3)	1334(2)	11137(3)	23(1)
C(8)	3020(4)	1532(2)	11719(3)	31(1)
C(9)	3474(4)	1546(2)	12673(3)	30(1)
C(10)	4551(4)	1366(2)	13027(3)	33(1)
C(11)	5184(4)	1158(2)	12456(3)	33(1)
C(12)	4722(3)	1131(2)	11509(3)	28(1)
C(13)	2541(3)	2359(2)	9715(3)	25(1)
C(14)	3191(3)	2952(2)	10226(3)	30(1)
C(15)	2905(4)	3723(2)	10068(3)	35(1)
C(16)	1972(4)	3931(2)	9407(3)	34(1)
C(17)	1326(4)	3357(2)	8894(3)	30(1)
C(18)	1614(3)	2576(2)	9042(3)	29(1)
C(19)	885(3)	1116(2)	7236(3)	26(1)

C(20)	-205(3)	1004(2)	7232(3)	26(1)
C(21)	-986(3)	1516(2)	6775(3)	30(1)
C(22)	-725(4)	2144(2)	6300(3)	34(1)
C(23)	338(4)	2242(2)	6270(3)	28(1)
C(24)	1145(3)	1735(2)	6733(3)	28(1)
C(25)	1666(3)	-425(2)	7200(3)	26(1)
C(26)	1920(3)	-1165(2)	7567(3)	28(1)
C(27)	1843(3)	-1811(2)	7004(3)	29(1)
C(28)	1498(4)	-1723(3)	6064(3)	36(1)
C(29)	1245(4)	-1001(3)	5680(3)	40(1)
C(30)	1317(4)	-356(2)	6244(3)	33(1)
C(1S)	6127(4)	500(3)	6135(4)	44(1)
C(2S)	6000(4)	895(3)	6901(4)	49(1)
C(3S)	6036(4)	1699(3)	6914(4)	45(1)
C(4S)	6183(3)	2102(3)	6173(3)	38(1)
C(5S)	6316(3)	1705(3)	5409(3)	37(1)
C(6S)	6283(4)	906(3)	5399(3)	41(1)

Table A-10. Bond lengths [Å] and angles [°] for **6.9**.

Mn(1)-C(3)	1.799(5)	C(4)-C(5)	1.538(6)
Mn(1)-C(1)	1.816(5)	C(5)-C(6)	1.520(6)
Mn(1)-C(2)	1.832(5)	C(7)-C(8)	1.380(6)
Mn(1)-N(1)	2.126(3)	C(7)-C(12)	1.392(6)
Mn(1)-P(2)	2.3396(14)	C(8)-C(9)	1.400(6)
Mn(1)-P(1)	2.3437(13)	C(9)-C(10)	1.374(6)
P(1)-C(7)	1.830(4)	C(10)-C(11)	1.383(6)
P(1)-C(4)	1.831(4)	C(11)-C(12)	1.392(6)
P(1)-C(13)	1.841(4)	C(13)-C(18)	1.390(6)
P(2)-C(19)	1.826(4)	C(13)-C(14)	1.408(6)
P(2)-C(25)	1.832(4)	C(14)-C(15)	1.380(6)
P(2)-C(6)	1.841(4)	C(15)-C(16)	1.382(6)
O(1)-C(1)	1.154(5)	C(16)-C(17)	1.384(6)
O(2)-C(2)	1.144(5)	C(17)-C(18)	1.397(6)
O(3)-C(3)	1.153(5)	C(19)-C(24)	1.400(6)
N(1)-N(2)	1.164(5)	C(19)-C(20)	1.409(6)
N(2)-N(3)	1.200(6)	C(20)-C(21)	1.372(6)
C(21)-C(22)	1.387(6)	C(2S)-C(3S)	1.384(7)
C(22)-C(23)	1.386(6)	C(3S)-C(4S)	1.374(7)
C(23)-C(24)	1.389(6)	C(4S)-C(5S)	1.390(6)
C(25)-C(26)	1.391(6)	C(5S)-C(6S)	1.375(6)
C(25)-C(30)	1.396(6)	C(3)-Mn(1)-C(1)	88.62(18)
C(26)-C(27)	1.387(6)	C(3)-Mn(1)-C(2)	90.69(19)
C(27)-C(28)	1.377(6)	C(1)-Mn(1)-C(2)	91.45(19)
C(28)-C(29)	1.372(6)	C(3)-Mn(1)-N(1)	174.65(16)
C(29)-C(30)	1.387(6)	C(1)-Mn(1)-N(1)	96.06(16)
C(1S)-C(6S)	1.372(7)	C(2)-Mn(1)-N(1)	86.61(16)
C(1S)-C(2S)	1.389(7)	C(3)-Mn(1)-P(2)	98.22(14)
C(1)-Mn(1)-P(2)	86.99(13)	N(1)-Mn(1)-P(2)	84.65(10)
C(2)-Mn(1)-P(2)	170.90(14)	C(3)-Mn(1)-P(1)	91.53(13)
C(1)-Mn(1)-P(1)	176.96(14)	C(2)-Mn(1)-P(1)	91.58(14)
N(1)-Mn(1)-P(1)	83.94(10)		

P(2)-Mn(1)-P(1)	89.99(4)	O(3)-C(3)-Mn(1)	176.0(4)
C(7)-P(1)-C(4)	104.01(19)	C(5)-C(4)-P(1)	112.9(3)
C(7)-P(1)-C(13)	101.39(18)	C(6)-C(5)-C(4)	114.2(3)
C(4)-P(1)-C(13)	100.99(18)	C(5)-C(6)-P(2)	117.7(3)
C(7)-P(1)-Mn(1)	112.71(13)	C(8)-C(7)-C(12)	119.2(4)
C(4)-P(1)-Mn(1)	114.39(14)	C(8)-C(7)-P(1)	117.6(3)
C(13)-P(1)-Mn(1)	121.16(14)	C(12)-C(7)-P(1)	123.2(3)
C(19)-P(2)-C(25)	101.88(19)	C(7)-C(8)-C(9)	120.6(4)
C(19)-P(2)-C(6)	106.66(19)	C(10)-C(9)-C(8)	119.4(4)
C(25)-P(2)-C(6)	98.42(19)	C(9)-C(10)-C(11)	120.9(4)
C(19)-P(2)-Mn(1)	113.46(14)	C(10)-C(11)-C(12)	119.4(4)
C(25)-P(2)-Mn(1)	118.06(14)	C(7)-C(12)-C(11)	120.4(4)
C(6)-P(2)-Mn(1)	116.31(14)	C(18)-C(13)-C(14)	117.9(4)
N(2)-N(1)-Mn(1)	117.2(3)	C(18)-C(13)-P(1)	122.3(3)
N(1)-N(2)-N(3)	175.4(4)	C(14)-C(13)-P(1)	119.7(3)
O(1)-C(1)-Mn(1)	175.6(4)	C(15)-C(14)-C(13)	120.8(4)
O(2)-C(2)-Mn(1)	176.1(4)	C(14)-C(15)-C(16)	120.8(4)
C(15)-C(16)-C(17)	119.4(4)	C(30)-C(25)-P(2)	120.4(3)
C(16)-C(17)-C(18)	120.3(4)	C(27)-C(26)-C(25)	121.3(4)
C(13)-C(18)-C(17)	120.9(4)	C(28)-C(27)-C(26)	119.5(4)
C(24)-C(19)-C(20)	118.9(4)	C(29)-C(28)-C(27)	120.6(4)
C(24)-C(19)-P(2)	124.2(3)	C(28)-C(29)-C(30)	119.8(4)
C(20)-C(19)-P(2)	116.9(3)	C(29)-C(30)-C(25)	121.1(4)
C(21)-C(20)-C(19)	120.2(4)	C(6S)-C(1S)-C(2S)	120.0(5)
C(20)-C(21)-C(22)	121.0(4)	C(3S)-C(2S)-C(1S)	119.4(5)
C(23)-C(22)-C(21)	119.3(4)	C(4S)-C(3S)-C(2S)	120.3(5)
C(22)-C(23)-C(24)	120.9(4)	C(3S)-C(4S)-C(5S)	120.2(5)
C(23)-C(24)-C(19)	119.7(4)	C(6S)-C(5S)-C(4S)	119.4(5)
C(26)-C(25)-C(30)	117.7(4)	C(1S)-C(6S)-C(5S)	120.7(5)
C(26)-C(25)-P(2)	121.8(3)		

VITA

Poulomi Ganguly was born in Kolkata, West Bengal, India, on May 23, 1978 to Achin and Ratna Ganguly. She grew up in New Delhi and Bangalore before graduating with her B.S. degree from St. Stephen's College, Delhi in 1999 and M.S. degree from the University of Delhi, Delhi, in 2001. She began her graduate studies at Texas A&M in January 2002 under the direction of Dr. Donald J. Darensbourg. Questions and comments may be directed to her mother at: UD090102, 1050/1 Survey Park, Kolkata-700075, West Bengal, India.